Strength of Unclipped Cold-Formed Knee-Walls Under Uniform Lateral Loading

Deanna M. Engelmeyer

Civil and Architectural Engineering and Construction Management Department

Milwaukee School of Engineering

Author Note

Deanna M. Engelmeyer, Civil and Architectural Engineering and Construction Management Department, Milwaukee School of Engineering.

A capstone project report submitted to the faculty of the Milwaukee School of Engineering in partial fulfillment of the requirements for the degree of Master of Science in Structural Engineering, June 3, 2018.

Correspondence concerning this report should be addressed to Deanna M. Engelmeyer, Civil and Architectural Engineering and Construction Management Department, Milwaukee School of Engineering, 1025 N Broadway, Milwaukee, WI 53202. E-mail: engelmeyerd@alumni.msoe.edu

Abstract

The industry standard for designing the moment-resisting connection of a cold-formed knee-wall is to provide a light gauge clip angle at the location of the connection. Because of the cantilevering nature of a knee-wall, clip angles provide additional rotational stiffness to effectively resist the moment that accumulates at the base. The purpose of this research initiative was to qualitatively and quantitatively measure the effects of a laterally loaded cold-formed knee-wall without the use of a light gauge clip angle. The experimental program included 18 full-scale tests. The three stud gauges, 18-, 16-, and 14-gauge, were tested under two base connection configurations: a structural steel channel and metal deck. Using the data obtained from the testing, the moment capacity of the unclipped knee-wall connection was calculated and compared to the published values for connections with a light gauge clip. Screw capacity tests were conducted to show why different connection limit states controlled for certain knee-wall tests. The testing showed that the Hillman machine screws can achieve a higher tensile rupture capacity than the generic machine screws, causing the stud-to-track connection to fail first by tear out. The tests performed on the metal deck base material did not produce as consistent results as the steel channel tests because of the constructability base connections. The tests attaching to the structural steel channel base material resulted in higher bending capacity because the rupture capacity of the machine screws is greater than the pullout capacity of the self-drilling screws.

Keywords: cold-formed steel framing, cold-formed knee walls, knee-wall connections, moment resistance, gauge testing, screw capacity testing, curtainwall construction

Acknowledgments

The completion of this capstone report would not have been possible without the assistance of many people and organizations. First and foremost, I would like to extend a thank you to my advisor, Dr. Christopher Raebel, for all his dedication and guidance in the production and completion of my research. Additionally, I would like to thank the committee members of this project, Dr. H. Peter Huttlemaier and Dr. Todd Davis, for all their support and insights into the study.

I would like to also acknowledge Jeff MacDonald, at Milwaukee School of Engineering, for all the extra time and hard work he put towards the construction and materials required for my testing.

I would like to give a special thanks to Karl Scherzer and his colleagues at Excel Engineering for not only the creation of my capstone project subject, but for all their expertise and help during the testing as well. I would also like to thank Germantown Iron and Steel for their generous donation of the steel angle and channel used in this experiment.

Finally, I would like to thank my family and friends. Their continued support during this process have made this educational journey possible.

Table of Contents

List of Figures

List of Tables

Nomenclature

Symbols

D – Displacement of knee-wall system

d – Depth of knee-wall members

$d_{pullout}$ – Distance between track-to-base-material screws

d_{shear} – Distance between stud-flange-to-track-flange screws

H – Height of knee-wall

L – Length of knee-wall

M – Moment

p – Wall pressure

P_{stud} – Tributary point load per stud

P_{total} – Total load reported by MTS actuators

s – Stud spacing of knee-wall

T – Tensile force in screw

θ – angular displacement or rotation of knee-wall system

w – Uniform distributed load

Abbreviations

AISI – American Iron and Steel Institute

ASCE – American Society of Civil Engineers

ASTM – American Society for Testing and Materials

avg – Average

BHS – Bake Hardenable Steel

C – Carbon

Cb – Columbium

Cr – Chromium

CS – Commercial Steel

CSEC – Construction Science and Engineering Center

Cu - Copper

CFS – Cold-Formed Steel Framing

D - Deck

DDS – Deep Drawing Steel

Displ – Displacement

DS – Drawing Steel

DWT – Draw Wired Transducers

EDDS – Extra Deep Drawing Steel

ft – Feet

GA. – Gauge

IBC – International Building Code

IN. – Inch

HSLAS – High Strength Low-Alloy Steel

HSLAS-F – High Strength Low-Alloy Steel with Improved Formability

HMSR – Hillman machine screw rupture

ksi – Kips per Square Inch

lb (or lbf) – Pounds

Mn – Manganese

Mo – Molybdenum

Nb – Niobium

ND – No Deck

Ni – Nickel

MSOE – Milwaukee School of Engineering

MSR – Generic machine screw rupture

P – Phosphorus

PDF's – Power Driven Fasteners

psi – Pounds per Square Inch

RCKW5.5 – Rigid Connector Knee-Wall clip

S – Sulfur

SDP – Self-drilling screw pullout

SDS – Self-drilling screw shear tear out

SFS – Special Forming Steel

SHS – Solution Hardened Steel

SS – Structural Steel

Ti – Titanium

UNO – Unless Noted Otherwise

V – Vanadium

wt – Weight

Glossary

Knee-wall – A wall, typically 3 feet or less in height, that does not span all the way up to the framing above, therefore, only having a single connection point back to the main structural system. This is also known as a *pony-wall*, *half-wall*, or a *cantilevering-wall*.

Electrical Discharge Machining (EDM) – A manufacturing metal cutting process that does not require physical contact between the metal and the EDM tool. The material of the metal is removed by a series of discrete electrical discharges allowing the metal particles to travel in a dielectric fluid. This is also known as *spark machining*, *spark eroding*, *die sinking*, *wire burning* or *wire erosion*.

Strength of Unclipped Cold-Formed Knee-Walls

Under Uniform Lateral Loading

Chapter 1: Introduction

In the construction of a building, the façade must be adequately supported in order to secure it in place while minimizing its potential for cracking and warping. The façade could be supported by a number of different structural materials, such as wood, cold-formed metal framing, concrete masonry units or precast concrete. Cold-formed steel framing is a common choice for the structural support of the façade often (Nowak & Shoemaker, 2012). Cold-formed steel framing is often found in low- to mid-rise buildings, because of its strength and non-combustible materials properties. It can be designed in load-bearing or curtainwall applications depending on the size, location and loading of the building.

Cold-formed framing is often used in curtainwall applications where it only needs to resist the lateral loading without any need to resist gravity loads (Nowak & Shoemaker, 2012). In these circumstances, a different primary structural system would support all of the gravity loads. In typical cold-formed curtainwall design, there are at least two connection points back to the main structure for support. These connections are designed as simple supports or slotted attachments that allow for vertical movement. However, there are special curtainwall applications, knee-walls, that only allow for a single connection point back to the main structure. Examples of these situations can be seen at parapet and railing locations of a building. Figure 1-1 illustrates a typical knee-wall application.

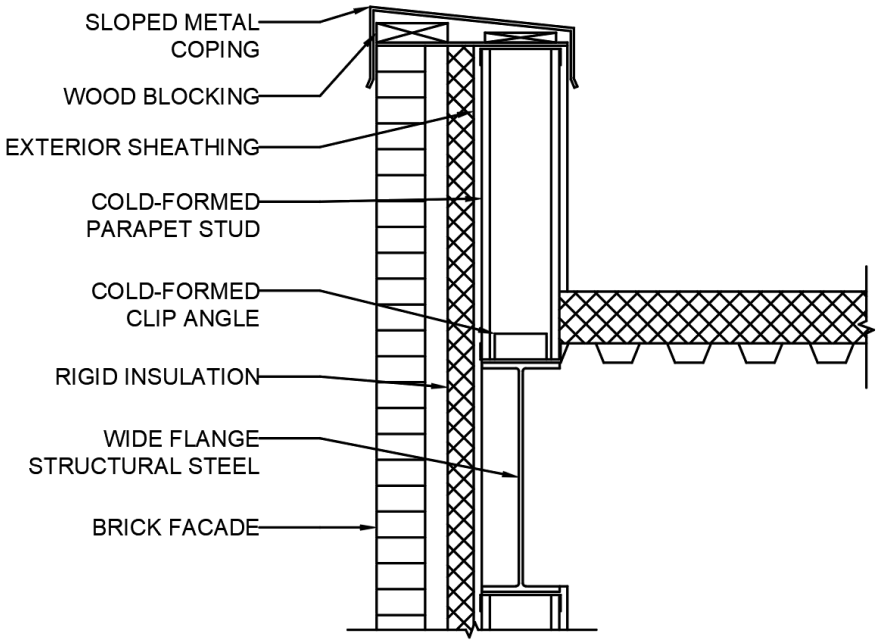

Figure 1-1. Typical knee-wall application.

Since knee-walls only allow for a single point of connection back to the primary structure, they are designed differently than the typical curtainwall connections. Knee-walls act as cantilevered beams; therefore, these single connection points are designed as fixed supports and must resist both moment and shear force. Moment resisting connections require special attention during design and construction to ensure the connection can develop its expected capacity.

Chapter 2: Literature Review and Present Practices

Cold-formed steel framing is increasing in popularity in the construction industry and need for relevant research on these structures is evident. Recent research initiatives have expanded the body of knowledge into design and construction of cold-formed framing. There are different applications of cold-formed steel in building structures. The relevant research relating to cold-formed steel properties and the design of knee-walls are included herein.

2.1 ASTM A1008: Standard Specification for Steel, Sheet, Cold-Rolled, Carbon, Structural, High-Strength Low-Alloy, High-Strength Low-Alloy with Improved Formability, Solution Hardened, and Bake Hardened

There are minimum material requirements for both structural and non-structural cold-formed framing that must be followed to ensure the safety of building occupants. ASTM A1008 provides standards for cold-rolled base metals for commercial steel (CS), drawing steel (DS), deep drawing steel (DDS), extra deep drawing steel (EDDS), special forming steel (SFS), structural steel (SS), high-strength low-alloy steel (HSLA), high-strength low-alloy steel with improved formability (HSLA-F), solution hardened steel (SHS), and bake hardenable steel (BHS) (ASTM International, 2016). Table 2.1-1 illustrates the allowable chemical compositions for the following cold rolled steel sheet designations determined by a heat analysis: SS, HSLAS, HSLAS-F, SHS and BHS.

Table 2.1-1

Chemical Composition for Cold Rolled Steel Sheets

Maximum Composition UNO (%)											
Designation[A]	**C**	**Mn**	**P**	**S**	**Cu**	**Ni**	**Cr**	**Mo**	**V**	**Cb/Nb**	**Ti**
SS											
Grade 25	0.20	0.60	0.035	0.035	0.20	0.20	0.15	0.06	0.008	0.008	0.025
Grade 30	0.20	0.60	0.035	0.035	0.20	0.20	0.15	0.06	0.008	0.008	0.025
Grade 33 (1)	0.20	0.60	0.035	0.035	0.20	0.20	0.15	0.06	0.008	0.008	0.025
Grade 33 (2)	0.15	0.60	0.20	0.035	0.20	0.20	0.15	0.06	0.008	0.008	0.025
Grade 40 (1)	0.20	1.35	0.035	0.035	0.20	0.20	0.15	0.06	0.008	0.008	0.025
Grade 40 (2)	0.15	0.60	0.20	0.035	0.20	0.20	0.15	0.06	0.008	0.008	0.025
Grade 45[C]	0.20	1.35	0.070	0.025	0.20	0.20	0.15	0.06	0.008	0.008	0.008
Grade 50	0.20	1.35	0.035	0.035	0.20	0.20	0.15	0.06	0.008	0.008	0.025
Grade 60	0.20	1.35	0.035	0.035	0.20	0.20	0.15	0.06	0.008	0.008	0.025
Grade 70	0.20	1.35	0.035	0.035	0.20	0.20	0.15	0.06	0.008	0.008	0.025
Grade 80	0.20	1.35	0.035	0.035	0.20	0.20	0.15	0.06	0.008	0.008	0.025
HSLAS											
Grade 45 (1)	0.22	1.65	0.04	0.04	0.20	0.20	0.15	0.06	0.005[B]	0.005[B]	0.005[B]
Grade 45 (2)	0.15	1.65	0.04	0.04	0.20	0.20	0.15	0.06	0.005[B]	0.005[B]	0.005[B]
Grade 50 (1)	0.23	1.65	0.04	0.04	0.20	0.20	0.15	0.06	0.005[B]	0.005[B]	0.005[B]
Grade 50 (2)	0.15	1.65	0.04	0.04	0.20	0.20	0.15	0.06	0.005[B]	0.005[B]	0.005[B]
Grade 55 (1)	0.25	1.65	0.04	0.04	0.20	0.20	0.15	0.06	0.005[B]	0.005[B]	0.005[B]
Grade 55 (2)	0.15	1.65	0.04	0.04	0.20	0.20	0.15	0.06	0.005[B]	0.005[B]	0.005[B]
Grade 60 (1)	0.26	1.65	0.04	0.04	0.20	0.20	0.15	0.06	0.005[B]	0.005[B]	0.005[B]
Grade 60 (2)	0.15	1.65	0.04	0.04	0.20	0.20	0.15	0.06	0.005[B]	0.005[B]	0.005[B]
Grade 65 (1)	0.26	1.65	0.04	0.04	0.20	0.20	0.15	0.06	0.005[B]	0.005[B]	0.005[B]
Grade 65 (2)	0.15	1.65	0.04	0.04	0.20	0.20	0.15	0.06	0.005[B]	0.005[B]	0.005[B]
Grade 70 (1)	0.15	1.65	0.04	0.04	0.20	0.20	0.15	0.16	0.005[B]	0.005[B]	0.005[B]
Grade 70 (2)	0.26	1.65	0.04	0.04	0.20	0.20	0.15	0.16	0.005[B]	0.005[B]	0.005[B]
HSLAS-F											
Grade 50	0.15	1.65	0.020	0.025	0.20	0.20	0.15	0.06	0.005[B]	0.005[B]	0.005[B]
Grade 60	0.15	1.65	0.020	0.025	0.20	0.20	0.15	0.06	0.005[B]	0.005[B]	0.005[B]
Grade 70	0.15	1.65	0.020	0.025	0.20	0.20	0.15	0.16	0.005[B]	0.005[B]	0.005[B]
Grade 80	0.15	1.65	0.020	0.025	0.20	0.20	0.15	0.16	0.005[B]	0.005[B]	0.005[B]
SHS											
	0.12	1.50	0.12	0.030	0.20	0.20	0.15	0.06	0.008	0.008	0.008
BHS											
	0.12	1.50	0.12	0.030	0.20	0.20	0.15	0.06	0.008	0.008	0.008

Note. Adapted from ASTM International, 2016. For additional information and requirements for this table, refer to ASTM A1008.

A: The number denoted in the parenthesis next to the grade represents the steel Type (for SS) or Class (for HSLAS)

B: These denote minimum values

C: This grade also has a maximum Nickel composition of 0.030

The different element compositions represented in Table 2.1-1 are suitable for welded connections. However, these materials must successfully bend 180° in any direction without cracking, otherwise the material can be subjected to rejection. Depending on the chemical composition and annealing method used to form these metals will determine the aging process seen throughout the life of the metal. Table 2.1-2 shows the minimum mechanical properties required for certain grades of cold rolled steel.

Table 2.1-2

Required Mechanical Properties for Cold Rolled Steel Sheets

Designation[A]	Yield Strength (ksi)	Tensile Strength (ksi)	Elongation in 2" (%)
SS			
Grade 25	25	42	26
Grade 30	30	45	24
Grade 33	33	48	22
Grade 40	40	52	20
Grade 45	45	60	20
Grade 50	50	65	18
Grade 60	60	75	12
Grade 70	70	85	6
Grade 80	80	82	N/A
HSLAS			
Grade 45 (1)	45	60	22
Grade 45 (2)	45	55	22
Grade 50 (1)	50	65	20
Grade 50 (2)	50	60	20
Grade 55 (1)	55	70	18
Grade 55 (2)	55	65	18
Grade 60 (1)	60	75	16
Grade 60 (2)	60	70	16
Grade 65 (1)	65	80	15
Grade 65 (2)	65	75	15
Grade 70 (1)	70	85	14
Grade 70 (2)	70	80	14
HSLAS-F			
Grade 50	50	60	22
Grade 60	60	70	18
Grade 70	70	80	16
Grade 80	80	90	14

Note. Adapted from ASTM International, 2016. For additional information and requirements for this table, refer to ASTM A1008. A: The number denoted in the parenthesis next to the grade represents the steel Class for HSLAS.

Two tension tests must be conducted for the cold rolled sheets when 50 tons or more of finished material is present. Two tension tests are also required when the testing specimen differs in thickness of at least 0.050 inches. In this circumstance the tension tests will consist of specimens at the locations of the thinnest and thickest parts of the material. When this tonnage or thickness requirement is not met, only one tension test is required. Two common methods for determining the yield strength of the steel are the 0.2% offset method and the 0.5% extension under load method.

According to the metallurgical analysis done for the material of this project, the cold-formed steel members conformed to structural steel Grade 40, as indicated in ASTM A1008. This was determined by one tension test of each type of metal used in this project. For additional information on the results, such as the stress-strain curves of each material tested, on this metallurgical analysis, refer to Appendix C of this document.

2.2 Mechanical Properties of Structural Stainless Steels by Tylek and Kuchta

Exterior cold-formed knee-wall applications, such as parapets, will be exposed to outdoor weather during their service life. Thus, the cold-formed framing must be corrosion resistant. To achieve corrosion resistance in stainless steel, chromium is the main alloying agent used, with only a maximum amount of carbon permitted to 1.2% (Tylek & Kuchta, 2014). Altering the amount of the alloying components in cold-form stainless steel, carbon, chromium, nickel and molybdenum, can have a significant influence on its mechanical and physical properties (Tylek & Kuchta, 2014).

There are different steel classifications for the different chemical compositions of the alloying metals: ferritic, austenitic, austenitic-ferritic, martensitic, and precipitation

hardening. However, out of these classifications, only ferritic, austenitic, and austenitic-ferritic metals with a maximum nominal yield strength of 70 ksi can be used in building structures (Tylek & Kuchta, 2014). The allowable ranges for these three stainless steel classifications are listed in Table 2.2-1.

Table 2.2-1

Chemical Composition Ranges for Structural Stainless Steels

Type of Stainless Steel	**Chemical Composition (wt%)**			
	Carbon (max)	**Chromium**	**Nickel**	**Molybdenum**
Ferritic	0.03 – 0.08	10.50 – 18.00	0 – 1.00	–
Austenitic	0.02 – 0.08	16.50 – 21.00	6.00 – 26.00	0 – 7.00
Austenitic-Ferritic	0.03	21.00 – 24.00	3.50 – 6.50	0.10 – 3.50

Note. Adapted from Tylek & Kuchta, 2014.

When comparing the three stainless steel classifications used in building structures, the ferritic, austenitic, and ferritic-austenitic each have specific mechanical property benefits depending on the combination of alloying content. The austenitic stainless steel has excellent ductility properties with an elongation after fracture of about 35% to 40% (Tylek & Kuchta, 2014). This good ductility comes from low amounts of carbon and nitrogen (Tylek & Kuchta, 2014). The ferritic stainless steel has the lowest hardness value out of the three, making it easier to drill into for connection attachments. The ferritic-austenitic steel holds the highest yield strength of the other two steel classifications due to its high content of nitrogen.

The cost of stainless steel is expensive because it contains extra alloying agents to make it corrosion resistant. Therefore, stainless steel is only used in areas that require it, such as

the exterior framing of the building structure and anywhere else that will be exposed to the outdoor elements. For all other situations that don't need corrosion resistive steel, such as interior railings or half-walls, carbon steel is typically used. A more cost efficient method of protecting the cold-formed framing from the outdoor elements would be to galvanize the cold-formed steel with a thin, exterior coating of stainless steel materials. When comparing the mechanical properties, the stress-strain curves of carbon steel and stainless steel are distinctly different from one another. The elastic portion of the stress-strain curve for stainless steel is non-linear, making it hard to determine when the metal transitions into its plastic state (Tylek & Kuchta, 2014). On the other hand, carbon steel has a linear elastic portion in the beginning, then a distinct transition into its plastic range (Tylek & Kuchta, 2014). There is also a physical distinction between carbon and stainless-steels. Carbon steel has a dull appearance, whereas stainless steel is visually shiny.

The steel used in this project represents that of carbon steel based on the shape of each gauge's stress-strain curve. However, the cold-formed pieces from the project have a shine to them, showing that they are galvanized. Illustrations of each gauge's stress-strain curve can be viewed in Appendix C, Figures C-1 through C-7.

2.3 ASTM A875: Standard Specification for Steel Sheet, Zinc-5% Aluminum Alloy-Coated by the Hot-Dip Process

An alternative option to full stainless-steel framing is to use galvanized carbon steel. This option is very common in the construction industry because it is an economical way to achieve corrosion resistance (ASTM International, 2013). Just like hot-rolled steel, a galvanizing metal used for cold-formed framing is a zinc-aluminum alloy. Like the cold-formed steel base metal, there are minimum requirements for galvanizing to adequately attain corrosion resistance. ASTM A875 provides standards for Zinc-5% Aluminum alloy type of galvanizing coating for cold-formed steel members (ASTM International, 2013). This zinc-aluminum coating is broken into two different types: zinc-5% aluminum-mischmetal alloy (Type 1) and zinc-5% aluminum-0.1% magnesium alloy (Type 2). Furthermore, the coating is available in two classes: minimized coating structure (Class A) and regular coating structure (Class B) (ASTM International, 2013).

In order to use this hot-dipped galvanizing technique, there are specific base metal and coating metal qualifications that must be met. This is to ensure the base metal adequately bonds to the coating metal to effectively resist corrosion of the base metal. The appropriate chemical requirements for the base metal are determined by a heat analysis of the metal. Table 2.3-1 represents the maximum values (unless otherwise shown) for each chemical element found for different types of base metals.

There are many tests to determine the chemical composition of the coating bath. Examples of some of the tests that can be done for the zinc-aluminum coating bath are Test Method E47 and Test Method E1277 (ASTM International, 2013). If there is any dispute resulting from the use of different tests, Test Method E1277 shall be the basis for

acceptance (ASTM International, 2013). The chemical make-up of the galvanizing coating bath can be seen in Table 2.3-2.

Table 2.3-1

Chemical Requirements for Heat Analysis Element

Maximum Composition UNO (%)											
Designation	**C**	**Mn**	**P**	**S**	**Cu**	**Ni**	**Cr**	**Mo**	**V**	**Cb**	**Ti**
SS											
Grade 33	0.20	-	0.04	0.04	0.20	0.20	0.15	0.06	0.008	0.008	0.025
Grade 37	0.20	-	0.10	0.04	0.20	0.20	0.15	0.06	0.008	0.008	0.025
Grade 50[A]	0.25	-	0.20	0.04	0.20	0.20	0.15	0.06	0.008	0.008	0.025
Grade 80	0.20	-	0.04	0.04	0.20	0.20	0.15	0.06	0.008	0.008	0.025
HSLAS											
Grade 50	0.20	1.20	-	0.035	0.20	0.20	0.15	0.16	0.01[B]	0.005[B]	0.01[B]
Grade 60	0.20	1.35	-	0.035	0.20	0.20	0.15	0.16	0.01[B]	0.005[B]	0.01[B]
Grade 70	0.20	1.65	-	0.035	0.20	0.20	0.15	0.16	0.01[B]	0.005[B]	0.01[B]
Grade 80	0.20	1.65	-	0.035	0.20	0.20	0.15	0.16	0.01[B]	0.005[B]	0.01[B]
HSLAS-F											
Grade 50	0.15	1.20	-	0.035	0.20	0.20	0.15	0.16	0.01[B]	0.005[B]	0.01[B]
Grade 60	0.15	1.20	-	0.035	0.20	0.20	0.15	0.16	0.01[B]	0.005[B]	0.01[B]
Grade 70	0.15	1.65	-	0.035	0.20	0.20	0.15	0.16	0.01[B]	0.005[B]	0.01[B]
Grade 80	0.15	1.65	-	0.035	0.20	0.20	0.15	0.16	0.01[B]	0.005[B]	0.01[B]

Note. Adapted from ASTM International, 2013. For additional information and requirements for this table, refer to ASTM A875.
A: Class 1 and 2 are listed. Class 3 has a maximum value Phosphorus value of 0.04
B: These denote minimum values

Table 2.3-2

Chemical Requirements for Coating Bath Type 2

Element	Composition (wt%)
Aluminum	4.5 – 6.2
Magnesium	0.06 – 0.15
Others, total, max (except iron)	0.01
Zinc	Remainder

Note. Adapted from ASTM International, 2013. For additional information and requirements for this table, refer to ASTM A875.

During the production of cold-formed framing pieces, there are a series of bends that are applied to the metal to produce the specified member shape. These bends can initiate cracks in the galvanizing coat at the bending locations. The factors that affect this issue include the thickness of the metal, the strength level, the degree of restraint during the bending process, the rolling direction, the chemistry and the microstructure. The Coating Bend Test is used to assess whether the coating was appropriately applied to the base metal (ASTM International, 2013). The testing specimen must be able to bend 180° in any direction without causing the exterior coating to flake on the outside of the bend only.

2.4 Residual Stresses in Cold-Formed Steel Member by Weng and Pekoz

The residual stresses developed in metal must be understood in order to provide an accurate structural design. Residual stresses in structural steel are the results of its imperfect formation process. When cold-formed steel is being produced, its cold-bending effect is the main source of its residual stresses (Weng & Pekoz, 1990). Other fabrication operations that also cause residual stresses in cold-formed steel are cutting, punching, and

welding of the metal (Weng & Pekoz, 1990). Because not every manufacturer produces the metal in the same manner, a vast collection of cold-formed steel from different suppliers was tested in their project to observe the effects of their residual stresses when they were axially compressed.

The method used long ago to measure the residual stresses in cold-formed steel is the conventional saw-cutting method (Weng & Pekoz, 1990). In this method, the cold-formed specimen is clamped down using vice grips, then cut using either a slitting saw or band saw supplied with fluid coolant. The strains of the cold-formed are measured to obtain the amount of residual stress in the member. Unfortunately, there are some notable drawbacks with this method. The vibrations produced from cutting the specimen can cause inconsistencies in strain gage readings, especially when thin-walled sections are used (Weng & Pekoz, 1990). Additional strain gage disturbances have been observed when the cold-formed sections are over-clamped resulting in permanent deformations.

A newer method that resolves these problems is electrical discharge machining (EDM) (Weng & Pekoz, 1990). This method cuts the metal using rapidly recurring current discharges between two electrodes. This cutting process doesn't require physical contact between the metal and the EDM tool. Therefore, the metal does not need to be clamped down as hard and the vibration of the metal greatly decreases during the cutting process. An illustration of the EDM setup can be viewed in Figure 2.4-1.

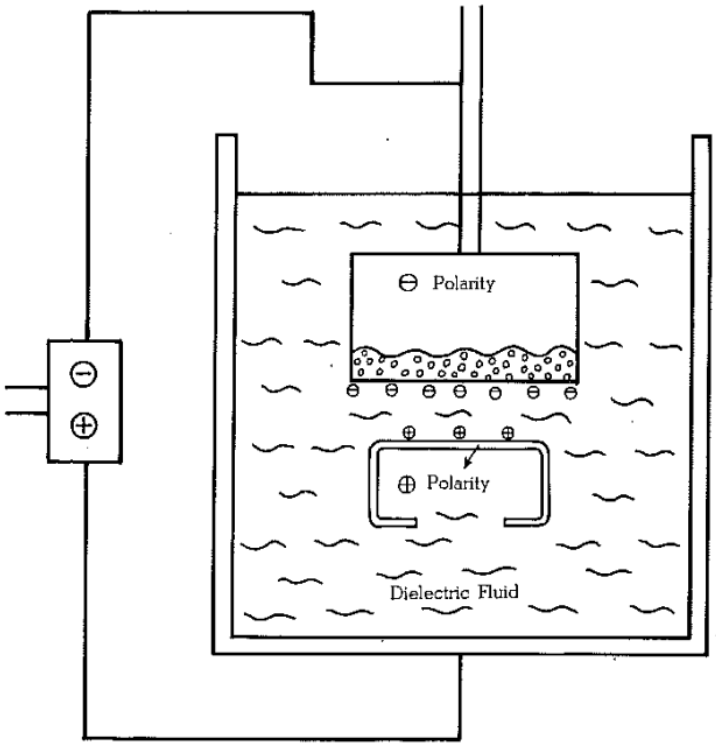

Figure 2.4-1. Measurement of residual stresses by EDM method. Adapted from "Residual Stresses in Cold-Formed Steel Members," by C. Weng and T. Pekoz, 1990, *Journal of Structural Engineering, 116*(6), p. 1614. https://doi.org/10.1061/(ASCE)0733-9445(1990)116:6(1611)

During an experiment reported by Weng and Pekoz (1990), six strain gages were placed along the web, flange, and return lip of a C-shaped cold-formed stud. These strain gages were only placed on half of the stud shape because symmetry can be applied to the other side. Each strain gage location measured both the inside and outside faces of the stud in the longitudinal direction. Locations of these strain gages along with sample residual strain results for a 16-gauge stud are shown in Figure 2.4-2.

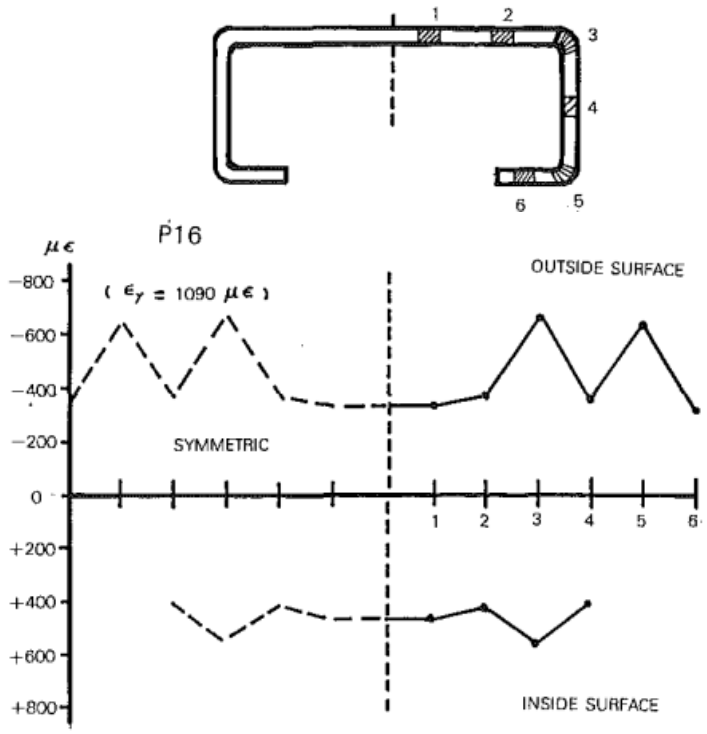

Figure 2.4-2. Measured residual strains of Section P16. Adapted from "Residual Stresses in Cold-Formed Steel Members," by C. Weng and T. Pekoz, 1990, *Journal of Structural Engineering, 116*(6), p. 1616. https://doi.org/10.1061/(ASCE)0733-9445(1990)116:6(1611)

Weng and Pekoz (1990) found that the compression residual stresses on the inside face of the studs were relatively the same magnitude as the tension residual stresses on the outside face of the stud. It was then concluded that a plastic section would develop along the inside face of the stud when axially compressed, because the residual compression stresses located there would add to the stresses caused by the external loading. Additionally, the residual stresses ranged from 25% to 70% of the yield stress, where the higher residual stresses were located at the corners or bends in the stud. This result was expected because most of the cold-working is done at the corners of the stud to create the bends. The yield stress was also larger at the stud corners because of strain hardening of the stud's metal during production. Because of this strain hardening, the residual stress is

assumed to be a conservative 50% of the yield strength throughout the entirety of the stud.

However, the residual stresses distributed through the thickness of the studs could not be measured, because the metal is too thin for the technology to measure the strain. Therefore, it is assumed that the stresses linearly distribute themselves through the stud thickness. All in all, further study into cold-formed residual stresses is recommended because the technology at the time of Weng and Pekoz's study limited the research needed to be done on the topic.

2.5 Connectors for Cold-Formed Steel Construction by SIMPSON Strong-Tie

Today's standards for connecting a light gauge knee-wall to the main structural system of a building is to feature the use of a light gauge steel clip angle (Simpson Strong-Tie Company, Inc., 2017, 1 June). This light gauge clip angle provides extra stiffness for the connection in order to reduce rotation of the knee-wall. Additionally, the extra screws needed to connect the angle clip to the cold-formed stud and track increase the shear and pull-out capacity of the connection (Simpson Strong-Tie Company, Inc., 2017, 1 June). SIMPSON Strong-Tie has designed their Rigid Connector for Knee-Wall (RCKW) clip angles specifically for these knee-wall applications (Simpson Strong-Tie Company, Inc., 2017, 1 June). They even offer an additional stiffener to the RCKW clip angle to further increase the capacity of the connection. Figure 2.5-1 shows the most commonly used RCKW clip as well as the RCKW clip that comes with the additional stiffener.

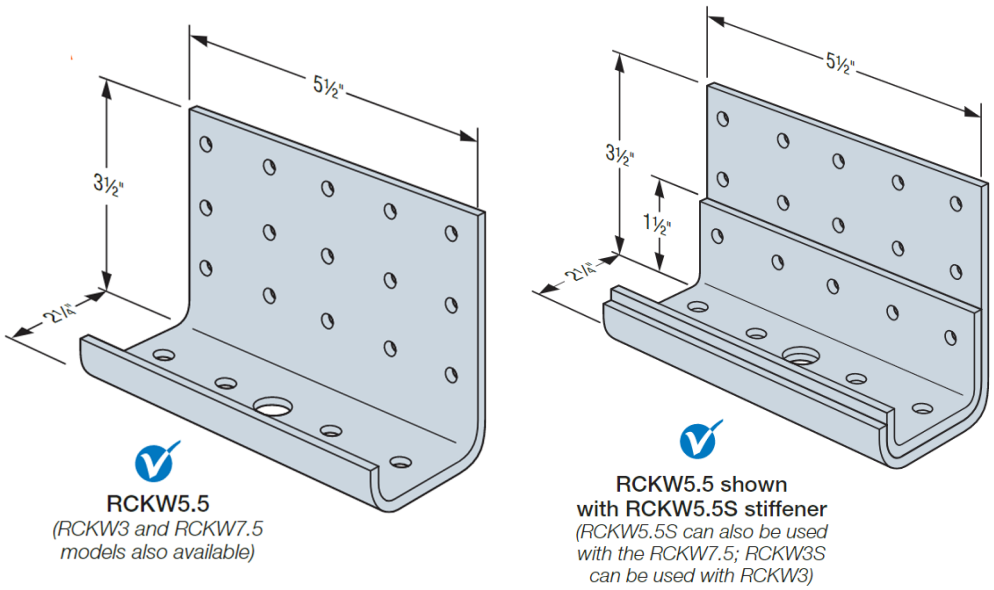

Figure 2.5-1. SIMPSON Strong-Tie RCKW Clip Angle. Adapted from *Connectors for Cold-Formed Steel Construction* [Catalog No. C-CF-2017], June 1, 2017, Pleasanton, CA.: Simpson Strong-Tie Company, Inc.

SIMPSON Strong-Tie references the 2015 IBC [which in turn relies on ASCE standard 7-10 and AISI standard S100-2012 (Simpson Strong-Tie Company, Inc., 2017, 1 June)] to calculate the moment developed at the connection location. Once the moment is determined, SIMPSON then provides tabulated moment capacities for their different RCKW clips. There are different tables depending on the base material and the location of the wall in relation to the base material (edge of slab, center of slab, etc). SIMPSON also provides additional tables that differentiate the capacities for seismic versus non-seismic situations. These capacity tables provide the required strength reductions for a concrete base material in its "cracked" condition.

Deflection of the knee-wall is also an important design consideration that SIMPSON Strong-Tie addresses. The building's façade has bending limitations to prevent cracking and warping. Therefore, even though a certain RCKW clip may work for the moment

design of the knee-wall, it may not abide by the deflection limitations of the façade. The IBC 2015 code permits the wind load to be taken as “0.42 times ‘component and cladding loads’ for deflections checks” (Simpson Strong-Tie Company, Inc., 2017, 1 June), because using the entire component and cladding wind load would produce an exceedingly conservative result.

Because the deflection curve was linear along the height of the experimental unclipped knee-wall, the experimental unclipped knee-wall and SIMPSON’s clipped knee-walls will be compared by easily converting each of their moment capacities into the loading conditions desired, allowable uniform lateral load and allowable wall pressure. Additionally, SIMPSON does not provide a table for a knee-wall base material of light gauge steel (metal deck) for their RCKW clips. Therefore, the only results that can be compared from this project are the tests that have the structural steel base material.

Chapter 3: Experimental Program

3.1 Introduction

The experimental testing for this project was conducted at the Milwaukee School of Engineering (MSOE) Construction Science and Engineering Center (CSEC). The goal of this experimental program was to determine the bending capacity of various gauges of cold-formed steel knee-walls connecting to two different base materials. The cold-formed knee-walls were subjected to a uniformly distributed load applied laterally along the top of the wall. This lateral load is reacted by moment, shear, and axial forces at the connection point at the bottom of the wall. The capacities of the knee-wall connection resulting from this experiment will be compared to the SIMPSON Strong-Tie tabulated capacities of knee-wall connections when a light-gauge clip angle is added to stiffen the attachment.

3.2 Test Specimen Overview

This experimental program consisted of a total of 18 tests. These 18 tests were divided evenly to test three different cold-formed gauges: 18-, 16-, and 14-gauge. Each of these three gauges were observed under two different base materials connection conditions: connection onto light gauge steel deck and connection to structural steel channel. Three trials of each different test were conducted. There was a specific naming convention used in order to differentiate tests. A sample illustration of this naming convention can be seen in Figure 3.2-1. Since the cold-formed knee-walls were attached to two different base materials, two different connection details were used. Figures 3.2-2 through 3.2-4 represent the base connection details used at each stud of the knee-wall.

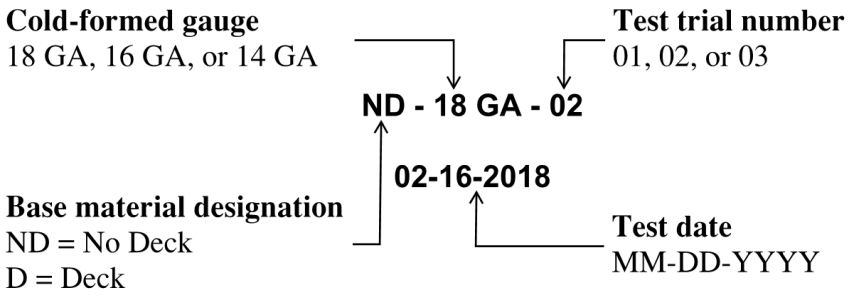

Figure 3.2-1. Experimental program naming convention.

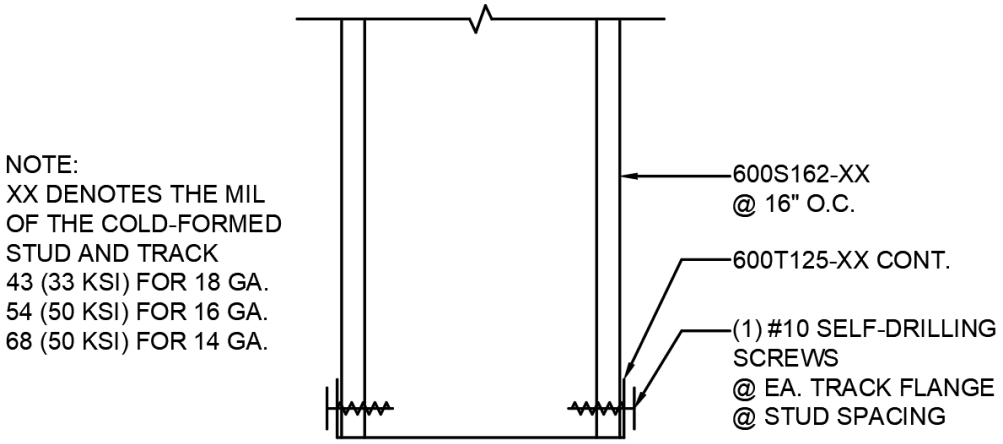

Figure 3.2-2. Stud to track connection detail.

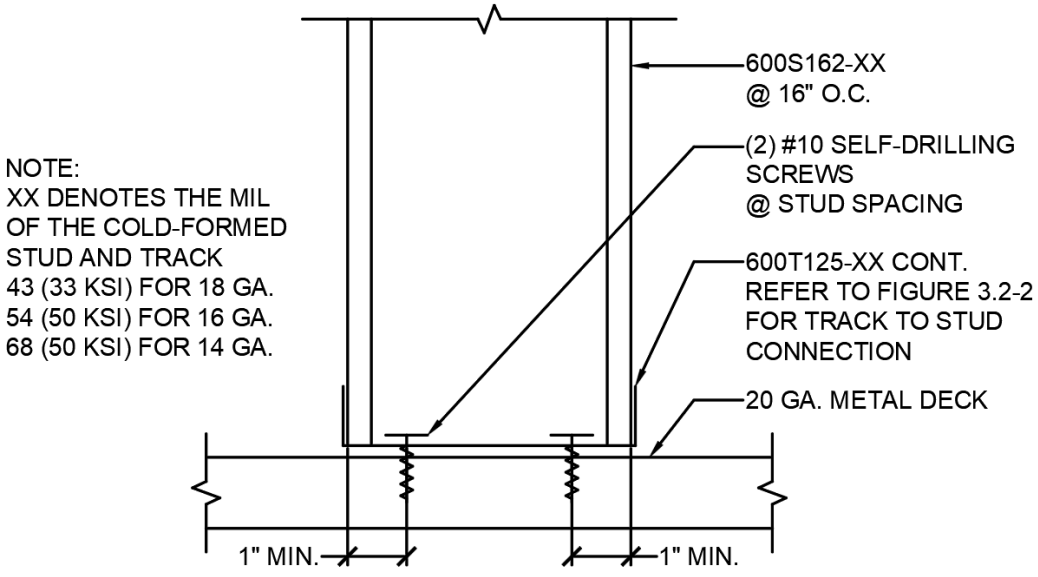

Figure 3.2-3. Base connection detail to metal deck.

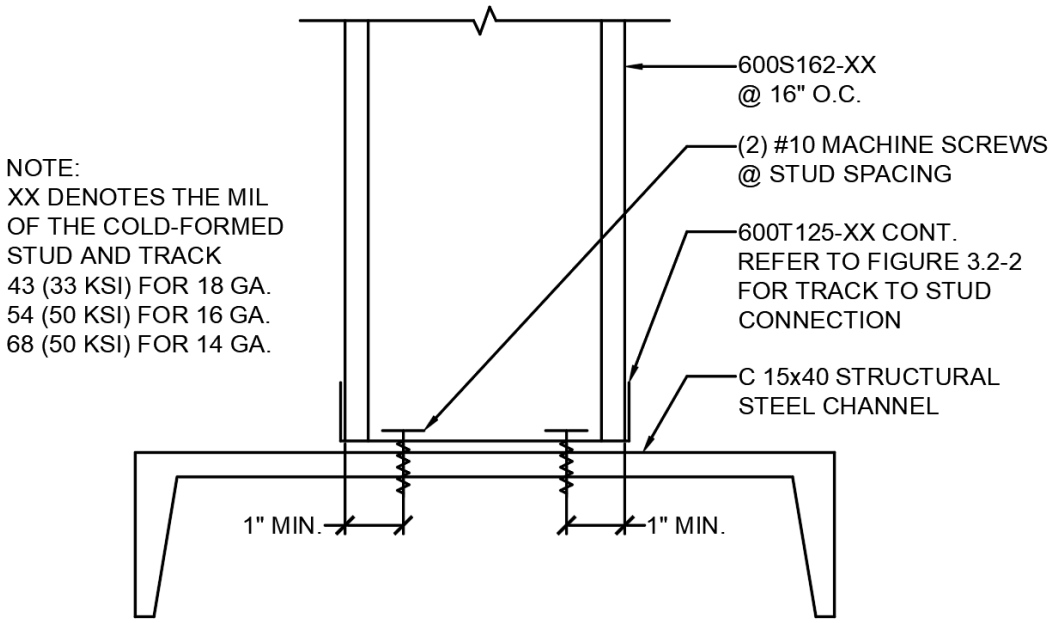

Figure 3.2-4. Base connection detail to structural steel.

The details illustrated in Figures 3.2-2 through 3.2-4 are similar to commonly used connections in order to best mimic what is seen in the field. The screws used to attach the cold-formed wall together as well as connect the knee-wall to the metal deck base material were #10 self-drilling screws. Typically, power-driven fasteners (PDF's) are used when connecting cold-formed steel framing to structural steel. However, if PDF's were used for this experimental project, the structural steel channel would not be reusable for more than one trial. In order to reuse the same structural steel channel for all 18 tests, #10 machine screws were used to attach the cold-formed knee-wall to the structural steel channel.

3.3 Screw Capacity Overview

Two different brands of machine screws were used due to the fact that materials were purchased as needed throughout the project. It was realized that the capacities of these

two different machine screw brands were not the same. This was initially realized because a different type of connection limit state controlled during the tests that used the name brand machine screw than the generic brand machine screws.

In order to fully investigate the capacity of these connections, screw capacity tests were conducted. These tests were designed to find the pull-out or rupture capacity for both the self-drilling screw and machine screw as well as the shear tear out capacity of only the self-drilling screw. Pictures of each screw capacity test setup can be seen in Figures 3.3-1 through 3.3-2.

Figure 3.3-1. Screw pullout/rupture capacity setup.

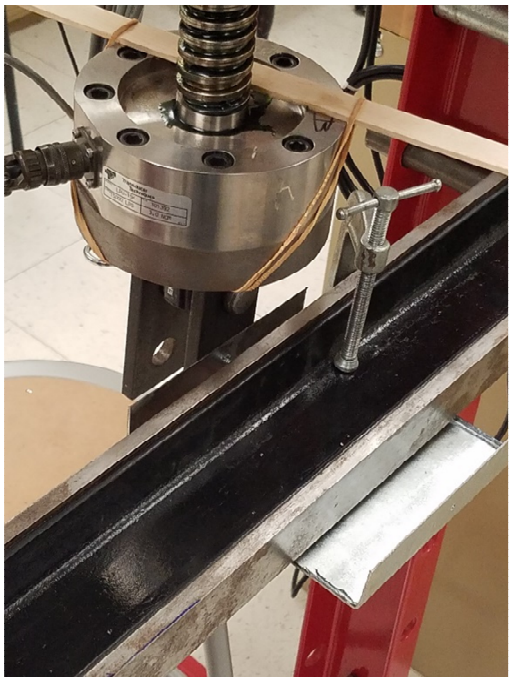

Figure 3.3-2. Screw shear capacity setup.

3.4 Test Assembly Overview

The test assembly was designed to best replicate how a cold-formed knee-wall would react in a realistic structural application. Common exterior cold-formed steel gauges were used in this experiment as well as typical connection patterns for the attachment of the studs to the track and attachment of the track to the two base materials tested. Figures 3.4-1 through 3.4-7 show how the cold-formed knee-wall was placed in the MSOE testing frame, how the lateral load was applied to the knee-wall as well as a visualization of the connection pattern used at the base of the knee-wall to resist the applied lateral load.

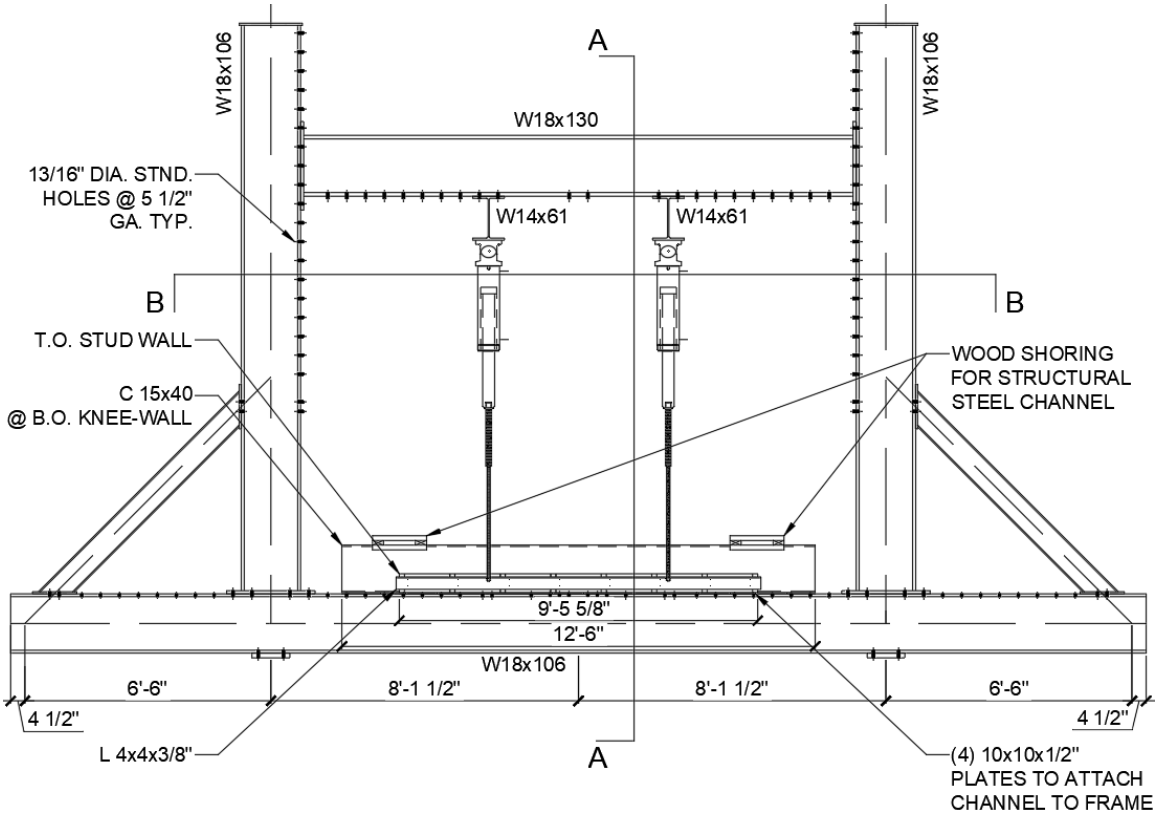

Figure 3.4-1. Front elevation of test setup.

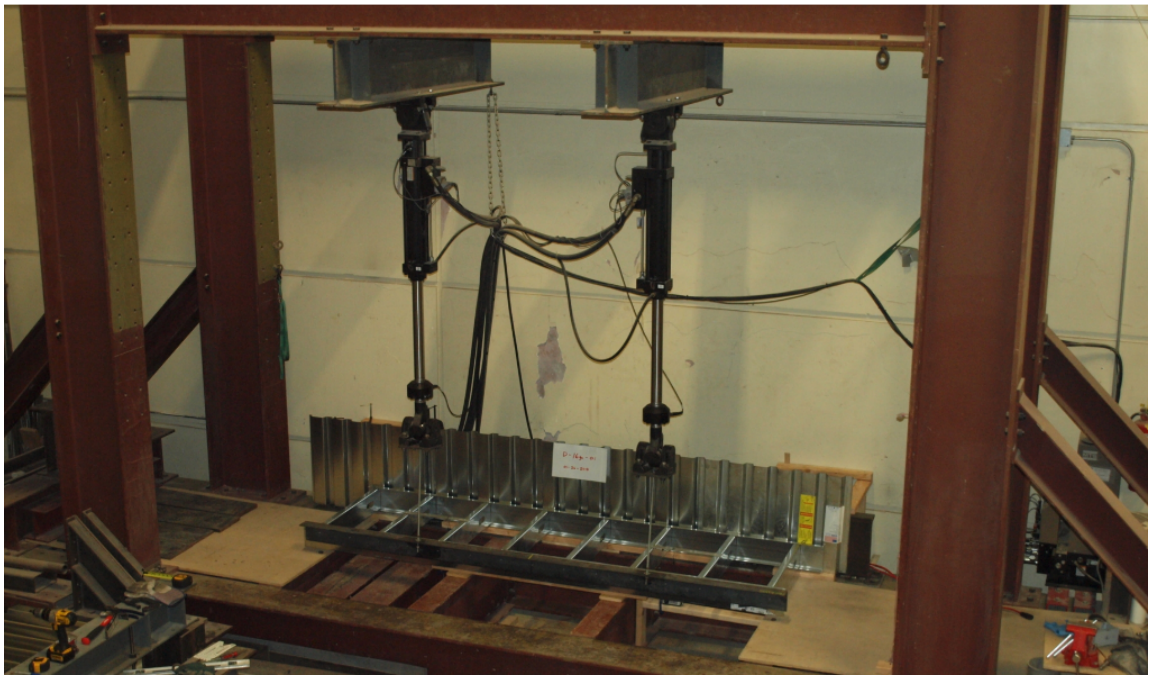

Figure 3.4-2. Test setup.

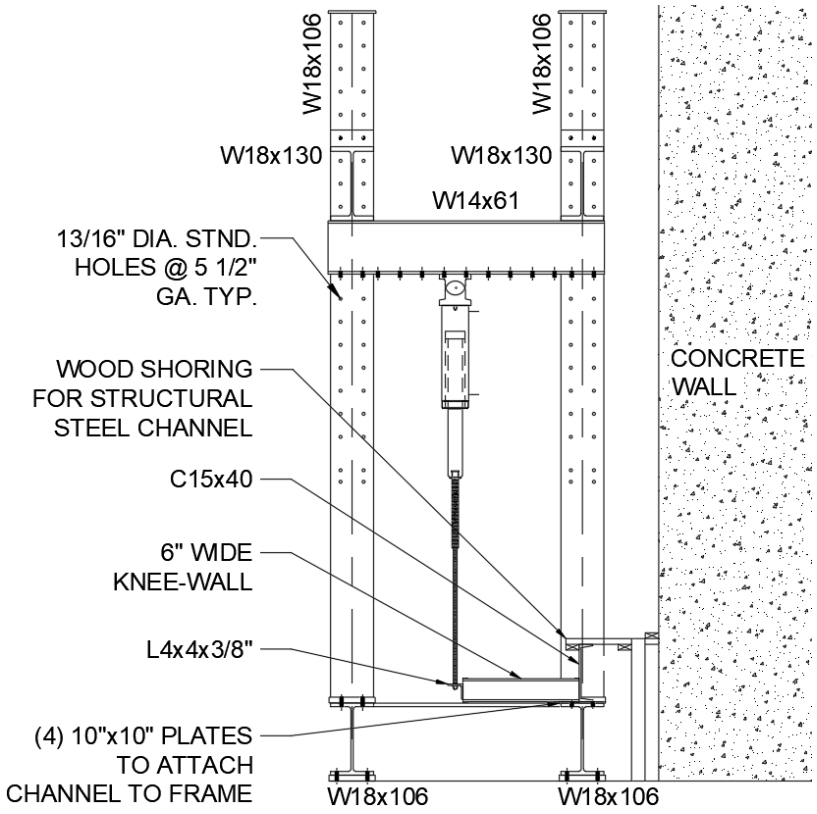

Figure 3.4-3. Side elevation of test setup (Section A-A).

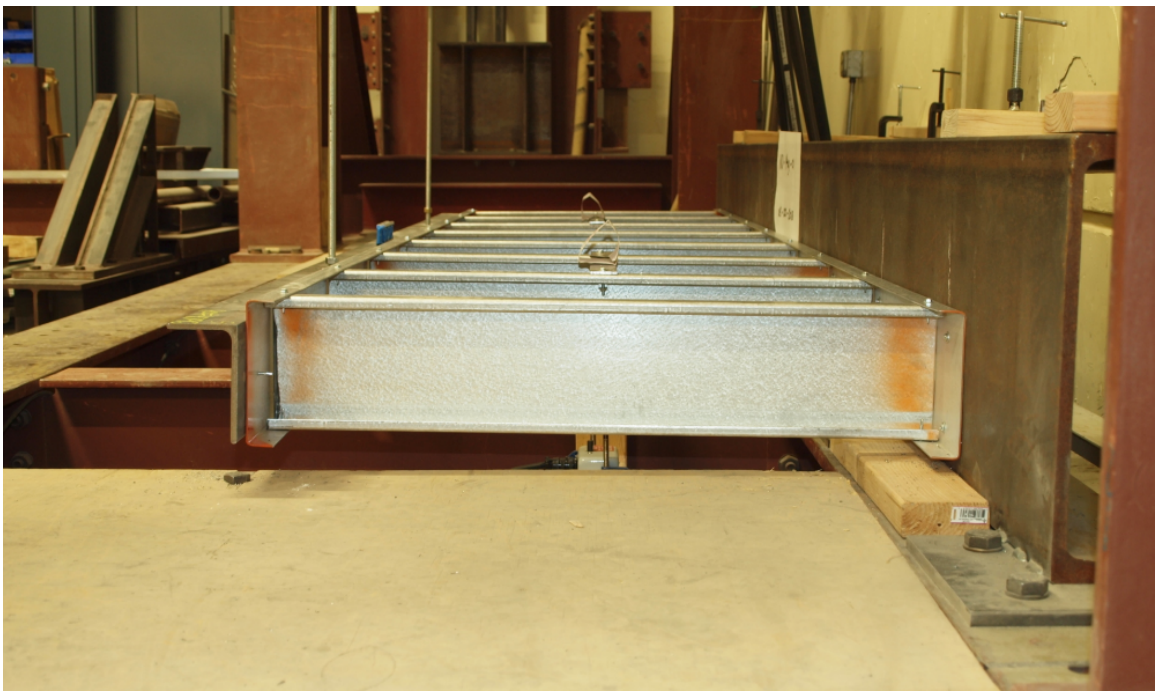

Figure 3.4-4. Test setup from side of frame.

The test assembly's applied load originated from two MTS 243.25 actuators powered by a 505.20 hydraulic pressure unit and a 293.11A-02 service manifold. Each MTS actuator has the ability to apply 22.2 kips of tensile force in a stroke of 20 inches. Knowing that the cold-formed knee-wall would not reach anywhere near these maximum force and displacement values before failing justified the use of the MTS actuators for this experiment. In addition to the force and displacement instrumentation provided by the actuators, two draw wire transducers (DWT's) were used to measure displacement at mid-height of each knee-wall test conducted. The DWT measurements were taken to validate that bending of the knee-wall out-of-plane was insignificant, and large deformation bending effects could be neglected.

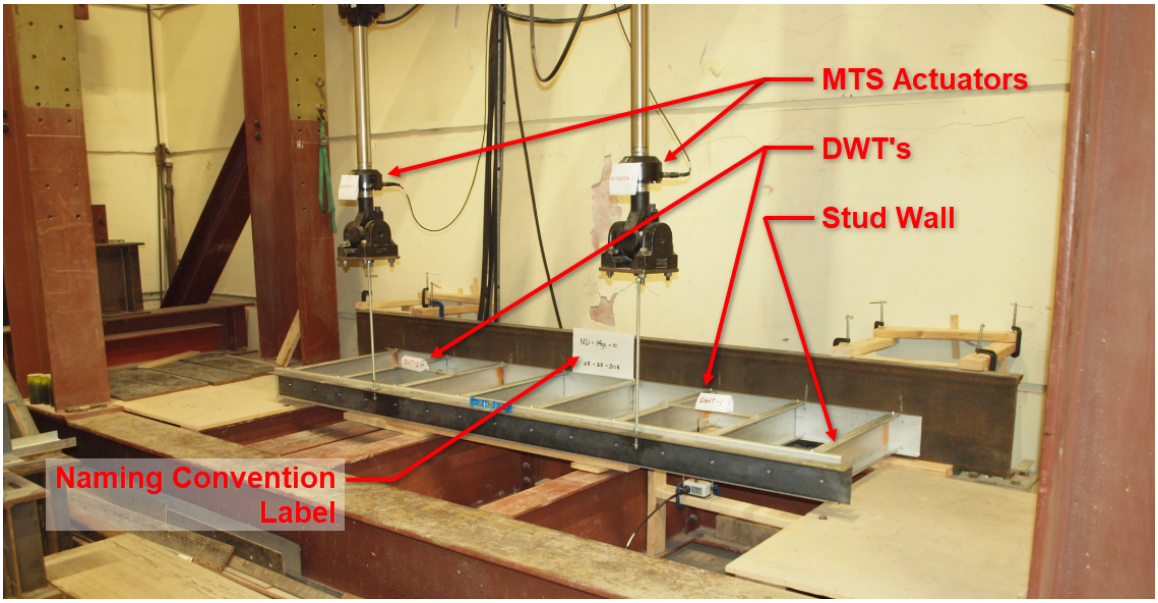

Figure 3.4-5. Test setup.

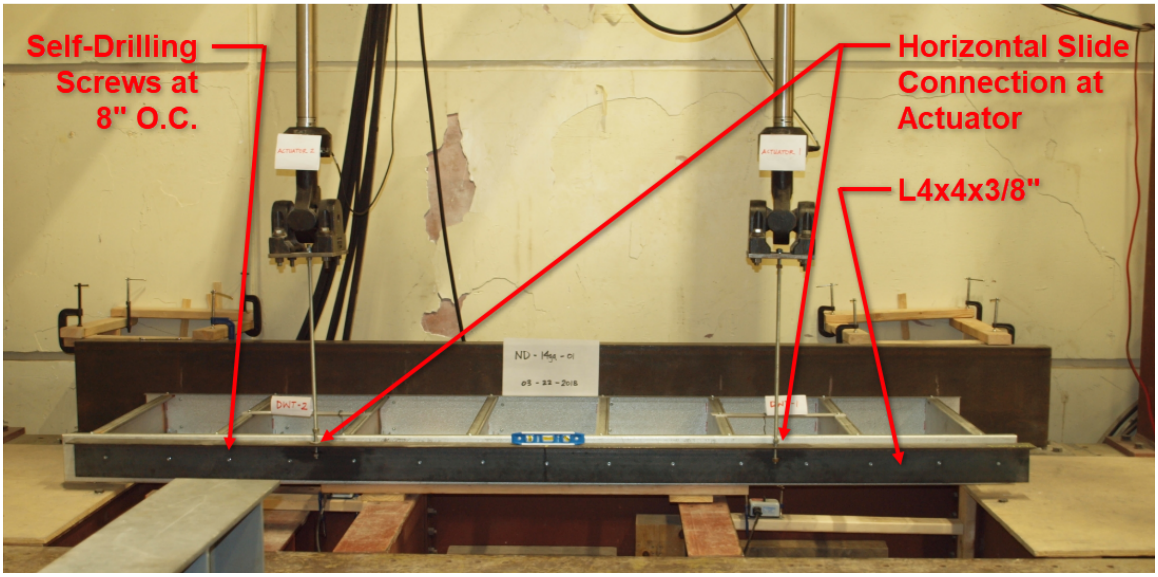

Figure 3.4-6. Knee-wall connection to actuator.

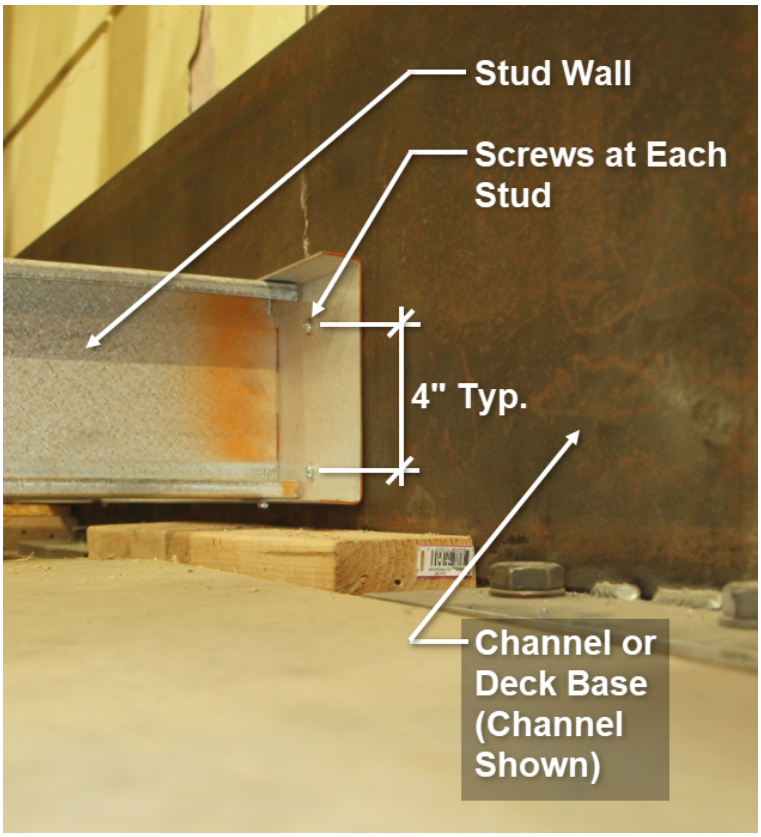

Figure 3.4-7. Knee-wall connection at base.

Figure 3.4-6 shows how the lateral load was applied to the top of the knee-wall. Although there were two connection points where the actuators attached to the steel angle, since the steel angle was much stiffer than the track and the steel angle was continuously attached to the top track of the knee-wall, the loading was considered to be uniform. The L4×4×⅜ in. angle consisted of a horizontal-slotted hole at each actuator-to-angle connection in order to keep the applied lateral force vertical. Otherwise as the knee-wall would "sweep back" as it deflected upward, the applied lateral load would stay perpendicular to the deflecting knee-wall and add undesired stresses to the system.

3.5 Test Procedure

3.5.1 Initial Test Frame Setup

The steel channel was prepared for experiment prior to installation to the frame. ½ in. diameter holes were drilled at 6 in. center-on-center and 16 in. center-to-center for the future attachment of the metal deck and cold-formed knee-wall to the steel channel, respectively. The spacing of each of these drilled holes were chosen to match the flute spacing of the metal deck and to match the stud spacing of the cold-formed knee-wall. The C15x40 steel channel was attached to the test frame with four PL½in. x10in. x10in. steel base plates bolted into the test frame's rear-floor-beam. The channel was welded to each of these plates after they had been bolted to the test frame. Figure 3.5.1-1 shows the connection of the channel to the base plate.

Figure 3.5.1-1. Welded connection of steel channel to base plate.

Lateral bracing was built and placed at both ends of the structural steel channel in order to provide the channel with additional lateral stiffness during the knee-wall experimental testing. This bracing, built out of dimensional lumber and attached to the concrete wall behind the test frame, was constructed so if the top of the channel were to rotate from the knee-wall loading, the bracing would resist the channel's rotation.

3.5.2 Pre-Test Procedure

Consistency of the pre-test procedure and inspection of the completed pre-testing setup was important in order to produce accurate and reliable results. The first step taken was determining which base condition was going to be tested: C15x40 steel channel or 20-gauge metal deck. When the metal deck is used, the deck was attached to the steel channel using #10 machine screws that were inserted into the pre-drilled holes spaced at 6 in. center-to-center. For the tests that required the steel channel base condition, no additional steps needed to be taken prior to wall placement.

Next, the pre-constructed cold-formed knee-wall was placed inside the testing frame. The wall was then attached to the base condition specified above: using #10 self-drilling screws for the metal deck base condition or #10 machine screws for the structural steel channel base. Once the knee-wall was attached to the base restraint, the top track was attached to the steel angle using #10 self-drilling screws at 8 in. center-to-center along the length of the wall. The two actuators were then connected to the steel angle by a ½ in. threaded steel rod through the two horizontal slotted-holes in the angle.

Two DWTs were placed at mid-height of the knee-wall between the actuator and the knee-wall's base. The final step was to take pictures of the pre-test condition and to take an initial horizontal measurement of the knee-wall's placement in the testing frame. This measurement, taken manually using a tape measure and a level, was the distance from the top track of the knee-wall to the inside edge of the test frame's front floor beam. A representation of this measurement can be seen in Figure 3.5.2-1. A final check of the installation of the test specimen was conducted prior to initiating a test. The final check ensured that no installation steps were over looked.

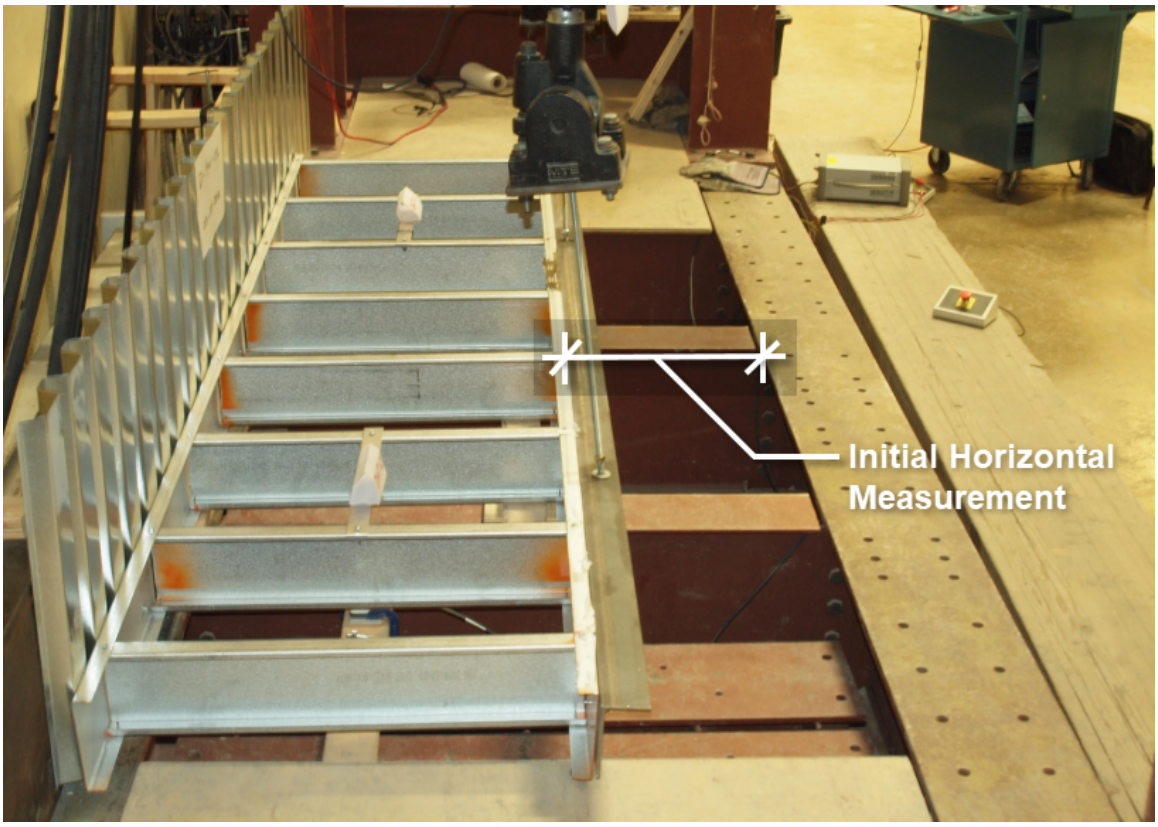

Figure 3.5.2-1. Initial horizontal measurement of cold-formed knee-wall.

3.5.3 Testing Procedure

Testing could commence once the specimen was properly installed. A consistent load application protocol was followed for all tests. All instrumentation was checked to make sure initial readings matched expected magnitudes. Then, the filename of the data file was inputted and saved to the test. The MTS system was operated in "displacement mode", meaning the actuators displaced a specified distance over a specified span of time. Displacement mode is appropriate for monotonic tests such as these.

The first set of displacement parameters moved the actuators up ½ in. over a duration of 30 seconds. The purpose of this small initial displacement was to move the actuators out of their full-stroke position. Occasionally the actuators show a slight pulse when

retracting from full-stroke, and this step allowed any data irregularities to be contained. The bolts connecting the threaded rods to the steel angle were not yet engaged in this stage of the testing procedure.

After the initial ½ in. displacement was completed, the bolts connecting the steel angle to the actuators were tightened so each actuator read approximately 25 to 30 lbs. This load engaged the system prior to initiating the main test protocol. The displacement parameters were changed to move the actuators up 10 in. over a duration of 300 seconds (5 minutes). This was the main test protocol, and data collected within this range were used to analyzed how the wall reacted under the lateral load produced by the vertical displacement of the actuators.

3.5.4 Post-Test Procedure

Once the full displacement of 10 in. was achieved, post-test pictures were taken of the knee-wall. Additionally, a horizontal measurement was taken for comparison to the initial horizontal measurement taken as part of the pre-test procedure. The final step was to remove the knee-wall from the testing frame. This included unscrewing the self-drilling screws from the top track and steel angle as well as unscrewing the bottom track from the specified base condition. Additional photos of the knee-wall's condition were taken. The post-test condition of this experiment can be seen in Figure 3.5.4-1

The testing data were plotted immediately after each test. This was done to confirm data accuracy and quality in order to make corrections or adjustments to the testing protocol if necessary. It should be noted that all tests resulted in quality data and only minor adjustments were made between tests. As such, all tests may be considered comparable.

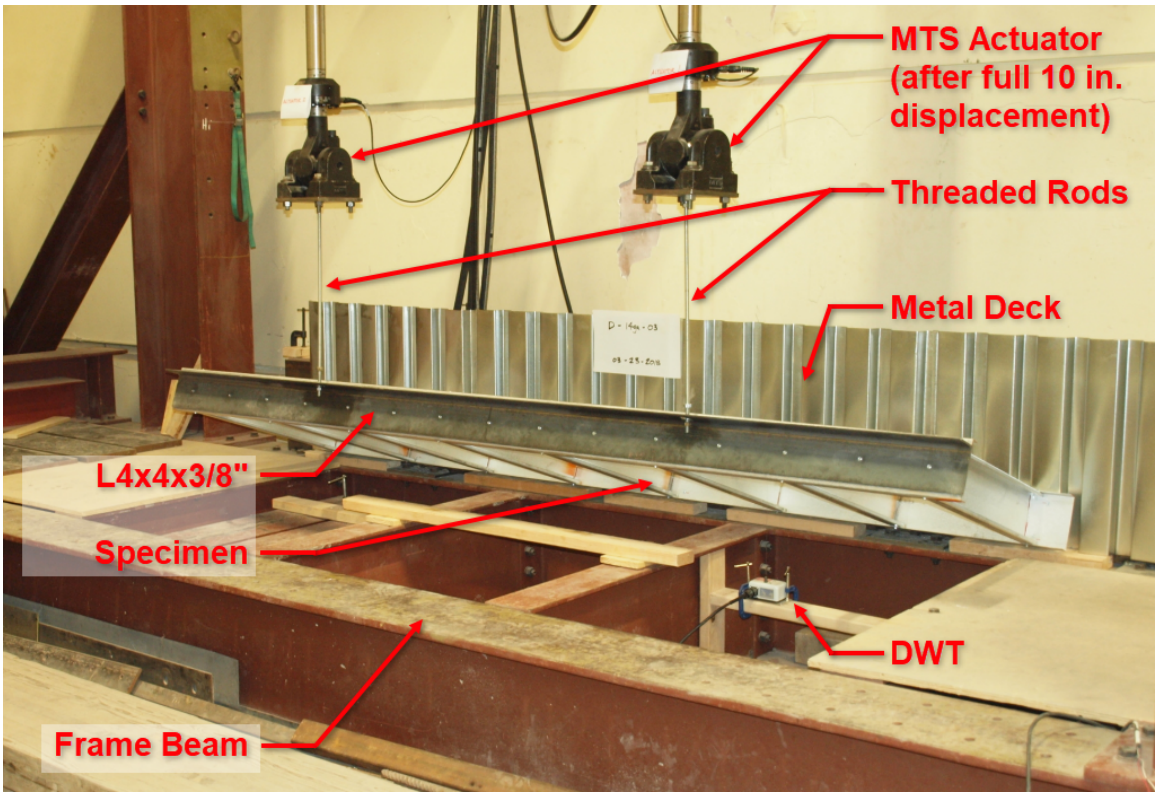

Figure 3.5.4-1. Typical test specimen after testing.

Chapter 4: Experimental Results

4.1 Introduction

A total of 18 unique tests were completed as part of the experimental program. Three different gauges of cold-formed were examined under two different base conditions. In order to ensure the experimental program has reliability and consistency, three trials were performed for each testing condition. The data collected from each test were confirmed through basic structural analysis.

4.2 Determination of Screw Forces at the Base Attachment

The moment capacity at the base connection is dependent on the pullout strength or rupture strength of the self-drilling screws or generic machine screws attaching the base track to the base material, respectively. Since the type of screw used in this experiment determines whether the pullout or rupture limit state controlled, both of these limit states will simply be referred to as *pullout* in the following discussion of the screw force calculation. Data collected from the two MTS actuators and DWT's were used to calculate screw forces. The load cell in the MTS actuators recorded the forces generated at each of their locations as they displaced the cold-formed knee-wall. The DWT's were located at mid-height of the wall in line with the actuators. Figure 4.2-1 shows force versus displacement of the knee-wall at the DWT locations and the actuator locations. Since the DWTs consistently read half of the displacement magnitude of the actuators for every test, it was concluded the cold-formed knee-wall deformed linearly. This conclusion allowed for simplified trigonometry to be used to calculate the forces at the base connection.

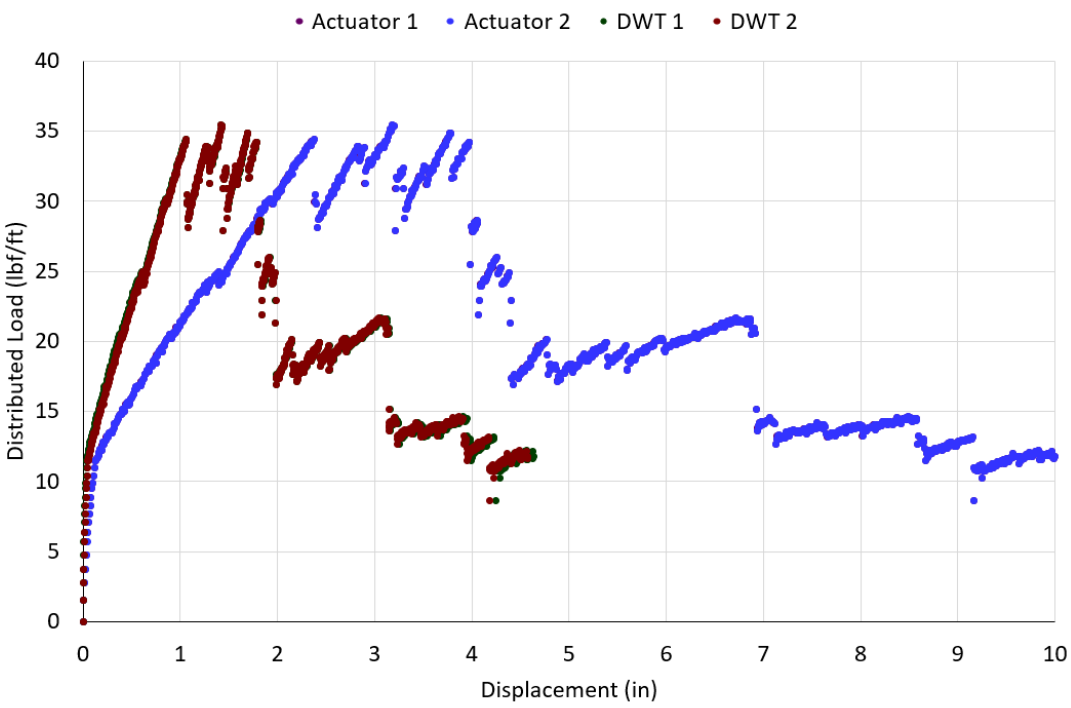

Figure 4.2-1. Distributed load versus displacement graph (D-18-01 shown).

The displacements reported by the MTS actuators were manually "zeroed" at the initial reading of the test, then the change in displacement was calculated on from the initial reading for the duration of the knee-wall test. The knee-wall's angular displacement or rotation, θ, was then calculated using the vertical wall displacement, D, and wall height, H:

$$\theta = \sin\left(\frac{D}{H}\right).$$

The two concentrated loads applied a uniformly distributed load on the top track by means of a stiff angle connected to the top track at regular intervals. The uniform load, w, is calculated using the total combined force read by the actuators, P_{total}, and the knee-wall length, L:

$$w = \frac{P_{total}}{L} .$$

By multiplying the uniformly distributed load by the cold-formed stud spacing of 16 in. center-on-center, one can calculate the tributary load of each stud, P_{stud}. Thus, the moment at the base connection, M, can be calculated:

$$M = P_{stud} H \cos(\theta) .$$

Figure 4.2-2 illustrates the moment, shear and axial forces acting on the cold-formed knee-wall due to the lateral loading along the top track of the cold-formed knee-wall. Figure 4.2-3 show the base connection's tension and compression forces due to the wall loading. This diagram of connection forces was simplified by assuming the resultant of the compression force was located at the location of the top screw in the base connection. The *pullout* force of the bottom screw, T, was then calculated using the distance between the top and bottom screw, $d_{pullout}$:

$$T = \frac{P_{stud} \sin(\theta)}{2} + \frac{M}{d_{pullout}} .$$

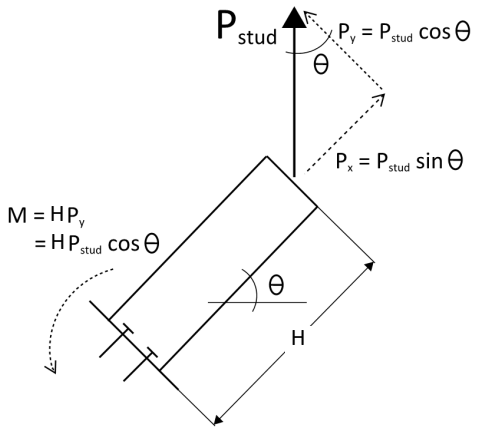

Figure 4.2-2. Knee-wall forces.

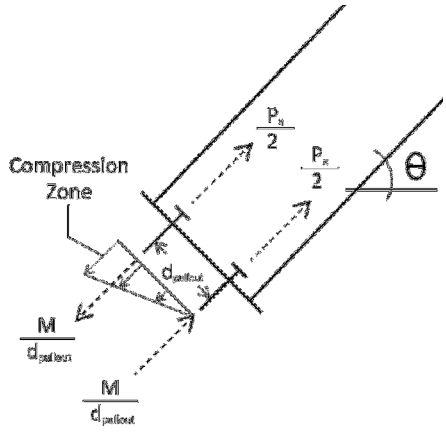

Figure 4.2-3. Pullout connection forces.

The calculation of the screw forces determines the capacity of the knee-wall since screw *pullout* was the controlling limit state for the majority of the tests. When *pullout* did not control the connection capacity, the stud-to-track screw tear out controlled. Figure 4.2-4 shows the shearing forces at the stud-to-track self-drilling screws developed by the lateral loading. The magnitude of this shearing force was calculated using the distance between the stud-to-track screws located on each side of the stud, d_{shear}:

$$T = \frac{P_{stud}\sin(\theta)}{2} + \frac{M}{d_{shear}}.$$

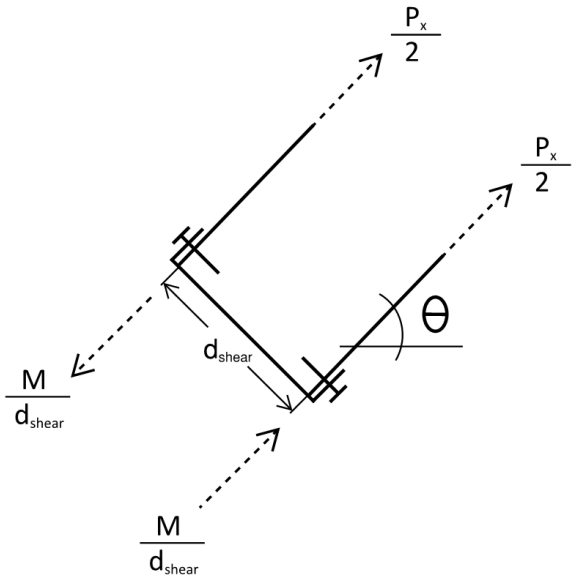

Figure 4.2-4. Shear connection forces.

A sample calculation of all screw forces can be found in Appendix A of this document.

4.3 Experimental Results

The following sections of the experimental results are organized by each testing trial conducted. Each section includes a description of the test along with before and after pictures of the cold-formed knee-wall base connection and tabulated values or graphical plots of the data accumulated throughout the duration of each experiment.

4.3.1 Screw Capacity Testing

Screw capacity tests were conducted because the different brands of screws used in this project caused different connection limit states to control. Each screw type was tested 5 to 6 times to ensure consistency in the data. Figures 4.3.1-1 through 4.3.1-3 are pictures of the before and after conditions of each of the three screw capacity tests. Table 4.3.1-1 contains a summary of the results for each screw capacity tests. For additional information pertaining to each individual screw capacity test, refer to Appendix D.

Table 4.3.1-1

Result Summary for Screw Capacity Testing

	Shear		Pullout/Rupture	
	# of Trials	Average Capacity (lbf)	# of Trials	Average Capacity (lbf)
#10 Generic Self-Drilling Screws	5	1084	6	296
#10 Generic Machine Screws	-	-	5	1403
#10 Hillman Machine Screws	-	-	5	1788

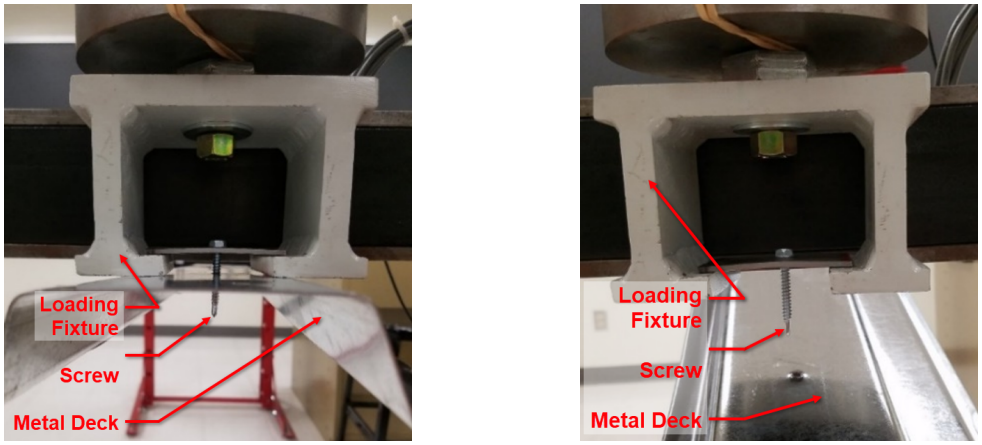

Figure 4.3.1-1. Self-drilling pullout pre-test and post-test positions.

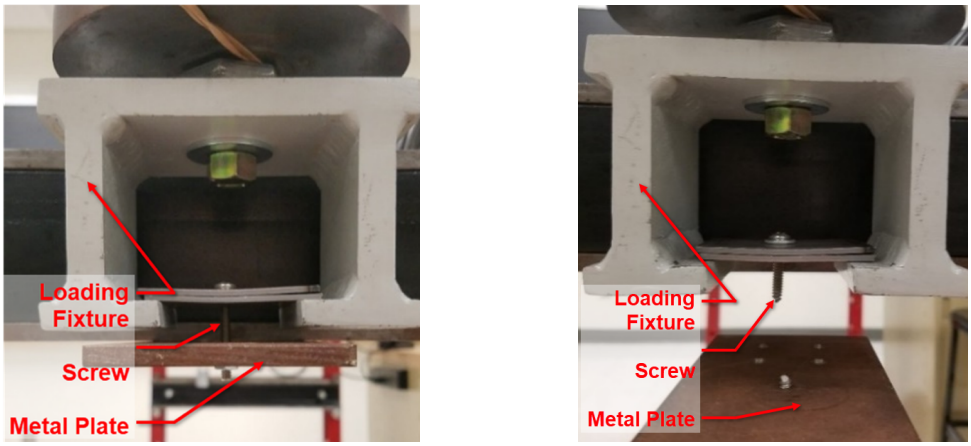

Figure 4.3.1-2. Machine rupture pre-test and post-test positions.

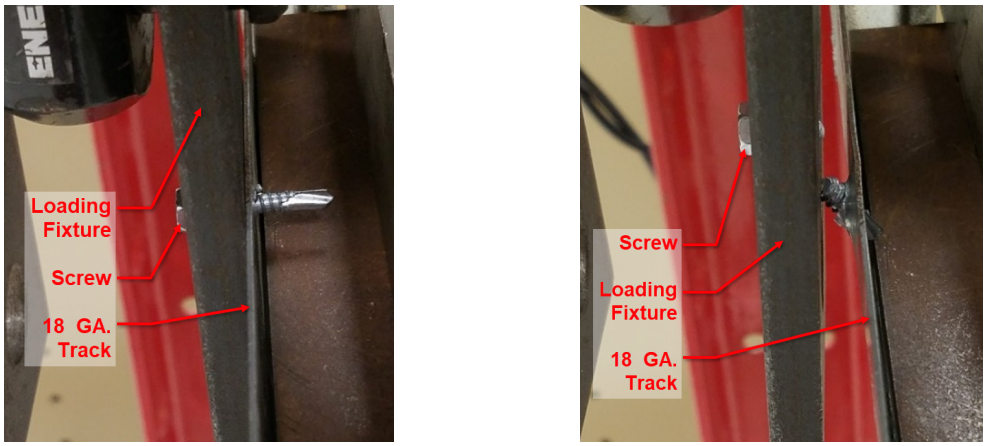

Figure 4.3.1-3. Self-drilling shear pre-test and post-test positions.

The results from the screw capacity tests confirmed why different limit state controlled during a few of the knee-wall tests. As seen from the results listed in Table 4.3.1-1, different brands of machine screws had different tensile rupture capacities. When the "generic" machine screws were used to attach the bottom track to the steel channel, machine screw tensile rupture was the governing limit state. Only when the Hillman machine screws were used did the limit state of the self-drilling screw tear out at the stud-to-track connection appear. These two different limit states can be observed in the cold-formed knee-wall result plots for the "no-deck" 18-gauge material.

4.3.2 18-Gauge on Metal Deck

Three trials were conducted for the 18-gauge cold-formed knee-wall for the metal deck base condition. These three trials were labeled D-18-01, D-18-02, and D-18-03. The base connection resisting the rotation of the cold-formed knee-wall consisted of two #10 self-drilling screws spaced 4 in. apart located at each stud. Figure 4.3.2-1 shows the moment versus rotation behavior of the 18-gauge cold-formed knee-wall connections. Figures 4.3.2-2 through 4.3.2-4 show the relationship of distributed loading to linear displacement of each individual 18-gauge test. On a few of the graphs, the data points of the two DWT's don't overlap each other exactly like the two actuator data points. This can be explained by slightly different distances from the actuator to the DWT's.

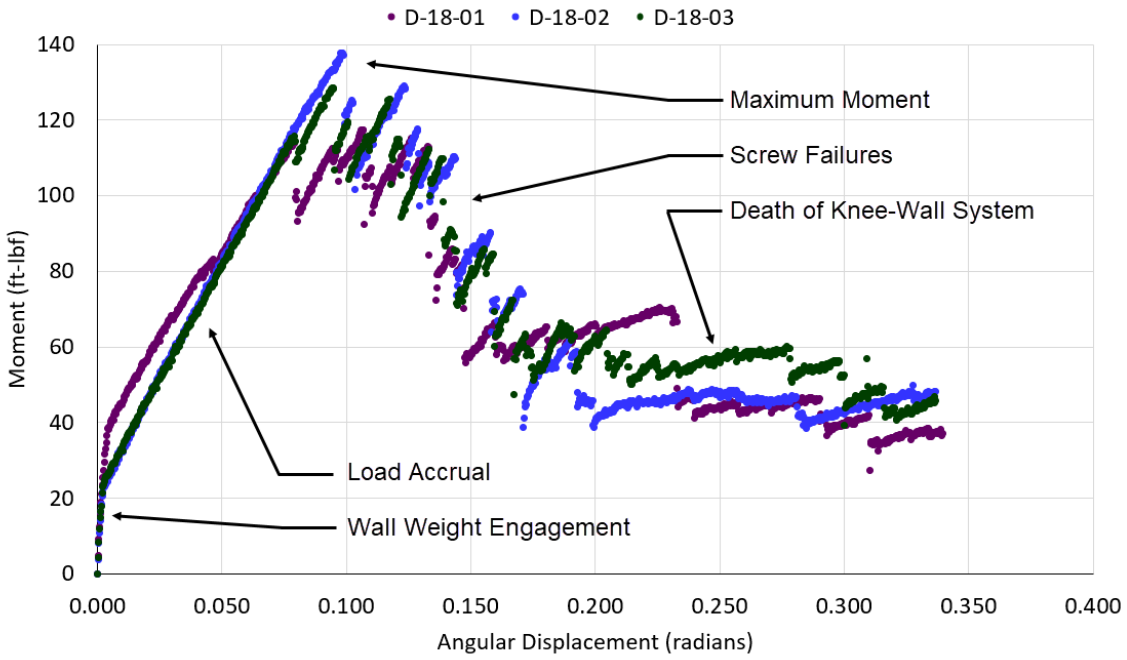

Figure 4.3.2-1. Moment versus rotation of 18-gauge on metal deck.

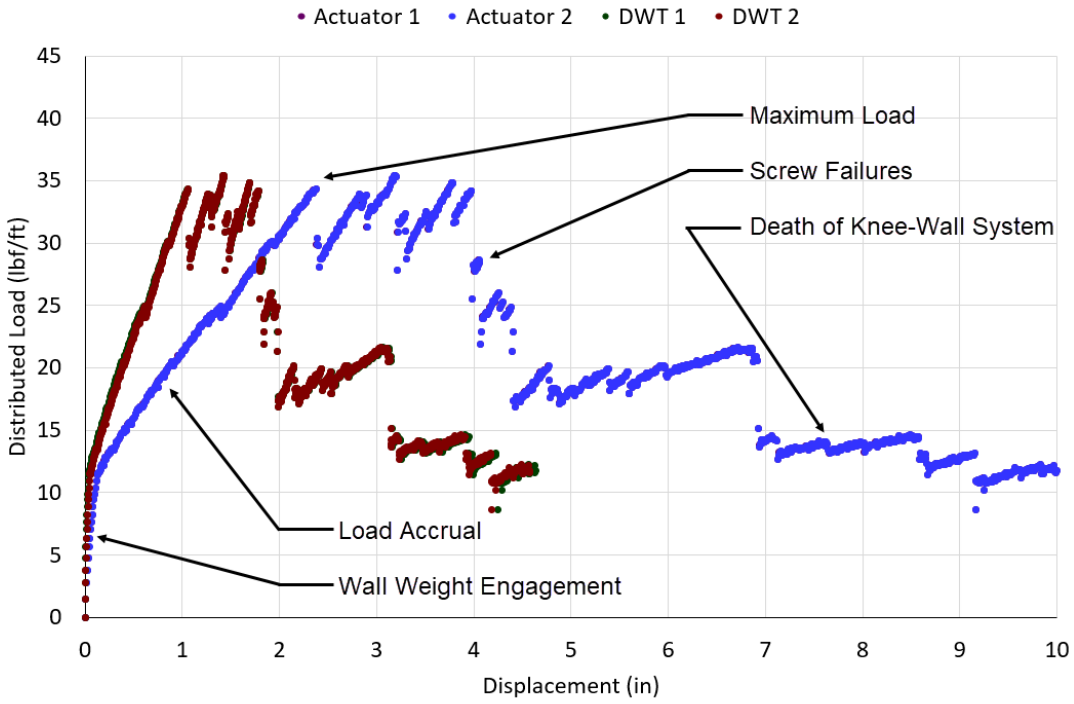

Figure 4.3.2-2. Distributed load versus displacement of test D-18-01.

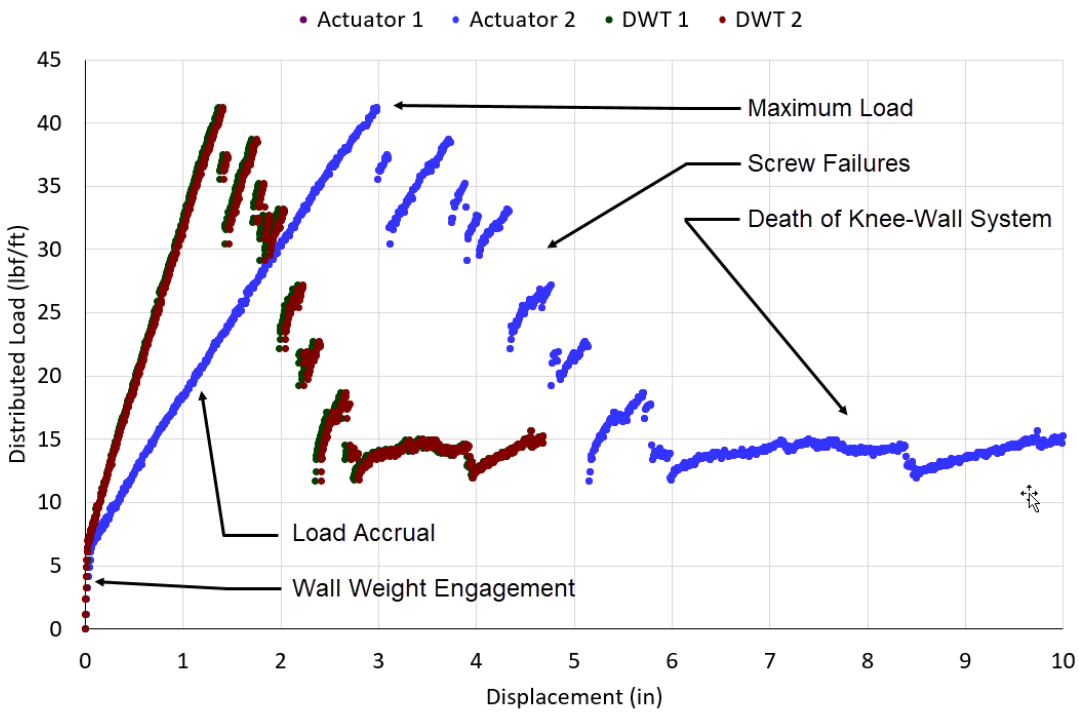

Figure 4.3.2-3. Distributed load versus displacement of test D-18-02.

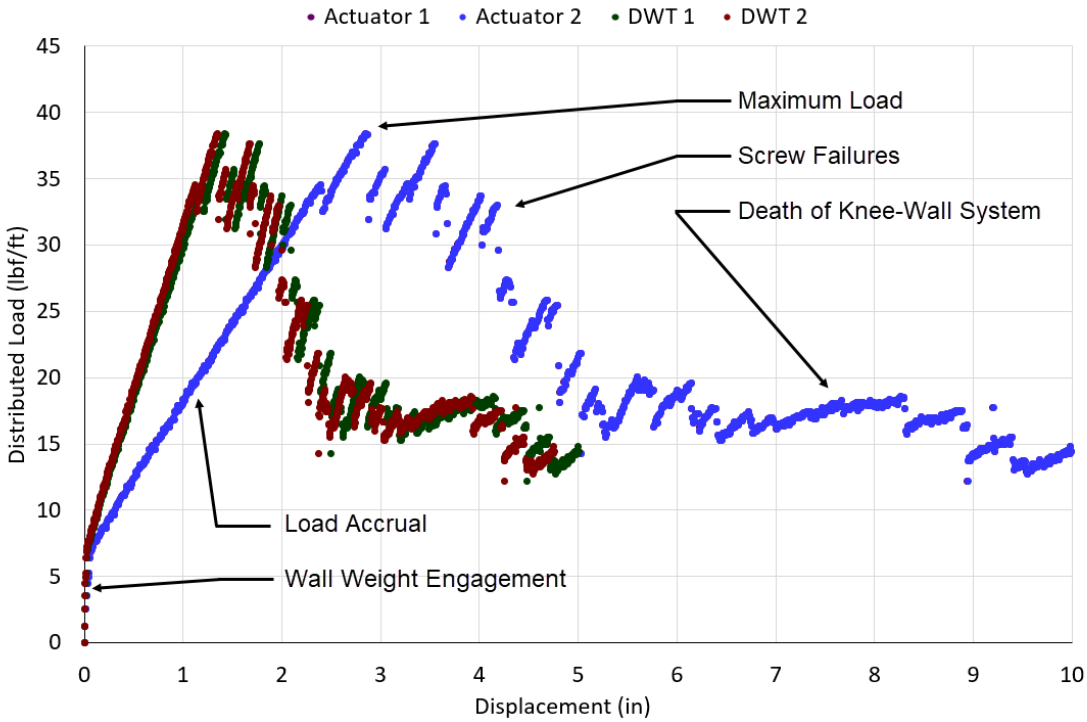

Figure 4.3.2-4. Distributed load versus displacement of test D-18-03.

Each graphical representation of the 18-gauge metal deck tests contains a wall weight engagement segment at the start of test. During this wall weight engagement, the MTS actuator system is gathering the weight of the cold-formed knee-wall, the structural steel angle, and all other connecting pieces of the actuator itself without any significant amount of displacement occurring. This signifies the part of the test where the connection elements, the self-drilling screws, are beginning to engage and transfer the load gathered into the metal deck base material.

Once the wall weight is fully engaged, the knee-wall starts to deform elastically until it reaches a maximum load where the first self-drilling screw at the base connection fails by its pullout limit state. Some of the tests conducted don't consist of a perfectly linear load accrual process. These small jumps throughout the load accrual process represent the slippage of the self-drilling screws. The self-drilling screws haven't completely pulled out of the metal deck yet, but some of their threads slipped through the metal deck, which is why these small jumps in the graph look similar to the complete failure of the screw. After this first self-drilling screw pulls out, the load on the knee-wall redistributes itself throughout the wall until the next self-drilling screw fails by its pullout limit state. This process repeats itself until all the bottom rows of self-drilling screws fail, where the cold-formed knee-wall system enters its final stage, its death. The graphical jumps in this process of the test are caused by the top row of self-drilling screws trying to resist the knee-wall deformation since they are now the only base connection elements that haven't failed. The knee-wall continues these small jumps until the testing ends at 10 in. of deformation.

Figures 4.3.2-5 through 4.3.2-10 are pictures of each 18-gauge metal deck trial before

and after the loading was applied to the cold-formed knee-wall. Each of these trials show how the cold-formed track deformed along the region of compression after the bottom row of self-drilling screws pulled out of the metal deck.

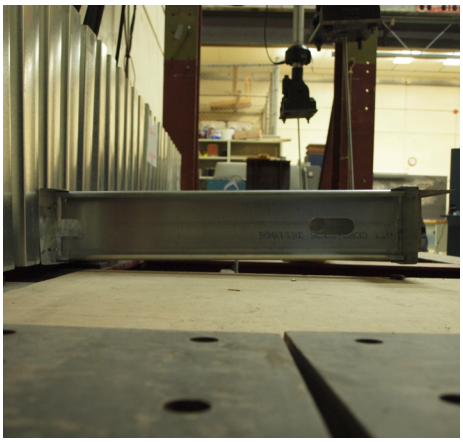

Figure 4.3.2-5. D-18-01 before test.

Figure 4.3.2-6. D-18-01 after test.

Figure 4.3.2-7. D-18-02 before test.

Figure 4.3.2-8. D-18-02 after test.

Figure 4.3.2-9. D-18-03 before test.

Figure 4.3.2-10. D-18-03 after test.

4.3.3 18-Gauge on Structural Steel Channel

Three trials were conducted for the 18-gauge cold-formed knee-wall for the structural steel channel base condition. These three trials were labeled ND-18-01, ND-18-02, and ND-18-03. The base connection resisting the rotation of the cold-formed knee-wall consisted of two #10 machine screws spaced 4 in. apart located at each stud. Figure 4.3.3-1 show the moment versus rotation behavior of the 18-gauge cold-formed knee-wall connections. Figures 4.3.3-2 through 4.3.2-4 show the relationship of distributed loading to linear displacement of each individual 18-gauge test. On a few of the graphs, the data points of the two DWT's don't overlap each other exactly like the two actuator data points. Once again, this can be explained by the slightly different distances from the actuator to the DWT's.

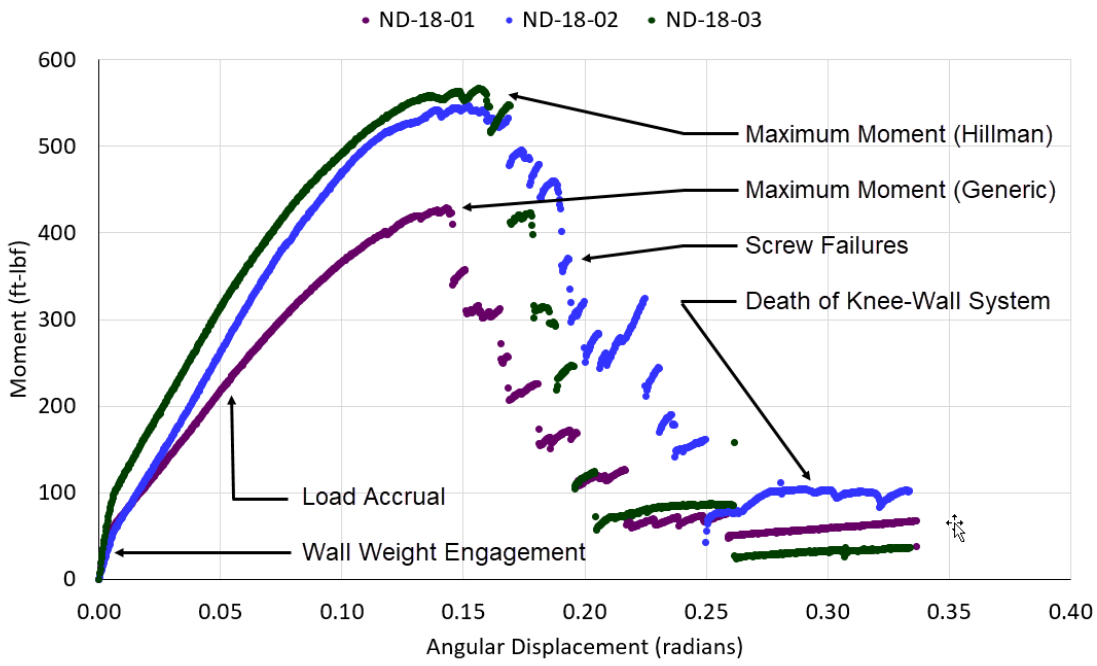

Figure 4.3.3-1. Moment versus rotation of 18-gauge on steel channel.

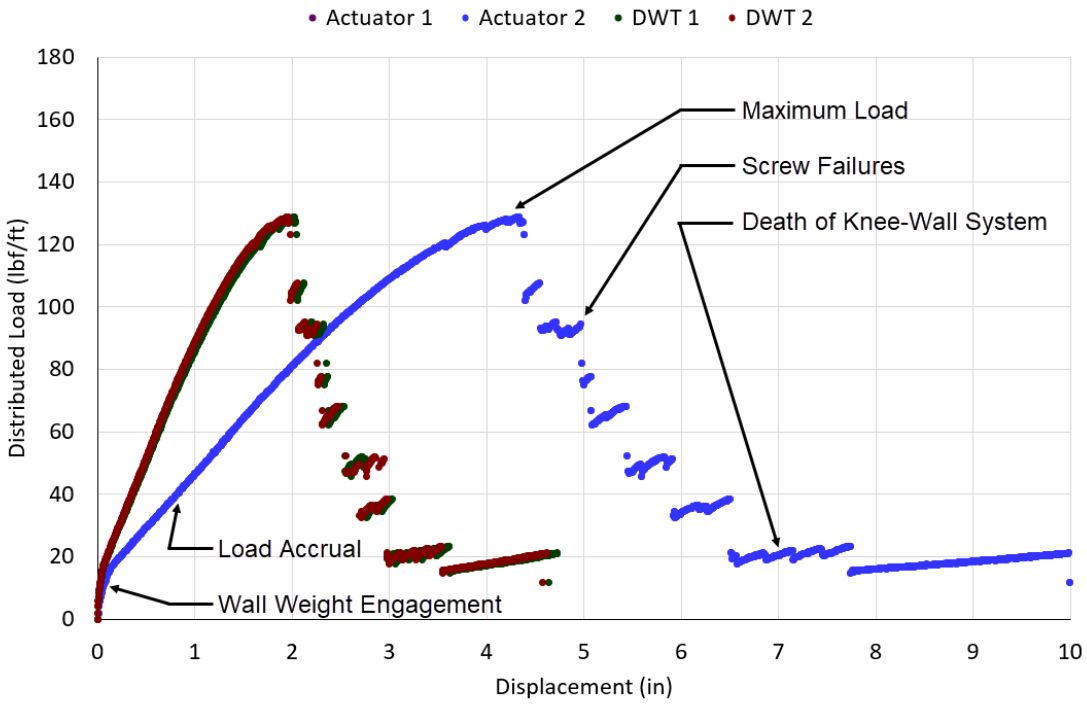

Figure 4.3.3-2. Distributed load versus displacement of test ND-18-01.

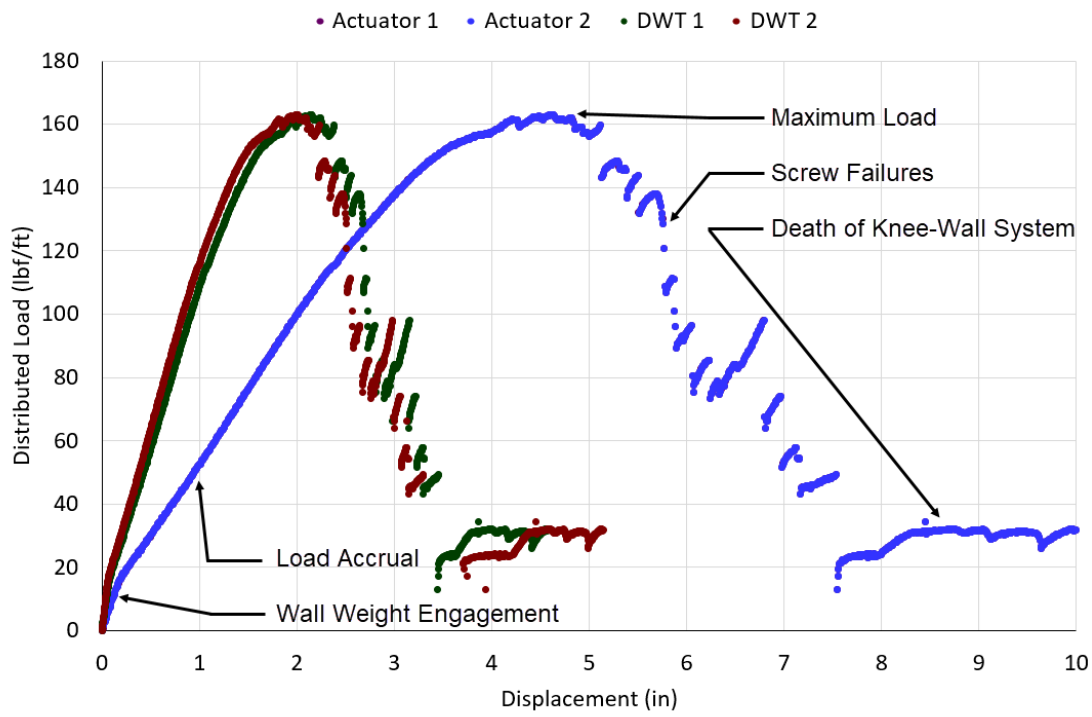

Figure 4.3.3-3. Distributed load versus displacement of test ND-18-02.

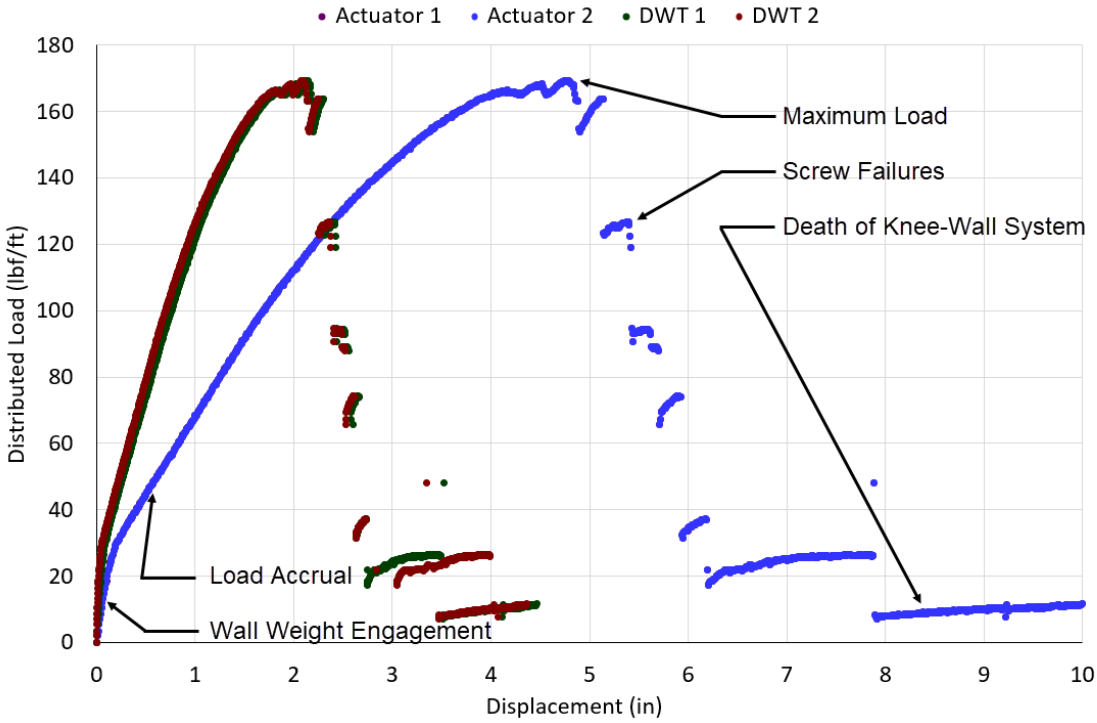

Figure 4.3.3-4. Distributed load versus displacement of test ND-18-03.

Each graphical representation of the 18-gauge structural steel channel tests contains a wall weight engagement segment at the start of test. During this wall weight engagement, the MTS actuator system is gathering the weight of the cold-formed knee-wall, the structural steel angle, and all other connecting pieces of the actuator itself without any significant amount of displacement occurring. This signifies the part of test where the connection elements, the machine screws, are beginning to engage and transfer the load gathered into the structural steel channel base material.

Once the wall weight is fully engaged, the knee-wall starts to deform elastically until it reaches a maximum load where the first connection element fails. The type connection failure was determined by the brand of machine screw used at the base connection. When the generic brand was used, the bottom row of those machine screws failed first by means of tensile rupture of the machine screw. When the Hillman screws were installed at the base connection, the controlling limit state of the cold-formed knee-wall system was tear out of the self-drilling screws used at the cold-formed knee-wall stud-to-track flange connection. This was observed in the data, as seen in Figure 4.3.3-1, by the difference in maximum moments the cold-formed knee-wall achieved before its first connection failure. For additional information on the capacity differences in the connection elements used in this project, refer to Section 4.3.1.

After the first connection element failure, the load on the knee-wall distributes itself throughout the wall until the next connection element failed. This process repeats itself until all the controlling connection elements failed, where the cold-formed knee-wall system enters its final stage, its death. The knee-wall continues in this stagnate stage until the testing ends at 10 in. of deformation.

Figures 4.3.3-5 through 4.3.3-10 are pictures of each 18-gauge structural steel channel trial before and after the loading was applied to the cold-formed knee-wall. Each of these trials show how the cold-formed track deformed along the region of compression after the bottom row of machine screws ruptured.

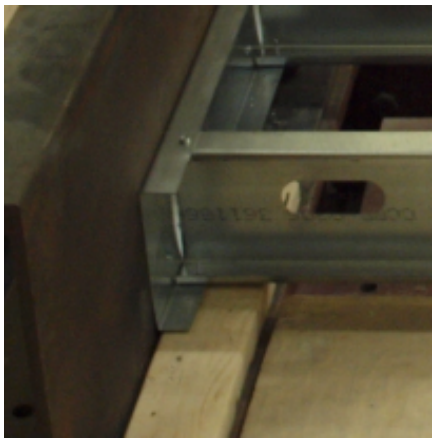

Figure 4.3.3-5. ND-18-01 before test.

Figure 4.3.3-6. ND-18-01 after test.

Figure 4.3.3-7. ND-18-02 before test.

Figure 4.3.3-8. ND-18-02 after test.

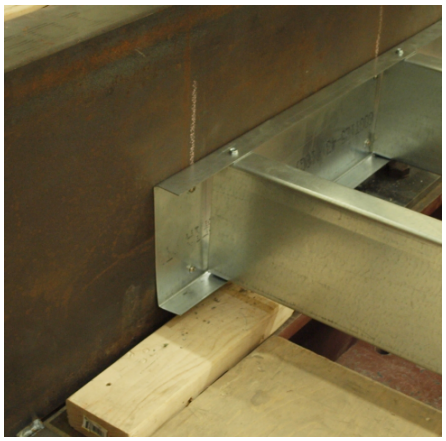

Figure 4.3.3-9. ND-18-03 before test.

Figure 4.3.3-10. ND-18-03 after test.

4.3.4 16-Gauge on Metal Deck

Three trials were conducted for the 16-gauge cold-formed knee-wall for the metal deck base condition. These three trials were labeled D-16-01, D-16-02, and D-16-03. The base connection resisting the rotation of the cold-formed knee-wall consisted of two #10 self-drilling screws spaced 4 in. apart located at each stud. Figure 4.3.4-1 shows the moment versus rotation behavior of the 16-gauge cold-formed knee-wall connections. Figures 4.3.4-2 through 4.3.4-4 show the relationship of distributed loading to linear displacement of each individual 16-gauge test. On a few of the graphs, the data points of the two DWT's don't overlap each other exactly like the two actuator data points. This can be explained by the slightly different distances from the actuator to the DWT's.

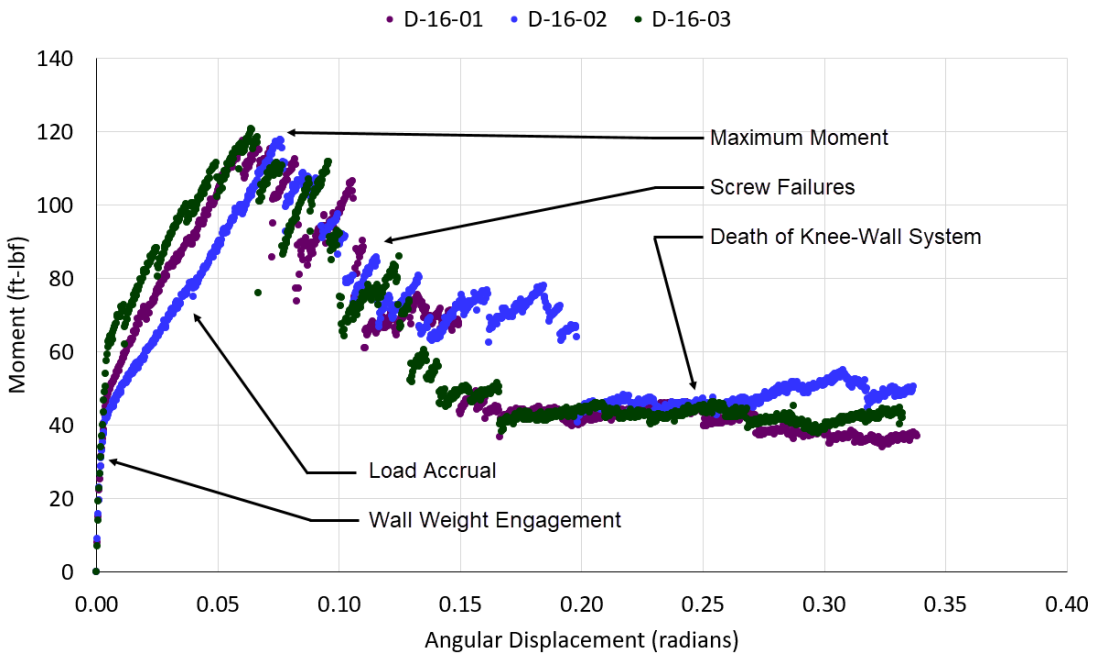

Figure 4.3.4-1. Moment versus rotation of 16-gauge on metal deck.

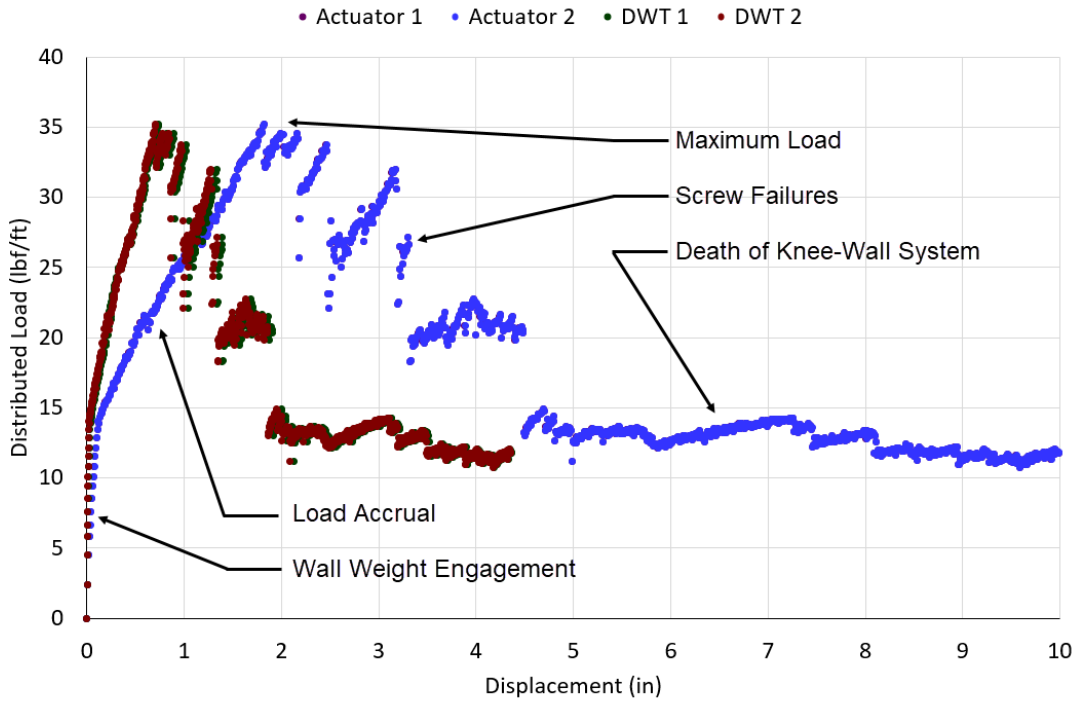

Figure 4.3.4-2. Distributed load versus displacement of test D-16-01.

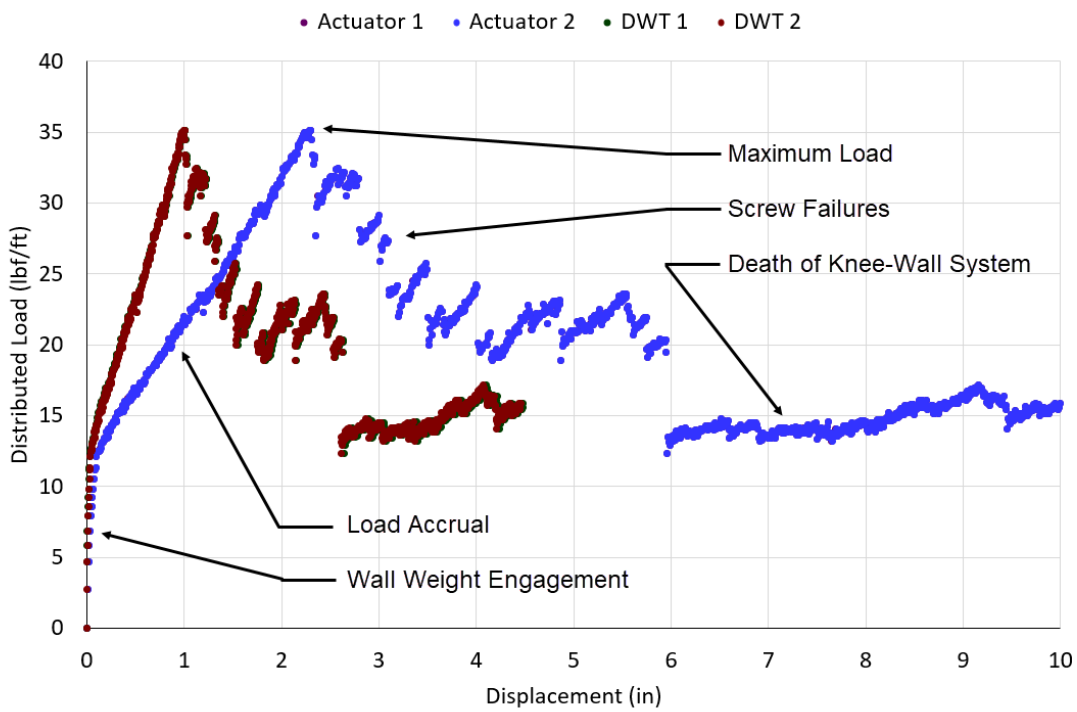

Figure 4.3.4-3. Distributed load versus displacement of test D-16-02.

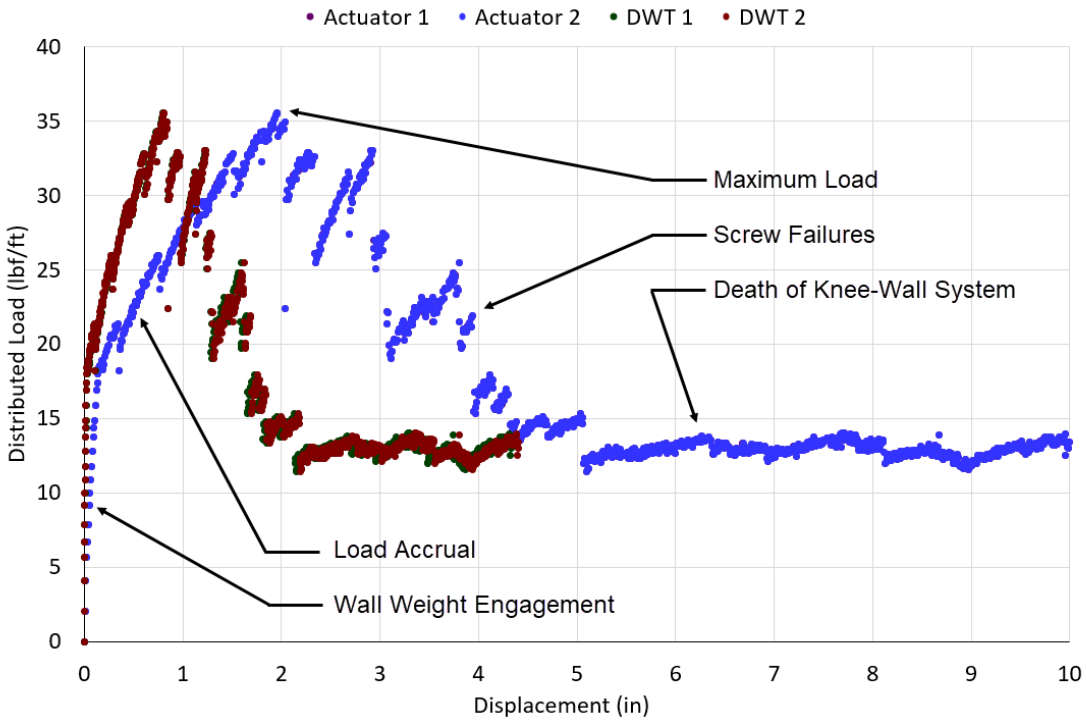

Figure 4.3.4-4. Distributed load versus displacement of test D-16-03.

Each graphical representation of the 16-gauge metal deck tests contains a wall weight engagement segment at the start of test. During this wall weight engagement, the MTS actuator system is gathering the weight of the cold-formed knee-wall, the structural steel angle, and all other connecting pieces of the actuator itself without any significant amount of displacement occurring. This signifies the part of test where the connection elements, the self-drilling screws, are beginning to engage and transfer the load gathered into the metal deck base material.

Once the wall weight is fully engaged, the knee-wall starts to deform elastically until it reaches a maximum load where the first self-drilling screw at the base connection fails by its pullout limit state. Some of the tests conducted don't consist of a perfectly linear load accrual process. These small jumps throughout the load accrual process represent the slippage of the self-drilling screws. The self-drilling screws haven't completely pulled out of the metal deck yet, but some of their threads slipped through the metal deck, which is why these small jumps in the graph look similar to the complete failure of the screw. After this first self-drilling screw pulls out, the load on the knee-wall redistributes itself throughout the wall until the next self-drilling screw fails by its pullout limit state. This process repeats itself until all the bottom rows of self-drilling screws fail, where the cold-formed knee-wall system enters its final stage, its death. The graphical jumps in this process of the test are caused by the top row of self-drilling screws trying to resist the knee-wall deformation since they are now the only base connection elements that haven't failed. The knee-wall continues these small jumps until the testing ends at 10 in. of deformation.

Figures 4.3.4-5 through 4.3.4-10 are pictures of each 16-gauge metal deck trial before

and after the loading was applied to the cold-formed knee-wall. Each of these trials show how the cold-formed track deformed along the region of compression after the bottom row of self-drilling screws pulled out of the metal deck.

Figure 4.3.4-5. D-16-01 before test.

Figure 4.3.4-6. D-16-01 after test.

Figure 4.3.4-7. D-16-02 before test.

Figure 4.3.4-8. D-16-02 after test.

Figure 4.3.4-9. D-16-03 before test.

Figure 4.3.4-10. D-16-03 after test.

4.3.5 16-Gauge on Structural Steel Channel

Three trials were conducted for the 16-gauge cold-formed knee-wall for the structural steel channel base condition. These three trials were labeled ND-16-01, ND-16-02, and ND-16-03. The base connection resisting the rotation of the cold-formed knee-wall consisted of two #10 machine screws spaced 4 in. apart located at each stud. Figure 4.3.5-1 shows the moment versus rotation behavior of the 16-gauge cold-formed knee-wall connections. Figures 4.3.5-2 through 4.3.5-4 show the relationship of distributed loading to linear displacement of each individual 16-gauge test. On a few of the graphs, the data points of the two DWT's don't overlap each other exactly like the two actuator data points. This can be explained by the slightly different distances from the actuator to the DWT's.

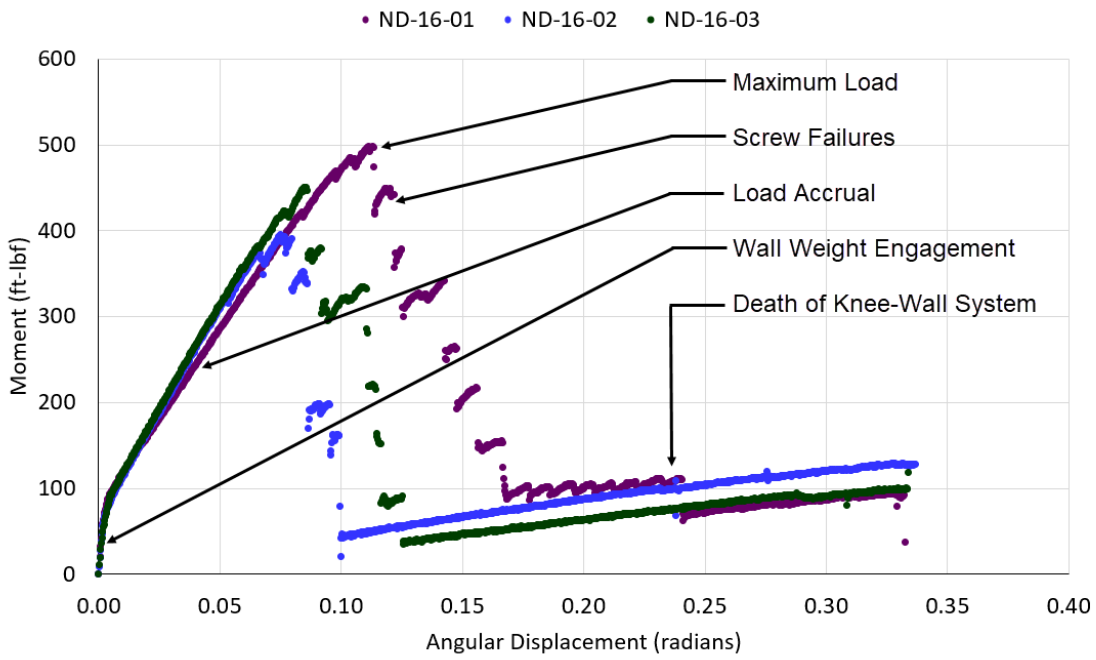

Figure 4.3.5-1. Moment versus rotation of 16-gauge on steel channel.

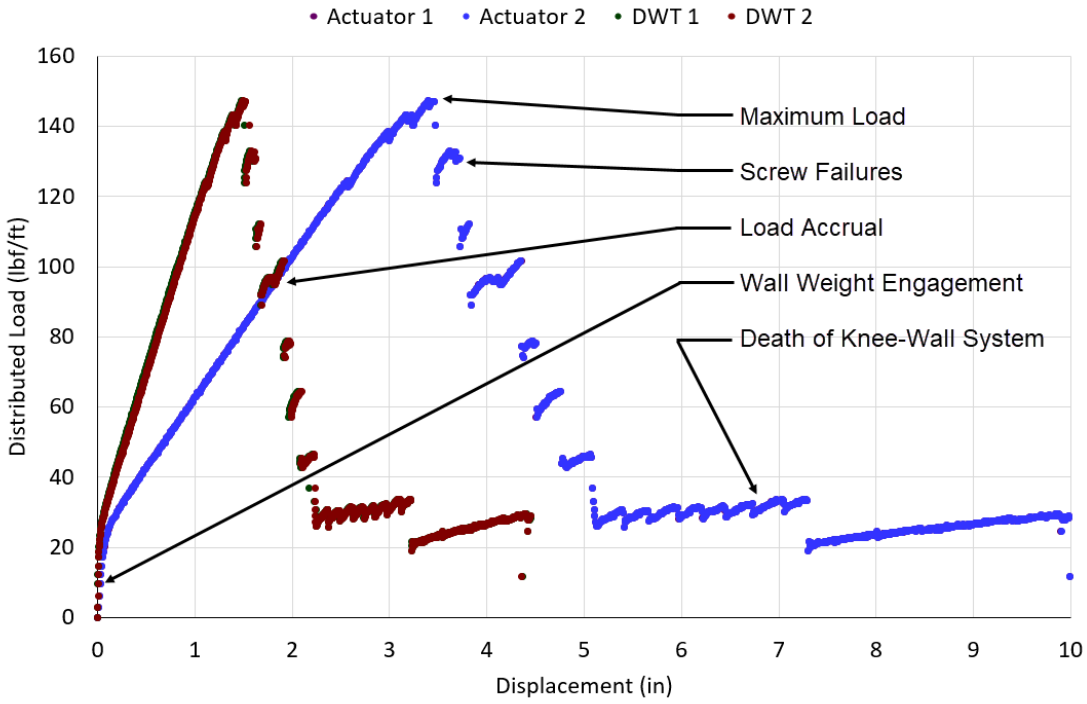

Figure 4.3.5-2. Distributed load versus displacement of test ND-16-01.

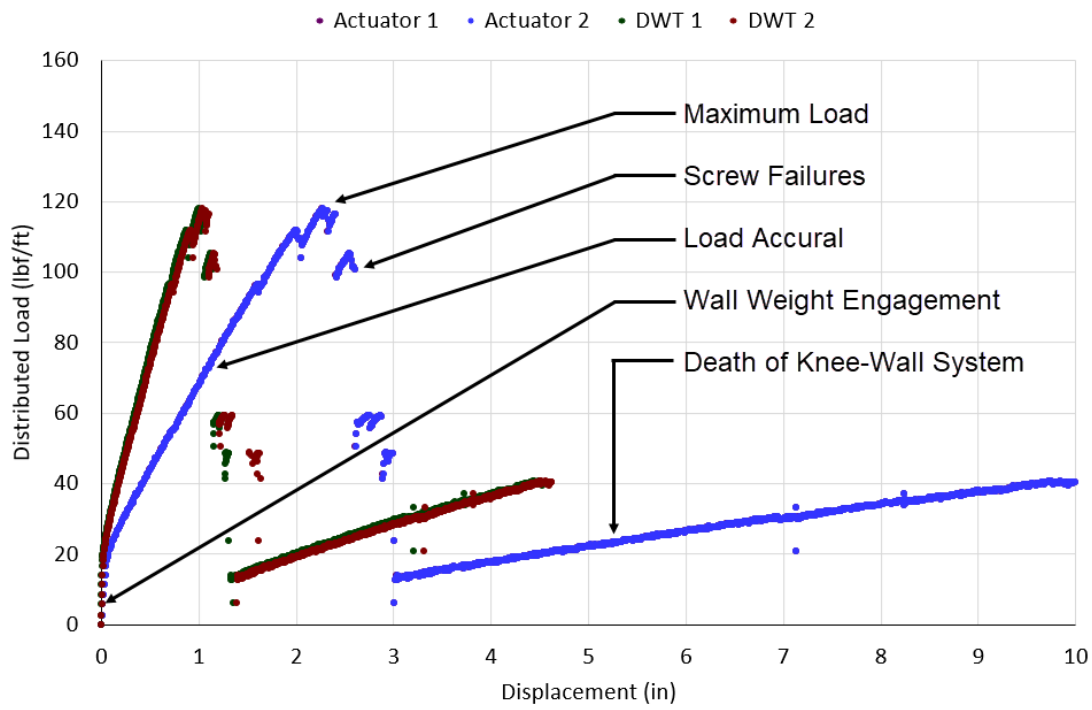

Figure 4.3.5-3. Distributed load versus displacement of test ND-16-02.

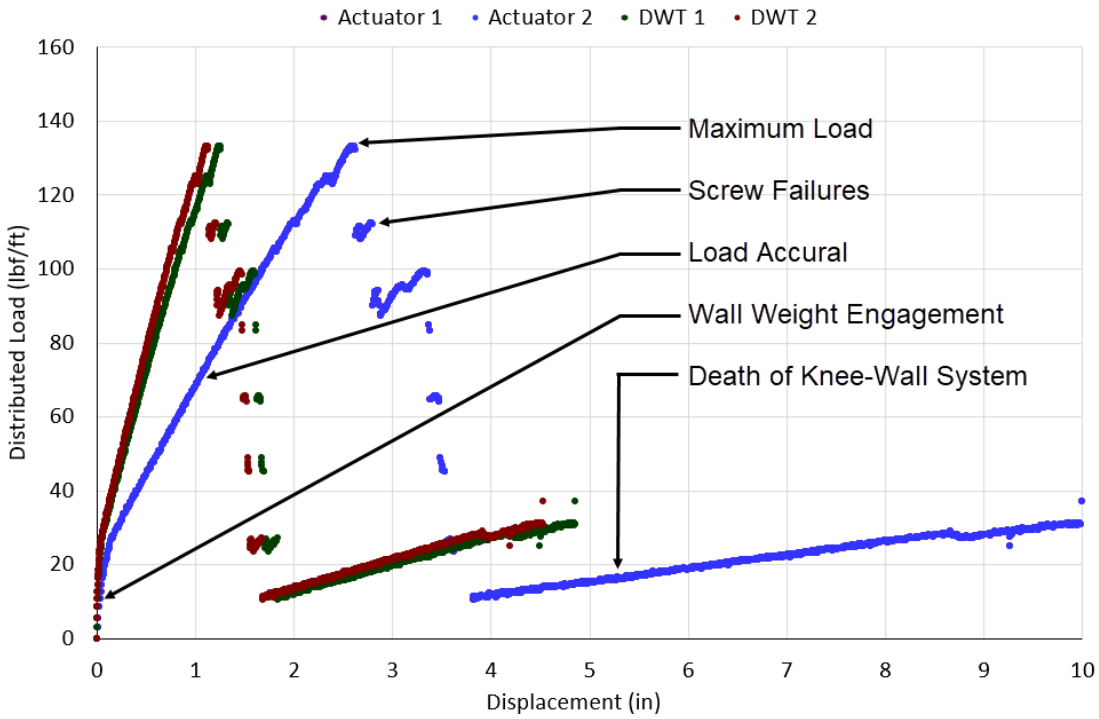

Figure 4.3.5-4. Distributed load versus displacement of test ND-16-03.

Each graphical representation of the 16-gauge structural steel channel tests contains a wall weight engagement segment at the start of test. During this wall weight engagement, the MTS actuator system is gathering the weight of the cold-formed knee-wall, the structural steel angle, and all other connecting pieces of the actuator itself without any significant amount of displacement occurring. This signifies the part of test where the connection elements, the machine screws, are beginning to engage and transfer the load gathered into the structural steel channel base material.

Once the wall weight is fully engaged, the knee-wall starts to deform elastically until it reaches a maximum load where the first machine screw at the base connection fails by its rupture limit state. After this first machine screw ruptured, the load on the knee-wall redistributes itself throughout the wall until the next machine screw fails by its rupture limit state. This process repeats itself until all the bottom rows of machine screws fail, where the cold-formed knee-wall system enters its final stage, its death. The graphical jumps in this process of the test are caused by the top row of machine screws trying to resist the knee-wall deformation since they are now the only base connection elements that haven't failed. The knee-wall continues these small jumps until the testing ends at 10 in. of deformation.

Figures 4.3.5-5 through 4.3.5-10 are pictures of each 16-gauge structural steel channel trial before and after the loading was applied to the cold-formed knee-wall. Each of these trials show how the cold-formed track deformed along the region of compression after the bottom row of machine screws ruptured.

Figure 4.3.5-5. ND-16-01 before test.

Figure 4.3.5-6. ND-16-01 after test.

Figure 4.3.5-7. ND-16-02 before test.

Figure 4.3.5-8. ND-16-02 after test.

Figure 4.3.5-9. ND-16-03 before test.

Figure 4.3.5-10. ND-16-03 after test.

4.3.6 14-Gauge on Metal Deck

Three trials were conducted for the 14-gauge cold-formed knee-wall for the metal deck base condition. These three trials were labeled D-14-01, D-14-02, and D-14-03. The base connection resisting the rotation of the cold-formed knee-wall consisted of two #10 self-drilling screws spaced 4 in. apart located at each stud. Figure 4.3.6-1 shows the moment versus rotation behavior of the 14-gauge cold-formed knee-wall connections. Figures 4.3.6-2 through 4.3.6-4 show the relationship of distributed loading to linear displacement of each individual 14-gauge test. On a few of the graphs, the data points of the two DWT's don't overlap each other exactly like the two actuator data points. This can be explained by the slightly different distances from the actuator to the DWT's.

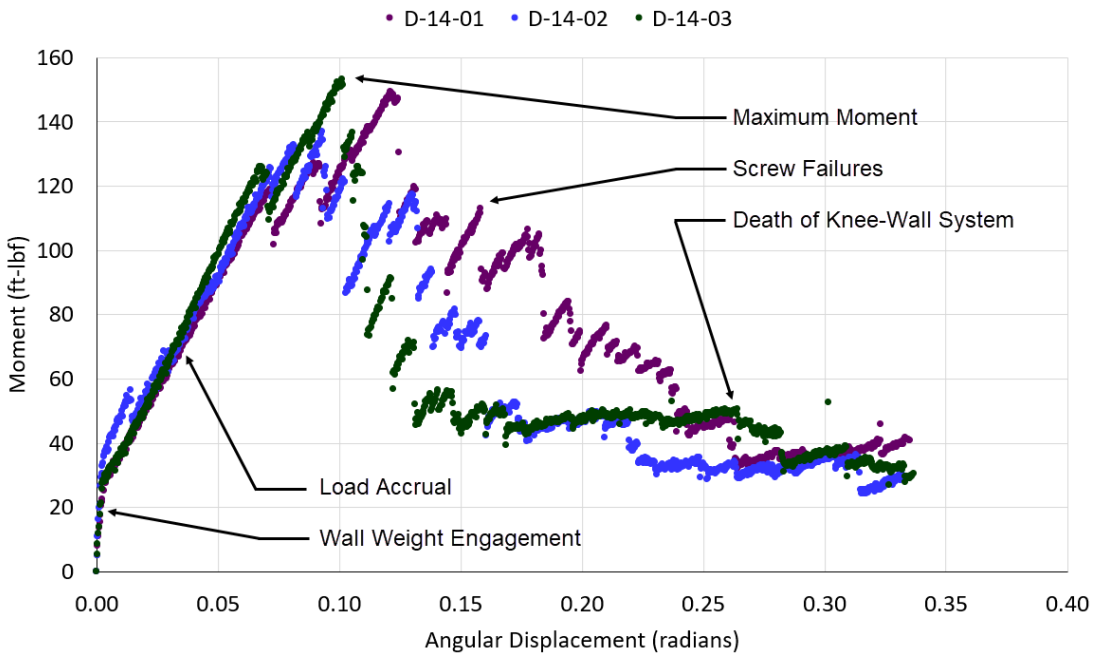

Figure 4.3.6-1. Moment versus rotation of 14-gauge on metal deck.

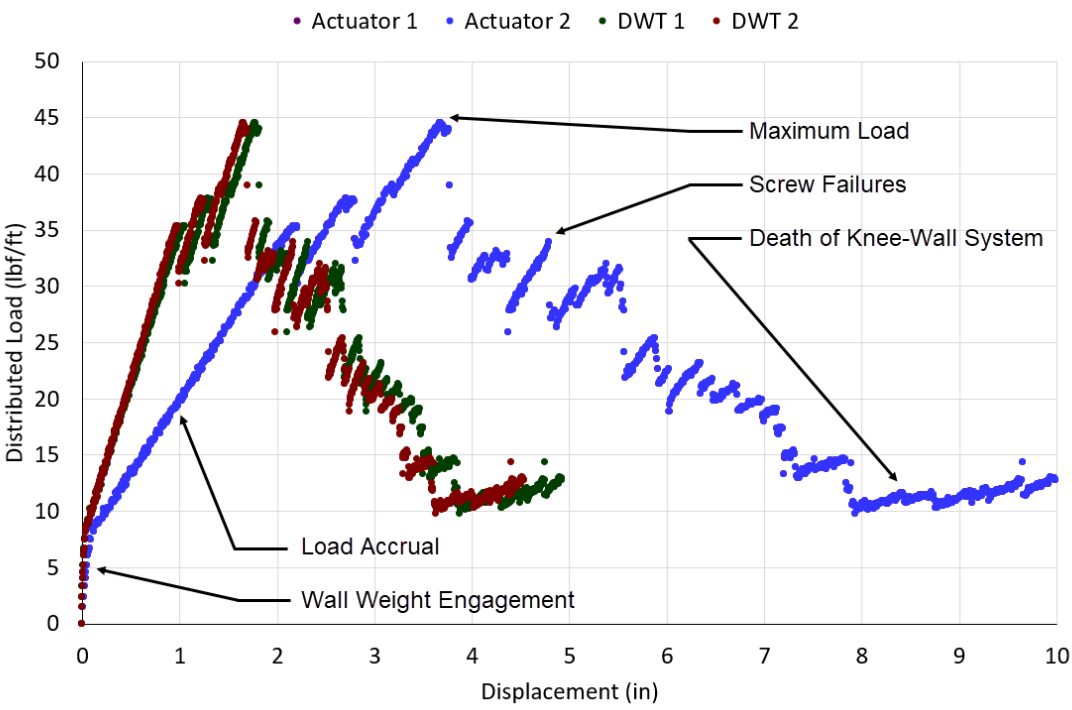

Figure 4.3.6-2. Distributed load versus displacement of test D-14-01.

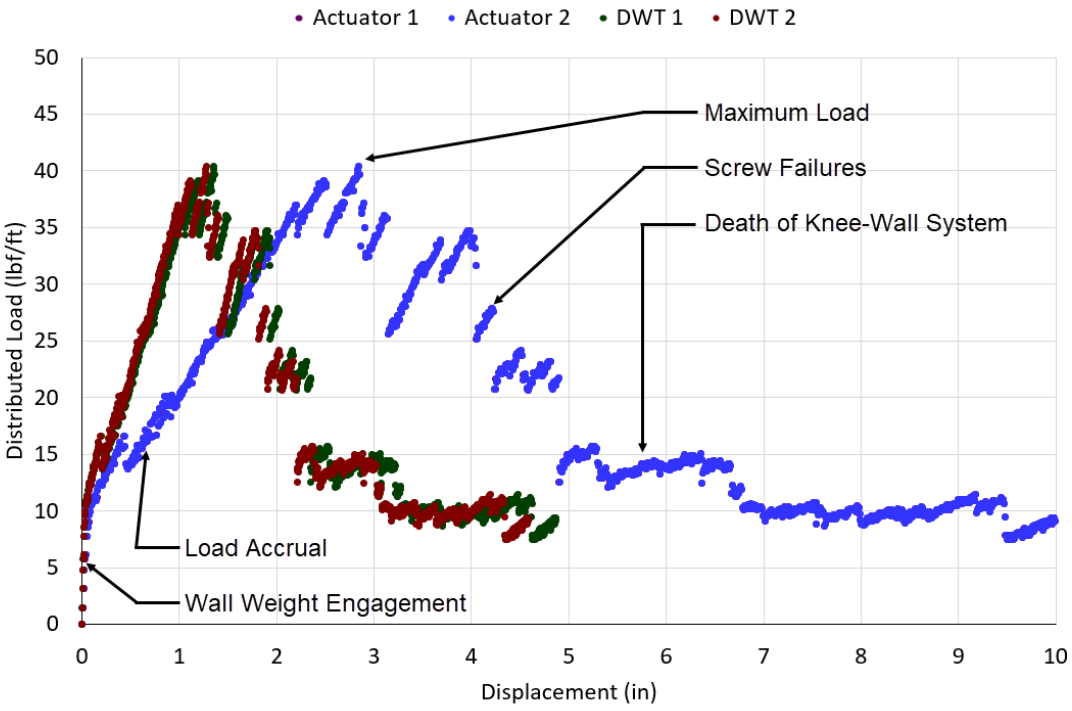

Figure 4.3.6-3. Distributed load versus displacement of test D-14-02.

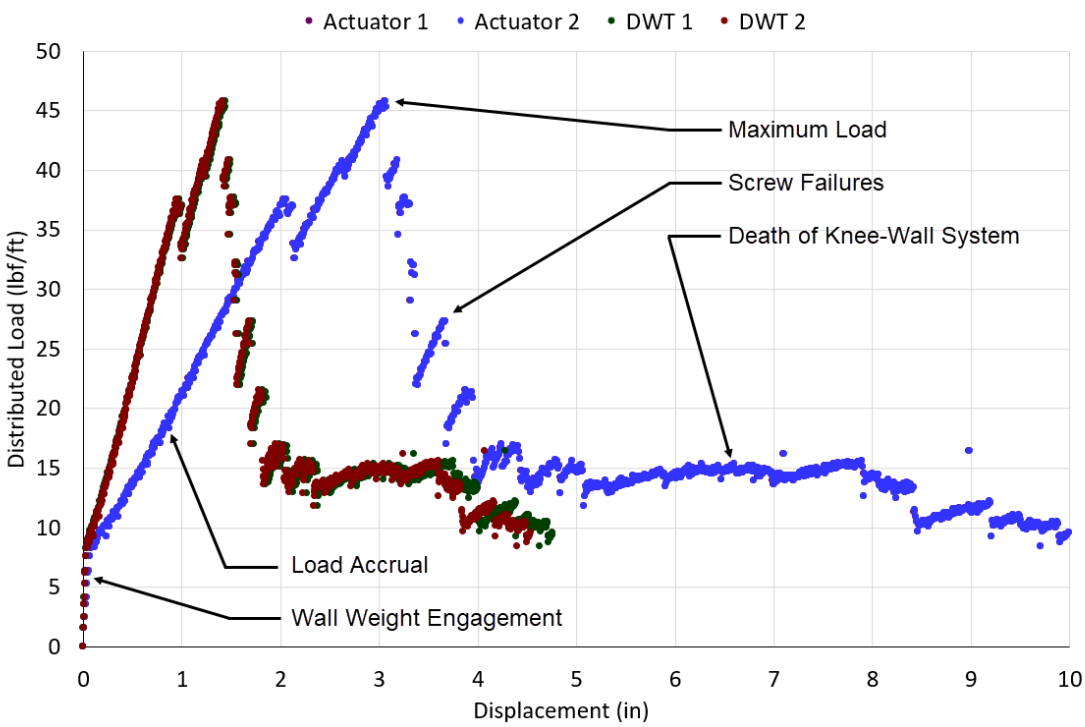

Figure 4.3.6-4. Distributed load versus displacement of test D-14-03.

Each graphical representation of the 14-gauge metal deck tests contains a wall weight engagement segment at the start of test. During this wall weight engagement, the MTS actuator system is gathering the weight of the cold-formed knee-wall, the structural steel angle, and all other connecting pieces of the actuator itself without any significant amount of displacement occurring. This signifies the part of test where the connection elements, the self-drilling screws, are beginning to engage and transfer the load gathered into the metal deck base material.

Once the wall weight is fully engaged, the knee-wall starts to deform elastically until it reaches a maximum load where the first self-drilling screw at the base connection fails by its pullout limit state. Some of the tests conducted don't consist of a perfectly linear load accrual process. These small jumps throughout the load accrual process represent the

slippage of the self-drilling screws. The self-drilling screws haven't completely pulled out of the metal deck yet, but some of their threads slipped through the metal deck, which is why these small jumps in the graph look similar to the complete failure of the screw. After this first self-drilling screw pulls out, the load on the knee-wall redistributes itself throughout the wall until the next self-drilling screw fails by its pullout limit state. This process repeats itself until all the bottom rows of self-drilling screws fail, where the cold-formed knee-wall system enters its final stage, its death. The graphical jumps in this process of the test are caused by the top row of self-drilling screws trying to resist the knee-wall deformation since they are now the only base connection elements that haven't failed. The knee-wall continues these small jumps until the testing ends at 10 in. of deformation.

Figures 4.3.6-5 through 4.3.6-10 are pictures of each 14-gauge metal deck trial before and after the loading was applied to the cold-formed knee-wall. Each of these trials show how the cold-formed track deformed along the region of compression after the bottom row of self-drilling screws pulled out of the metal deck.

Figure 4.3.6-5. D-14-01 before test.

Figure 4.3.6-6. D-14-01 after test.

Figure 4.3.6-7. D-14-02 before test.

Figure 4.3.6-8. D-14-02 after test.

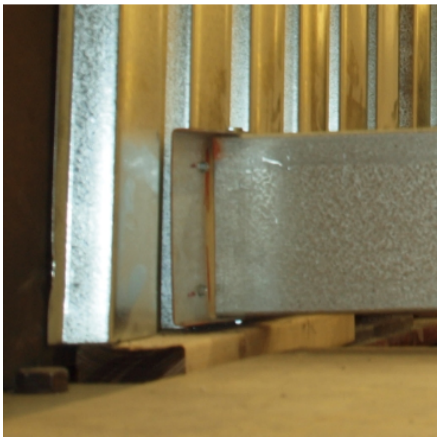

Figure 4.3.6-9. D-14-03 before test.

Figure 4.3.6-10. D-14-03 after test.

4.3.7 14-Gauge on Structural Steel Channel

Three trials were conducted for the 14-gauge cold-formed knee-wall for the structural steel channel base condition. These three trials were labeled ND-14-01, ND-14-02, and ND-14-03. The base connection resisting the rotation of the cold-formed knee-wall consisted of two #10 machine screws spaced 4 in. apart located at each stud. Figure 4.3.7-1 shows the moment versus rotation behavior of the 14-gauge cold-formed knee-wall connections. Figures 4.3.7-2 through 4.3.7-4 show the relationship of distributed loading to linear displacement of each individual 14-gauge test. On a few of the graphs, the data points of the two DWT's don't overlap each other exactly like the two actuator data points. This can be explained by the slightly different distances from the actuator to the DWT's.

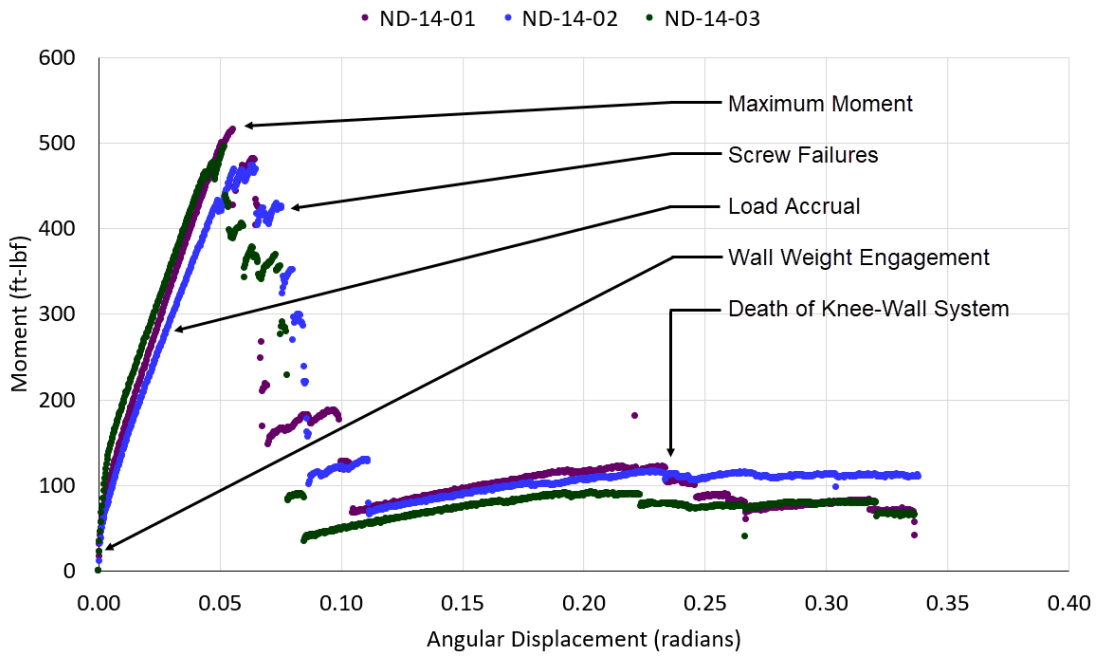

Figure 4.3.7-1. Moment versus rotation of 14-gauge on steel channel.

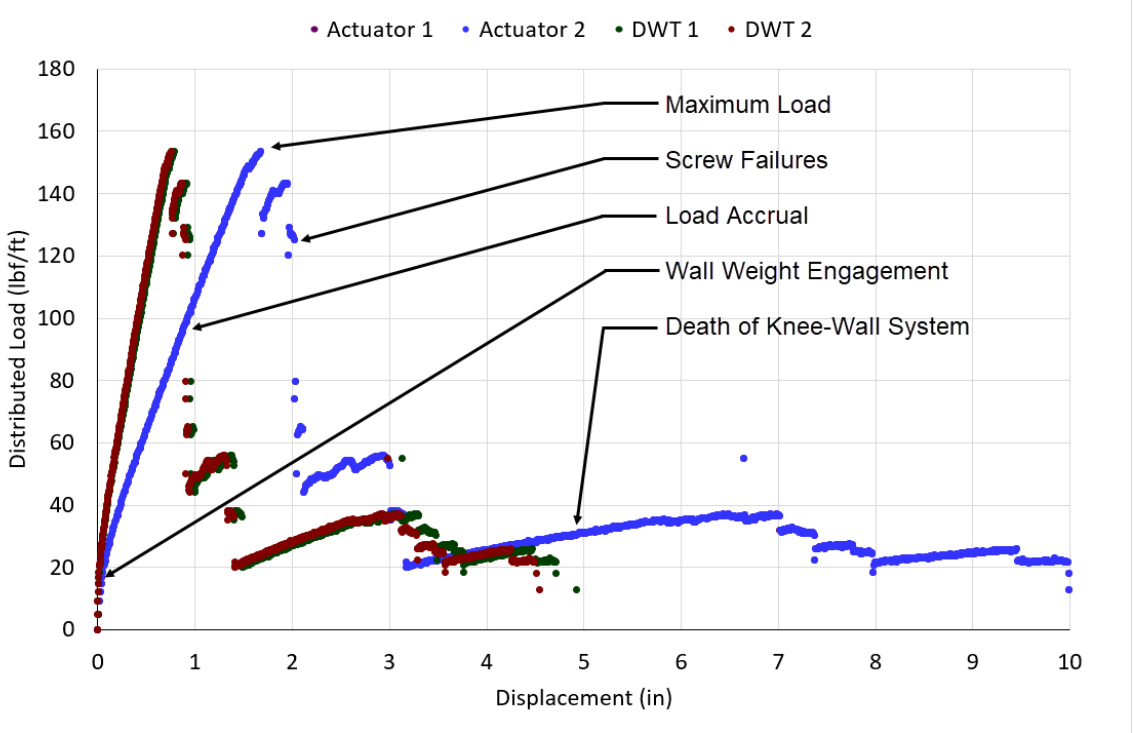

Figure 4.3.7-2. Distributed load versus displacement of test ND-14-01.

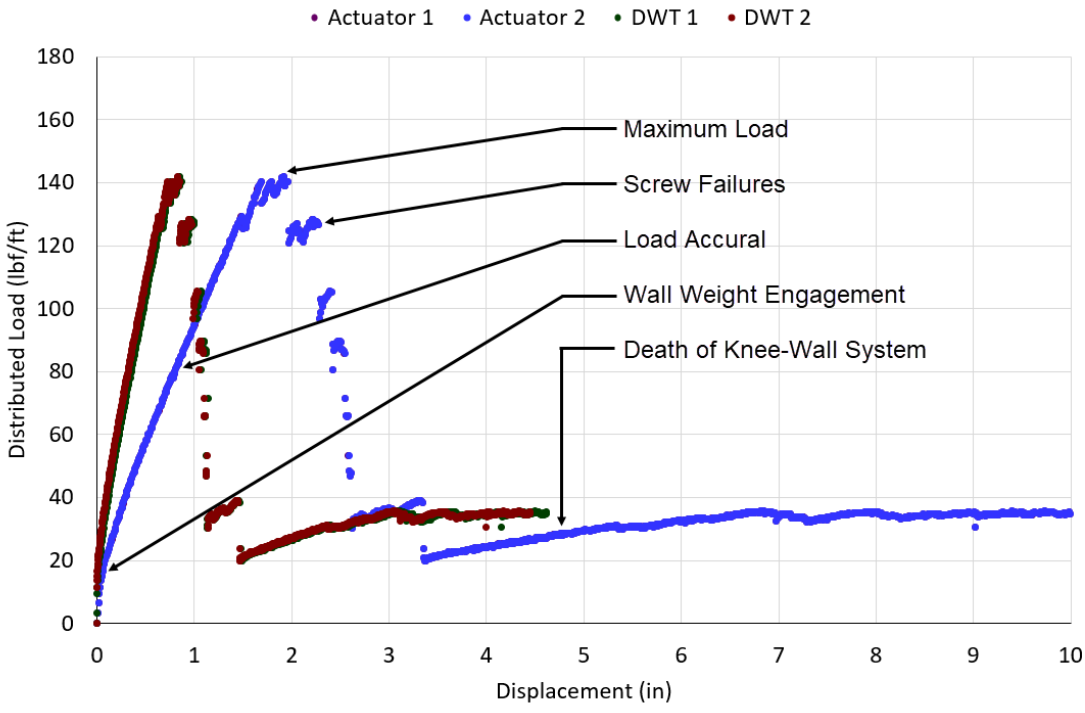

Figure 4.3.7-3. Distributed load versus displacement of test ND-14-02.

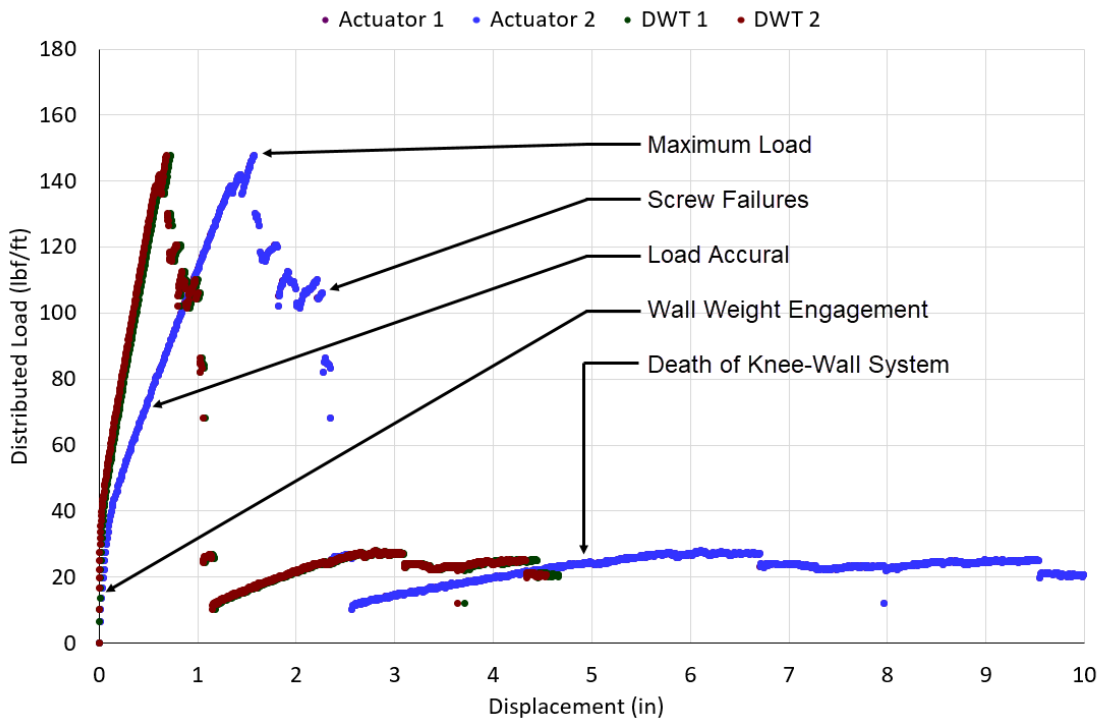

Figure 4.3.7-4. Distributed load versus displacement of test ND-14-03.

Each graphical representation of the 14-gauge structural steel channel tests contains a wall weight engagement segment at the start of test. During this wall weight engagement, the MTS actuator system is gathering the weight of the cold-formed knee-wall, the structural steel angle, and all other connecting pieces of the actuator itself without any significant amount of displacement occurring. This signifies the part of test where the connection elements, the machine screws, are beginning to engage and transfer the load gathered into the structural steel channel base material.

Once the wall weight is fully engaged, the knee-wall starts to deform elastically until it reaches a maximum load where the first machine screw at the base connection fails by its rupture limit state. After this first machine screw ruptured, the load on the knee-wall redistributes itself throughout the wall until the next machine screw fails by its rupture

limit state. This process repeats itself until all the bottom rows of machine screws fail, where the cold-formed knee-wall system enters its final stage, its death. The graphical jumps in this process of the test are caused by the top row of machine screws trying to resist the knee-wall deformation since they are now the only base connection elements that haven't failed. The knee-wall continues these small jumps until the testing ends at 10 in. of deformation.

Figures 4.3.7-5 through 4.3.7-10 are pictures of each 14-gauge structural steel channel trial before and after the loading was applied to the cold-formed knee-wall. Each of these trials show how the cold-formed track deformed along the region of compression after the bottom row of machine screws ruptured.

Figure 4.3.7-5. ND-14-01 before test.

Figure 4.3.7-6. ND-14-01 after test.

Figure 4.3.7-7. ND-14-02 before test.

Figure 4.3.7-8. ND-14-02 after test.

Figure 4.3.7-9. ND-14-03 before test.

Figure 4.3.7-10. ND-14-03 after test.

Chapter 5: Data Analysis

5.1 Introduction

The data collected for the duration of the experimental testing were employed to compare the three different gauges of cold-formed knee-walls. Each of the three gauges were observed under two different base materials, 20-gauge metal deck and C15×40 channel. To compare the data for each of these testing scenarios, the maximum moments they accumulated before the first connection element failure was observed. These maximum moments value was then used to calculate the screw's pullout capacity, rupture capacity, or shear capacity, depending on which brand and type of screw was used for the attachment of the knee-wall to the base material.

5.2 Screw Capacity Data Comparison

Different connection limits states controlled for different cold-formed knee-wall tests. Screw capacity tests were performed to better understand why the connection limit states were not consistent among tests. Tables 5.2-1 through 5.2-2 contain values for the maximum capacity the screws reached before the first screw failure. Table 5.2-3 shows the results of the screw capacity tests.

Table 5.2-1

Maximum Screw Capacities for Tests on Metal Deck

Test	Self-Drilling Pullout
	lbf
D-18-01	345
D-18-02	414
D-18-03	349
D-16-01	354
D-16-02	355
D-16-03	357
D-14-01	451
D-14-02	413
D-14-03	457

Table 5.2-2

Maximum Screw Capacities for Tests on Steel Channel

Test	Screw Brand	Machine Screw Rupture (base connection	Self-Drilling Shear (stud-to-track connection)
		lbf	lbf
ND-18-01	Generic	1241	838
ND-18-02*	Hillman	1617	1084
ND-18-03*	Hillman	1659	1112
ND-16-01	Generic	1434	955
ND-16-02	Generic	1177	793
ND-16-03	Generic	1347	901
ND-14-01	Generic	1552	1045
ND-14-02	Generic	1412	955
ND-14-03	Generic	1493	1006

*Note: * signifies stud-to-track self-drilling screw tear out limit state controlled*

Table 5.2-3

Result Summary for Screw Capacity Testing

	Shear		Pullout/Rupture	
	# of Trials	Average Capacity (lbf)	# of Trials	Average Capacity (lbf)
#10 Generic Self-Drilling Screws	5	1084	6	296
#10 Generic Machine Screws	-	-	5	1403
#10 Hillman Machine Screws	-	-	5	1788

The pullout and rupture values shown from the cold-formed knee-wall tests (Tables 5.2-1 through 5.2-2) were quite consistent between the different scenarios tested, except for the two of the 18-gauge tests attached to the structural steel channel (ND-18-02 and ND-18-03). The screws connecting the track to the base material in these two tests achieved much higher tension forces than any of the other tests conducted. It was during these two tests that the Hillman machine screws were used to attach the cold-formed knee-wall to the steel channel instead of the generic brand that were used in the rest of the steel channel tests. The Hillman brand screws were proven through the screw capacity tests to have a higher rupture capacity. Additionally, the screw capacity test results show the average shear failure of the self-drilling screws located at the track flanges to be 1084 lbs. The only two tests that accumulated stud-to-track shearing forces at 1084 lbs or higher were the two tests that used the Hillman machine screws (ND-18-02 and ND-18-03). When comparing the cold-formed knee-wall results to the screw capacity test results, the screw capacity tests achieved higher pullout values than the screws in the cold-formed knee-wall tests by a couple hundred pounds. This could be explained by the tightening of the screws during the cold-formed knee-wall tests. When attaching the cold-formed knee-wall to the structural steel channel, the machine screws were tightened to remove any

slack or movement of the knee-wall. This introduced a pre-tension force within the screw prior to the test loading. The screws from the screw capacity tests were able to achieve a higher capacity because they were not pre-tensioned prior to testing.

5.3 Data Comparison

The three cold-formed steel gauges tested in this experiment were 18-, 16-, and 14-gauge metal. Each of these gauges were tested under two different base materials, 20-gauge metal deck and a C15×40 steel channel. Tables 5.3-1 through 5.3-2 illustrate the maximum moments each cold-formed knee-wall test achieved before the first connection element failure. Figures 5.3-1 through 5.3-3 represent all of the cold-formed steel gauges applied with each of the two base materials.

Table 5.3-1

Moments for Deck Tests

Test	Maximum Moment
	ft-lbf
D-18-01	114
D-18-02	137
D-18-03	116
D-16-01	118
D-16-02	118
D-16-03	119
D-14-01	149
D-14-02	137
D-14-03	152

Table 5.3-2

Moments for Channel Tests

Test	Maximum Moment ft-lbf
ND-18-01	410
ND-18-02	533
ND-18-03	547
ND-16-01	474
ND-16-02	390
ND-16-03	447
ND-14-01	515
ND-14-02	469
ND-14-03	496

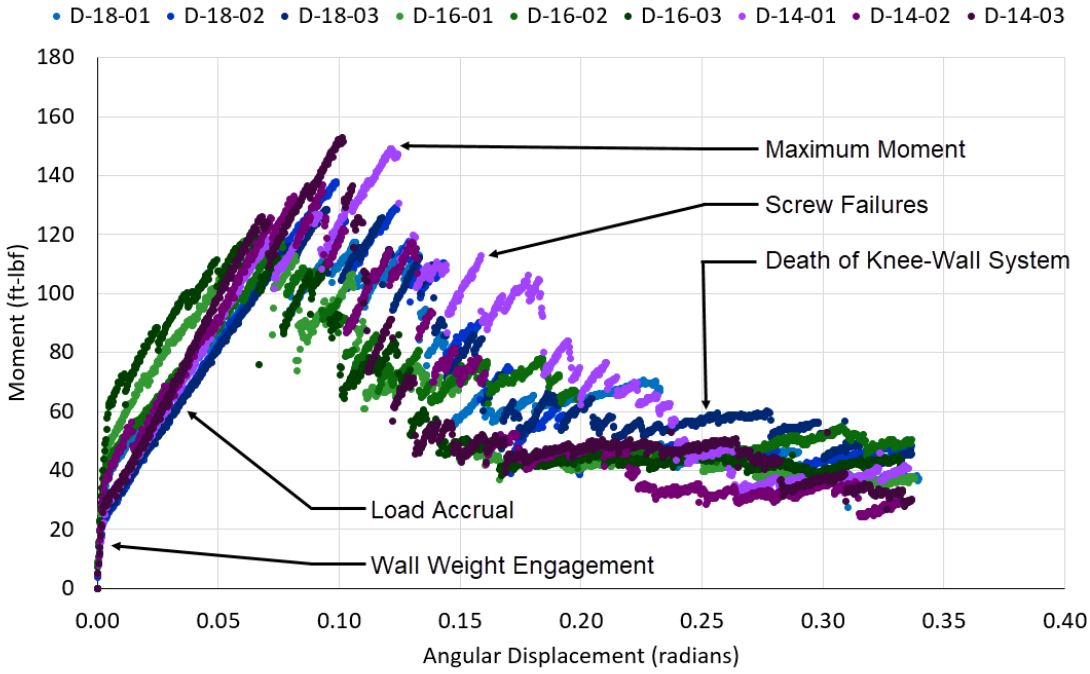

Figure 5.3-1. Moment versus rotation of metal deck tests.

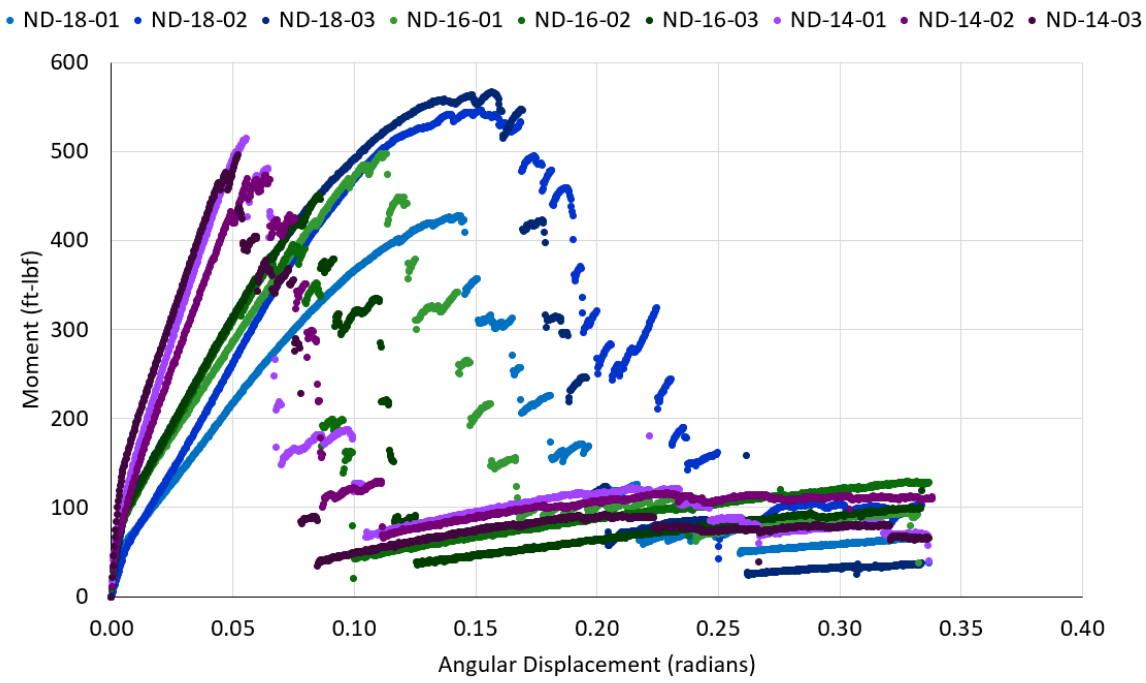

Figure 5.3-2. Moment versus rotation of steel channel tests.

There was not a huge variation in the maximum moments for each gauge tested on the metal deck base condition, only having a standard deviation and coefficient of variation of 14.1 and 11.0%, respectively. The holes for the machine screws were predrilled into the steel channel. This provided a consistent connection spacing that could not change from test to test. Additionally, it was assumed the maximum moment magnitude achieved for each cold-formed gauge attached to the metal deck should descend in order of descending cold-formed gauge thickness. These tests do not illustrate that because the 18-gauge cold-formed knee-walls reached higher moments than the 16-gauge knee-walls. This can be explained through the constructability of the cold-formed knee-wall attachment to the metal deck. The deck flutes were spaced at approximately six inches center-on-center, whereas the knee-wall attachment points were supposed to be 16 in. center-on-center. Therefore, the spacing of the connection points varied along the length

of the wall due to the deck flutes not aligning with the knee-wall stud spacing. However, this condition is also apparent in a real construction circumstance, so the tests mimic real-world installation. Additionally, the screws at each connection point were supposed to be spaced four inches apart. Because of the awkward angle the screws were inserted at on the testing frame, the spacing between the screws varied from connection point to connection point.

The tests completed on the steel channel base material consisted of a larger range of maximum moments achieved, having a standard deviation and coefficient of variation of 41.6 and 594.3%, respectively (excluding the tests that used the Hillman machine screws). The results of tests using the steel channel base material performed more as expected. The maximum moment magnitudes achieved ascended by the order of ascending cold-formed gauge thickness. Additionally, as the thickness of cold-formed steel increased, the ductility of the knee-wall decreases. As seen in Figure 5.3-2, the brand of machine screw or the type of connection failure did not affect the ductility of the cold-formed knee-wall, these factors only affected the bending capacity of the cold-formed knee-wall. The 18- and 16-gauge cold-formed material achieved about three times and two times more rotation than the 14-gauge material before their first connection element failure, respectively.

In order to compare the experimental results to commonly applied industry standards, a comparison to SIMPSON's RCKW5.5 clips will be done. Table 5.3-3 illustrates the comparison between the lateral line loads and pressures allowed on the wall based on the bending capacity of the experimental and SIMPSON base connections. The table uses a knee-wall height of 30 in. and a stud spacing of 16 in. center-on-center. SIMPSON does

not provide tabulated values for 14-gauge knee-walls or connections to a metal deck base material, therefore the only comparison that was done included the 18- and 16-gauge knee-wall tests to the steel channel base material. Additionally, SIMPSON's tabulated values include a factor of safety of three, in accordance with AISI S100-16. Therefore, this safety factor was applied to the average experimental moment capacity magnitude. It should be noted that the average moment capacity value for the 18-gauge cold-formed knee-walls in Table 5.3-3 did not include the tests that used the Hillman machine screws.

Table 5.3-3

Comparison to SIMPSON Strong-Tie Values on Structural Steel

	18-gauge		16-gauge	
	Experimental (average)	SIMPSON (Tabulated)	Experimental (average)	SIMPSON (Tabulated)
Moment Capacity (ft-lb)	137	530	146	536
Allow. Line Load (plf)	41	159	44	161
Allow. Wall Pressure (psf)	33	127	35	129

The moment capacity magnitudes, collected from the experimental results and the SIMPSON tables, were used in the following equation along with the stud spacing, s, and the knee-wall height, H, to obtain the allowable lateral line load along the top track of the knee-wall:

$$w = \frac{M}{sH}.$$

The following equation was used to obtain the allowable knee-wall pressure, p. It was derived using an equation compatible for cantilevering walls under a uniform distributed

load. The uniform distributed load was then converted into the wall pressure by dividing the load by the stud spacing, s:

$$p = \frac{2M}{sH^2}.$$

Using the RCKW5.5 clip at each knee-wall base connection increases the allowable top track line load and allowable wall pressure by almost four times as much. Even though SIMPSON's allowable line load and wall pressure values were calculated using the same information as the experimental values (e.g. wall height and stud spacing), some assumptions SIMPSON made differed from the parameters of the experimental tests. Their RCKW5.5 tabulated values assume (4) #12 screws to attach the light gauge clip to the structural steel and (6) #12 screws to the cold-formed stud, as opposed to the #10 screws used in the experimental tests. Therefore, the use of stronger screws is part of the reason why the RCKW5.5's moment capacities are higher than the moment capacities from the experimental tests (not solely from the clip itself).

Chapter 6: Discussion and Conclusion

6.1 Introduction

This section summarizes the results of this experimental testing and explains the impact of this research to the construction committee.

6.2 Discussion of Experimental Results

This project consisted measuring the bending capacity of unclipped cold-formed knee-walls using a total of 18 tests. Half of these tests were observed over a 20-gauge metal deck base material and the other half were observed over a C15×40 steel channel base material. Each base condition tests three different gauge thickness of cold-formed steel, 18-, 16-, and 14-gauge. In order to provide this project with consistent and reliable results, three trials of each type of test were taken.

The knee-wall tests performed on the metal deck base material produced slightly different results from the knee-wall tests attached to the structural steel channel by the way that the moment capacity did not increase as the gauge thickness of the knee-wall increased. This difference in the data was attributed to the screw pullout of the metal deck being the controlling limit state of the connection failure as well as the lack of consistency in the connections of the knee-wall to the metal deck base material. These inconsistencies include the spacing of the deck flutes not matching the spacing of each connection location on the knee-wall, and the spacing of each screw not consistently being screwed in at four inches at each connection location.

The tests attaching the knee-wall to the structural steel channel base material resulted in higher bending capacity due to the fact that the machine screws' tensile rupture capacity is more than the pullout capacity of the self-drilling screws. The change in ductility in

each gauge of cold-formed knee-wall tested was well distinguished during these steel channel tests. The thicker the cold-formed material was, the less ductile the knee-wall system became.

The screw capacity tests for the self-drilling screws and the machine screws proved why different connection limit states controlled for some of the cold-formed knee-wall tests. The Hillman brand named screws achieved a higher screw tensile rupture force, resulting in the self-drilling screws attaching the cold-formed stud to the track failed first by shear tear out.

6.3 Comparison to SIMPSON's RCKW5.5 Clip

Although the bending capacities for knee-walls without a clip at each of their base connections were almost four times less than SIMPSON's tabulated values for knee-walls using the RCKW5.5 clips, there are some advantages the construction industry can take away from this data, upon more research and testing performed on the subject. The use of a light gauge clip angle increases both the material and labor costs of the project. Even though the material and labor costs associated with the installation per clip is quite small, it can add up quickly throughout the duration of the construction process. If a knee-wall did not require the installation of a light gauge clip angle, the construction team could save time and money for the owner of the project.

6.4 Conclusion

The main conclusion to take away from this experimental cold-formed knee-wall project is the opportunity for cost saving. The data resulting from this project show that 30 in. tall cold-formed knee-walls do have a small amount of bending capacity and could possibly

be implemented into lightly loaded construction projects, upon more research and testing performed on this subject. However, since the capacity of an unclipped knee-wall is so small, there are not many situations where it is adequate for the design loading of the building.

6.5 Need for Future Research

This project only tested a small number of unclipped knee-wall scenarios. Therefore, there is a need for future research to expand the knowledge of this subject. Future research could consider using concrete as a base material, possibly changing the compressive strength of the concrete from test to test. The testing performed for this experiment only tested six in. deep cold-formed members, therefore comparing different depths of the cold-formed members could be another future research subject. Additionally, the connection detail for each base condition in this experiment consisted of two #10 screws spaced four in. apart from each other. Altering the screw size or spacing is another possible subject that could be experimented in the future.

References

American Iron and Steel Institute [AISI]. (2012). *North American specification for the design of cold-formed steel structural members (AISI S100)*. In *Cold-formed steel manual: AISI manual*. (2013). Washington, D.C.: American Iron and Steel Institute.

American Society for Testing and Materials [ASTM International]. 2013. *Standard specification for steel sheet, zinc-5% aluminum alloy-coated by the hot-dip process* [ASTM A875/A875M – 13]. In *Annual book of ASTM standards 2013* [Volume 01.06: Metallic-Coated Iron and Steel Products]. West Conshohocken, PA: ASTM International. https://doi.org/ 10.1520/A0875_A0875M-13

American Society for Testing and Materials [ASTM International]. 2016. *Standard specification for steel, sheet, cold-rolled, carbon, structural, high-strength low-alloy, high-strength low-alloy with improved formability, solution hardened, and bake hardenable* [ASTM A1008/A1008M – 16]. In *Annual book of ASTM standards 2016* [Volume 01.03: Metallic-Coated Iron and Steel Products]. West Conshohocken, PA: ASTM International. https://doi.org/ 10.1520/A1008_A1008M-16

Metallurgical Associates, Inc. (2018). *Tensile properties* [Technical report]. Waukesha, WI.: Metallurgical Associates, Inc.

Nowak, M., & Shoemaker, L. (2012, March). Trends in cold-formed steel. *Structure Magazine,* 49. Retrieved from http://www.structuremag.org/?p=3820

Simpson Strong-Tie Company, Inc. (2017, June 1). *Connectors for cold-formed steel construction* [Catalog No. C-CF-2017]. Pleasanton, CA.: Simpson Strong-Tie

Company, Inc.

Tylek, I., & Kuchta, K. (2014). Mechanical properties of structural stainless steels. *Technical Transactions Civil Engineering, 4,* 60-79. Retrieved from https://suw.biblos.pk.edu.pl/downloadResource&mId=1231453

Weng, C. C., & Pekoz, T. (1990). Residual stresses in cold-formed steel members. *Journal of Structural Engineering, 116*(6), 1611-1625. https://doi.org/10.1061/(ASCE)0733-9445(1990)116:6(1611)

Appendix A: Sample Knee-wall Connection Calculation

Given:

A six in. knee-wall, made of 18-gauge material, has a height of 30 in., a length of 9 ft 6 in., and a stud spacing every 16 in. center-on-center connected to a C15×40 channel. The knee-wall is connected the steel channel at each stud using #10 machine screws with a screw distance of four in. There is a uniform load applied to the top of the knee-wall produced by two MTS actuators. The following table is a set of sample data recorded by the MTS system that recorded the displacement of the knee-wall and the force applied by each of the two actuators along with the displacement readings at the DWT located at mid-height of the knee-wall:

Actuator 1		**Actuator 2**		**DWT 1**	**DWT 2**
Displ	**Force**	**Displ**	**Force**	**Displ**	**Displ**
in	**Lbf**	**in**	**lbf**	**in**	**in**
4.386	594.786	4.385	575.643	2.046	1.982

Find the worst-case tensile force in the track-to-stud screw and the worst-case shear force in the stud-to-track screw at the given displacement.

Summary of given knee-wall information:

Knee-wall Parameter	Symbol	Value
Height	H	30 in.
Length	L	9.5 ft
Depth	d	6 in.
Stud-to-track screw distance	d_{shear}	6 in.
Stud Spacing	s	16 in.
Track-to-base-material distance	$d_{pullout}$	4 in.

Average displacement of knee-wall:

$$D = \frac{D_1 + D_2}{2}$$

$$D = \frac{4.386in + 4.385in}{2}$$

$$D = 4.3855in$$

Angular Displacement or Rotation of knee-wall at given displacement:

$$\theta = \sin\left(\frac{D}{H}\right)$$

$$\theta = \sin\left(\frac{4.3855in}{30in}\right)$$

$$\theta = 0.14566rad$$

Total load applied to knee-wall at given displacement:

$$P_{total} = P_1 + P_2$$

$$P_{total} = 594.786lbs + 575.643lbs$$

$$P_{total} = 1170.429lbs$$

Equivalent uniform distributed load along top track of knee-wall:

$$w = \frac{P_{total}}{L}$$

$$w = \frac{1170.429 lbs}{9.5 ft}$$

$$w = 123.203 plf$$

Tributary point load seen at each stud:

$$P_{stud} = ws$$

$$P_{stud} = (123.203 plf)(16 in)\left(\frac{1 ft}{12 in}\right)$$

$$P_{stud} = 164.271 lbs$$

Moment at base connection caused by lateral load:

$$M = P_{stud} H \cos(\theta)$$

$$M = (164.271 lbs)(30 in)(\cos(0.14566 rad))\left(\frac{1 ft}{12 in}\right)$$

$$M = 406.328 ft \cdot lb$$

Tensile force in bottom track-to-base-material screw:

$$T = \frac{P_{stud} \sin(\theta)}{2} + \frac{M}{d_{pullout}}$$

$$T = \frac{(164.271 lbs)(\sin(0.14566 rad))}{2} + \frac{406.328 ft \cdot lb}{(4 in)\left(\frac{1 ft}{12 in}\right)}$$

$$T = 1230.906 lbs$$

Shearing force in bottom stud-to-track-screw:

$$T = \frac{P_{stud} \sin(\theta)}{2} + \frac{M}{d_{shear}}$$

$$T = \frac{(164.271 lbs)(\sin(0.14566 rad))}{2} + \frac{406.328\, ft \cdot lb}{(6in)\left(\frac{1\, ft}{12 in}\right)}$$

$$T = 824.578 lbs$$

Appendix B: Shop Drawings

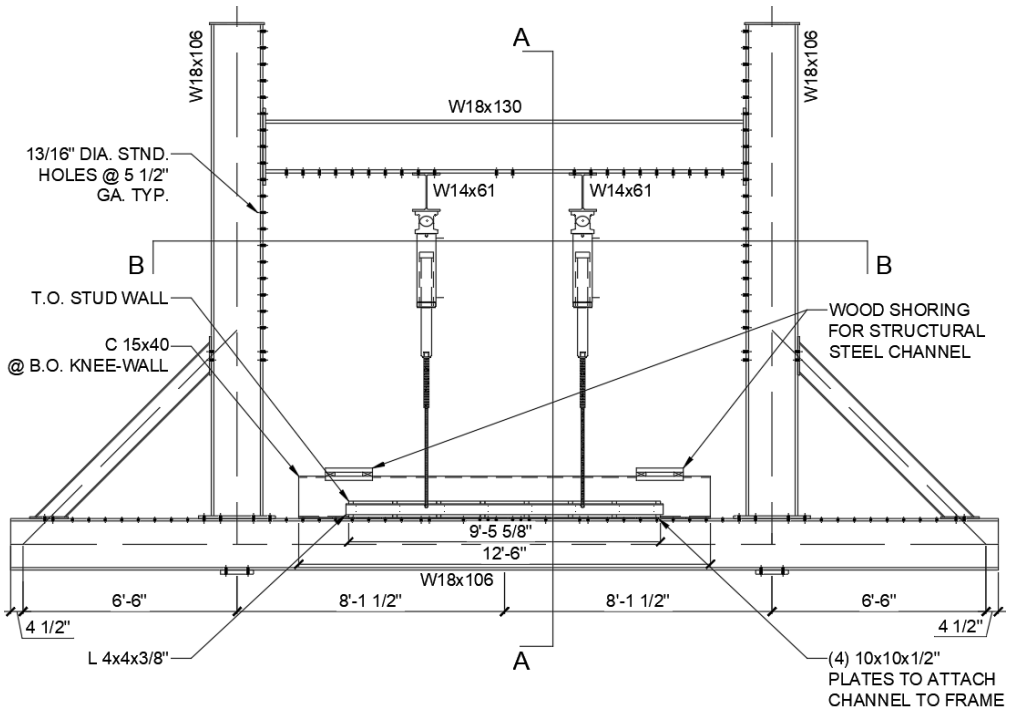

Figure B-1. Front elevation of test setup.

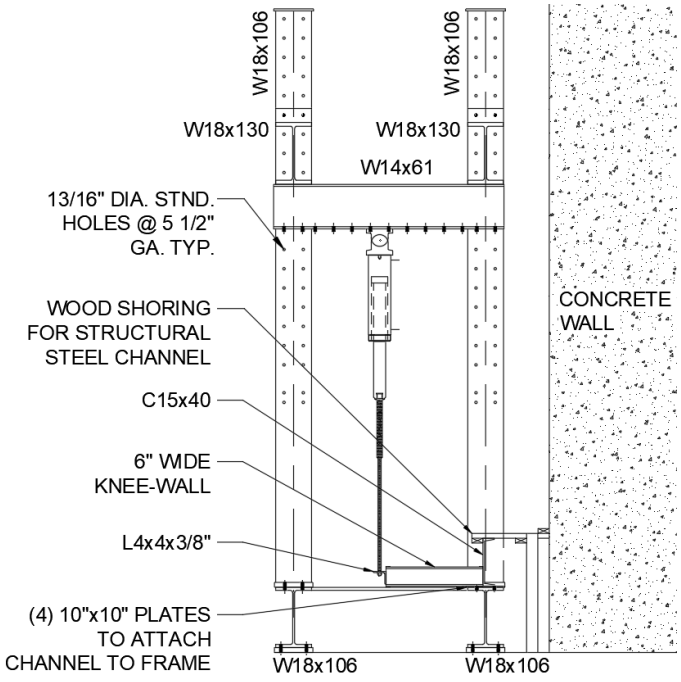

Figure B-2. Side elevation of test setup (Section A-A).

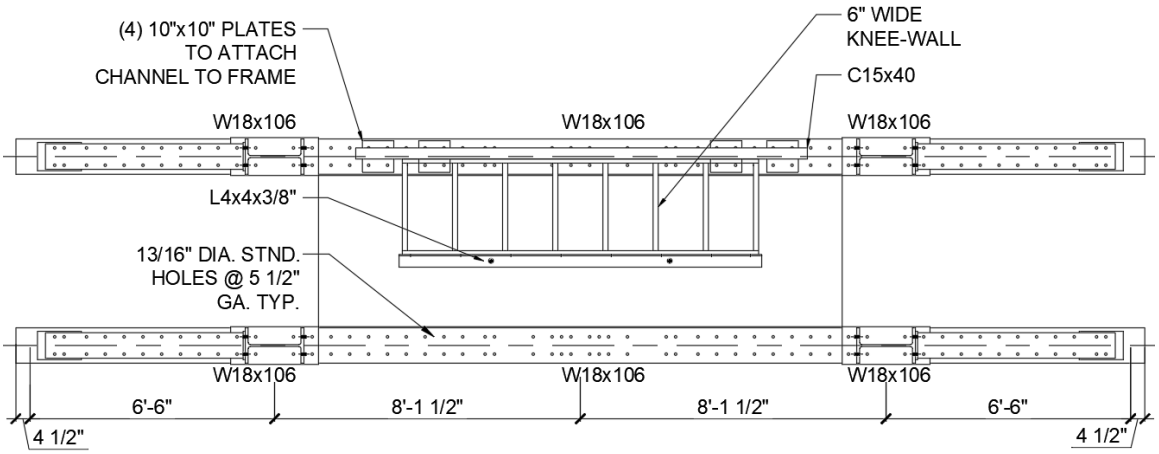

Figure B-2. Top view of test setup (Section B-B).

Appendix C: Material Testing

Metallurgical Associates, Inc. performed the metallurgic analysis of each of the different metals used in this project. Tests were completed on the 20-gauge metal decking as well as 18-, 16-, and 14-gauge studs and tracks. They were tested in comparison with the ASTM A1008 minimum standards. Refer to Section 2.1 in Chapter 2 for additional information on the property requirements for ASTM A1008. Table C-1 contains a summary of a complete list of tested values MAI performed on the metals they were provided with. Following is a breakdown of the testing information done for each piece of metal.

Table C-1

Tensile Properties

Property	Stud			Track			20-Ga Metal Deck	ASTM A1008, SS Grade 40
	18-Ga	16-Ga	14-Ga	18-Ga	16-Ga	14-Ga		
Specimen Width (in)	0.501	0.502	0.502	0.502	0.502	0.502	0.502	0.500
Specimen Thickness (in)	0.069	0.056	0.076	0.045	0.055	0.045	0.033	Material Thickness
Specimen Length (in)	2.00	2.00	2.00	2.00	2.00	2.00	2.00	2.0
Tensile Strength (psi)	74,300	81,500	65,500	65,000	81,500	65,200	76,000	52,000 min.
Yield Strength (psi)[1]	57,800	59,500	56,600	50,500	60,500	50,900	61,500	40,000 min.
Elongation (%)	28	23	25	26	26	24	26	20 min.

Note. 1: At 0.2% offset. Adapted from "Tensile Properties," by Metallurgical Associates, Inc., 2018, Waukesha, WI: Metallurgical Associates, Inc.

C.1 18-Gauge Material Testing

The 18-gauge material was the lightest of the cold-formed pieces tests. These pieces were purchased at a local Menard's. The tracks arrived at the MSOE testing lab in 10 ft sections and the studs arrived in length of 16 ft. Therefore, the tracks did not require any additional cutting, but the studs needed to be cut down to 30 in long pieces. The studs also included punched out holes in the web at 24 in on center. A circular saw was used to cut the studs. According to the two stress-strain curves below, both the stud and the track are made of carbon steel. Due to their shiny appearance, these pieces seem to be galvanized as well.

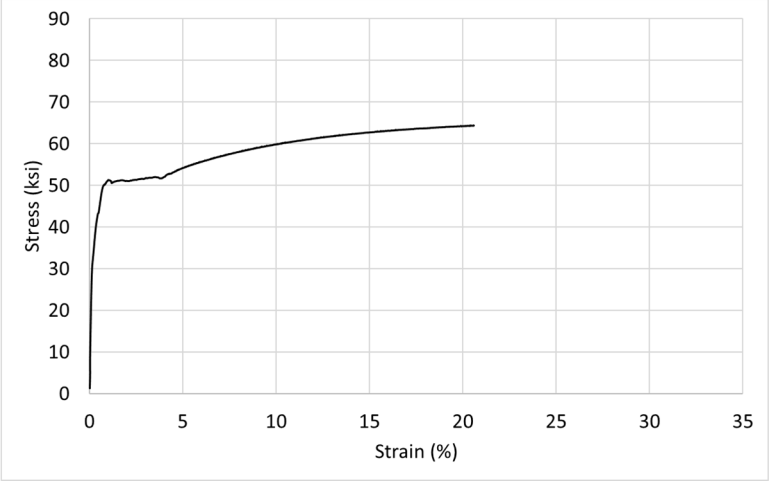

Figure C-1. Stress-strain curve of 18-gauge cold-formed stud. Adapted from "Tensile Properties," by Metallurgical Associates, Inc., 2018, Waukesha, WI: Metallurgical Associates, Inc.

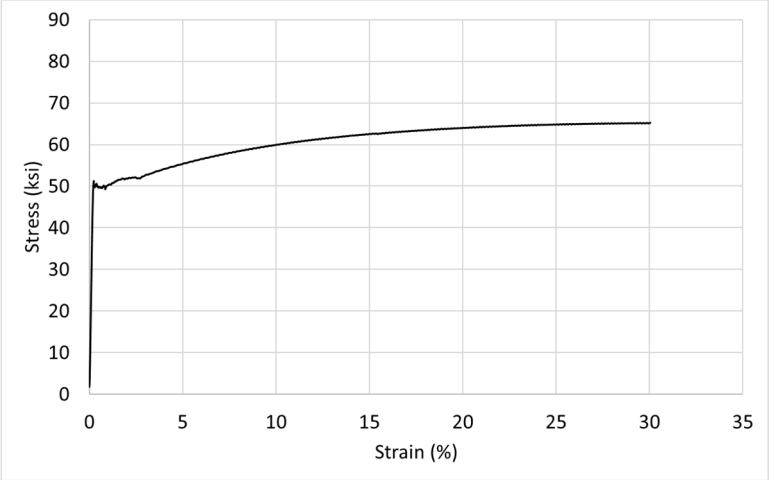

Figure C-2. Stress-strain curve of 18-gauge cold-formed track. Adapted from "Tensile Properties," by Metallurgical Associates, Inc., 2018, Waukesha, WI: Metallurgical Associates, Inc.

C.2 16-Gauge Material Testing

The 16-gauge metal was the second thickest cold-formed steel to be tested in this experiment. These pieces were also bought at Menard's in the same lengths and quantities as the 18-gauge material. Therefore, the same cuts were applied to these pieces in the lab. They were also made of galvanized carbon steel. However, the type carbon steel the 16-gauge pieces were made of was stronger than the 18-gauge carbon steel.

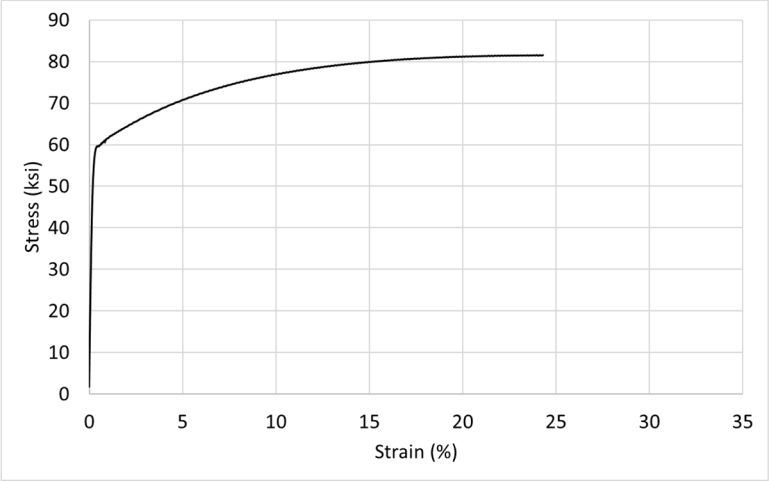

Figure C-3. Stress-strain curve of 16-gauge cold-formed stud. Adapted from "Tensile Properties," by Metallurgical Associates, Inc., 2018, Waukesha, WI: Metallurgical Associates, Inc.

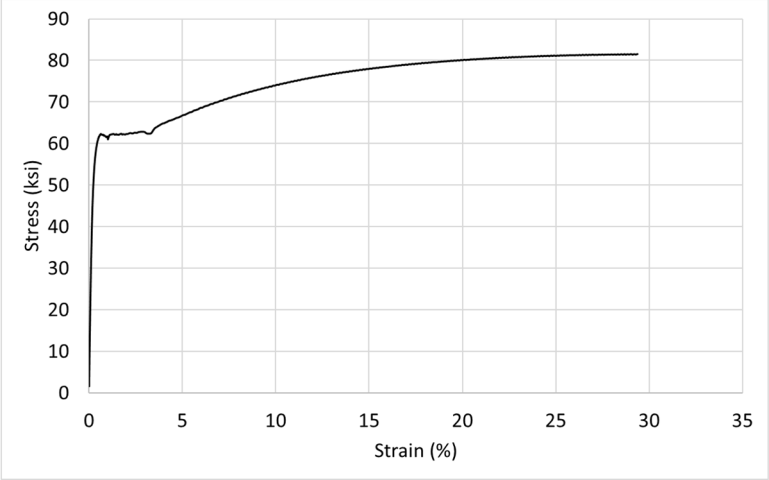

Figure C-4. Stress-strain curve of 16-gauge cold-formed track. Adapted from "Tensile Properties," by Metallurgical Associates, Inc., 2018, Waukesha, WI: Metallurgical Associates, Inc.

C.3 14-Gauge Material Testing

The 14-gauge material was the thickest cold-formed steel tested for this project. This gauge of metal was purchased from a commercial distributor, Home Lumber. Both the studs and tracks were cut to the required length needed for the project by a blade that

didn't produce as much deformation as the circular saw from the MSOE lab. These studs did not include any punched-out holes along the length of it web.

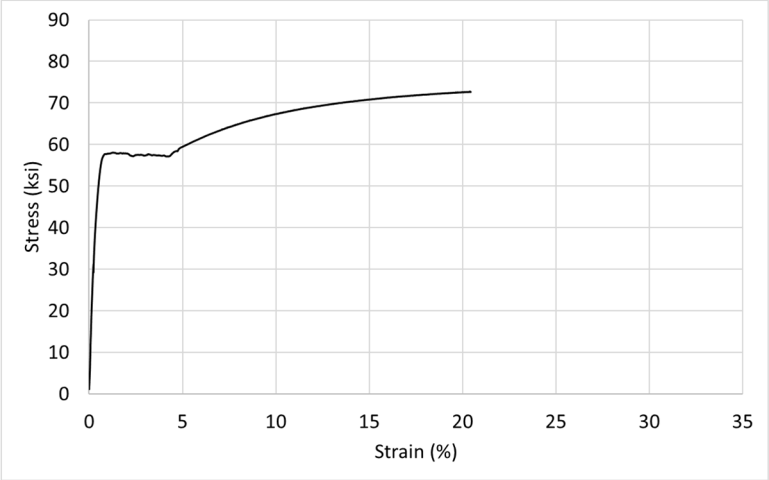

Figure C-5. Stress-strain curve of 14-gauge cold-formed stud. Adapted from "Tensile Properties," by Metallurgical Associates, Inc., 2018, Waukesha, WI: Metallurgical Associates, Inc.

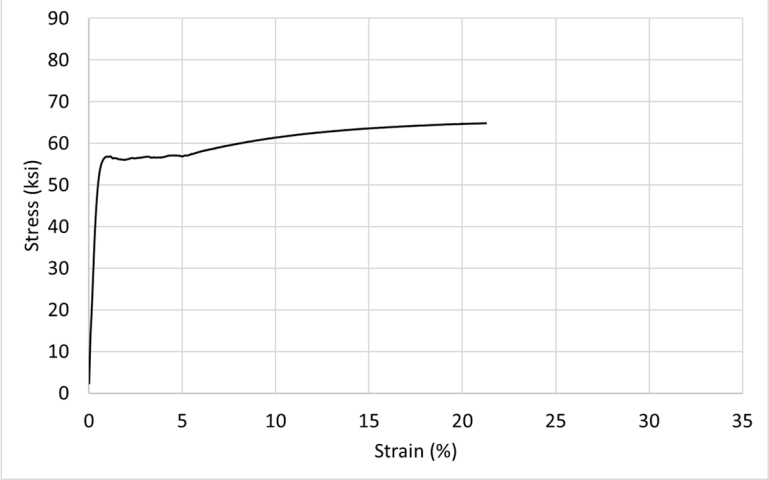

Figure C-6. Stress-strain curve of 14-gauge cold-formed track. Adapted from "Tensile Properties," by Metallurgical Associates, Inc., 2018, Waukesha, WI: Metallurgical Associates, Inc.

C.4 Additional Material Testing

An additional metal that was tested for this project was the 20-gauge metal decking. The metal deck was one of the base conditions observed along with the structural steel channel. The one-and-a-half-inch-deep decking was purchased at Cordeck of Kenosha and arrive to the MSOE lab in 3 ft long by 2 ft tall sections.

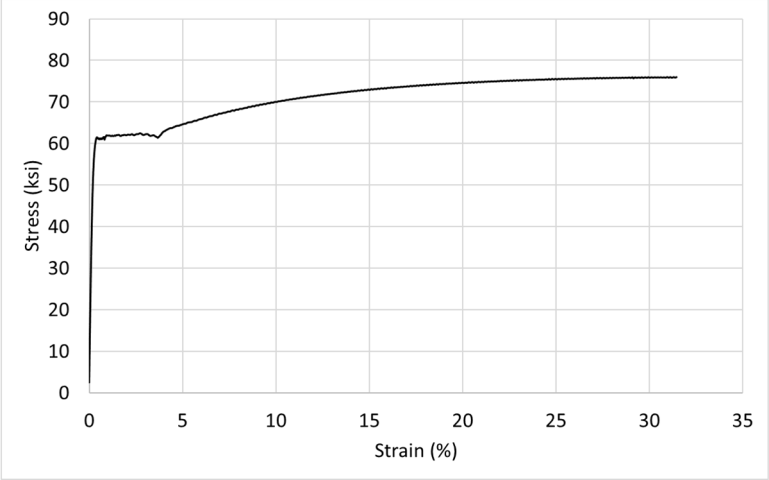

Figure C-7. Stress-strain curve of 20-gauge metal deck. Adapted from “Tensile Properties,” by Metallurgical Associates, Inc., 2018, Waukesha, WI: Metallurgical Associates, Inc.

Appendix D: Screw Capacity Testing

Screw capacity tests were completed in one of MSOE's small testing laboratories. The screw capacity tests consisted of three different setups in order to determine the pullout and shear capacities of the different types of screws used in the cold-formed knee-wall experiment: #10 generic self-drilling screws, #10 generic machine screws, and Hillman brand #10 machine screws. These tests were performed in order to determine why different limit states occurred during the cold-formed knee-wall experiment when certain combinations of screws were used. Table D-1 illustrates a summary of the results of the various screw capacity tests completed.

Table D-1

Summary of Screw Capacity Test Results

	Shear		Pullout/Rupture	
	# of Trials	Average Capacity (lbf)	# of Trials	Average Capacity (lbf)
#10 Generic Self-Drilling Screws	5	1084	6	296
#10 Generic Machine Screws	-	-	5	1403
#10 Hillman Machine Screws	-	-	5	1788

D.1 Pullout Screw Capacity Testing

D.1.1 Self-Drilling Screws

Number 10 self-drilling screws were used to attach the cold-formed knee-wall to the metal deck base condition. While the uniform lateral load was applied to the knee-wall, the controlling limit state was the pullout of these self-drilling screws. Figure D.1.1-1 is a

graphical representation of all how the self-drilling screws reacted in the pullout test. Table D.1.1-1 summarizes the maximum self-drilling pullout (SDP) values from each trial as well the average value based on these maximum values.

Table D.1.1-1

Self-Drilling Screw Pullout Results

Test	01	02	03	04	05	06	Average
Maximum Pullout (lbf)	288	313	281	282	310	303	296

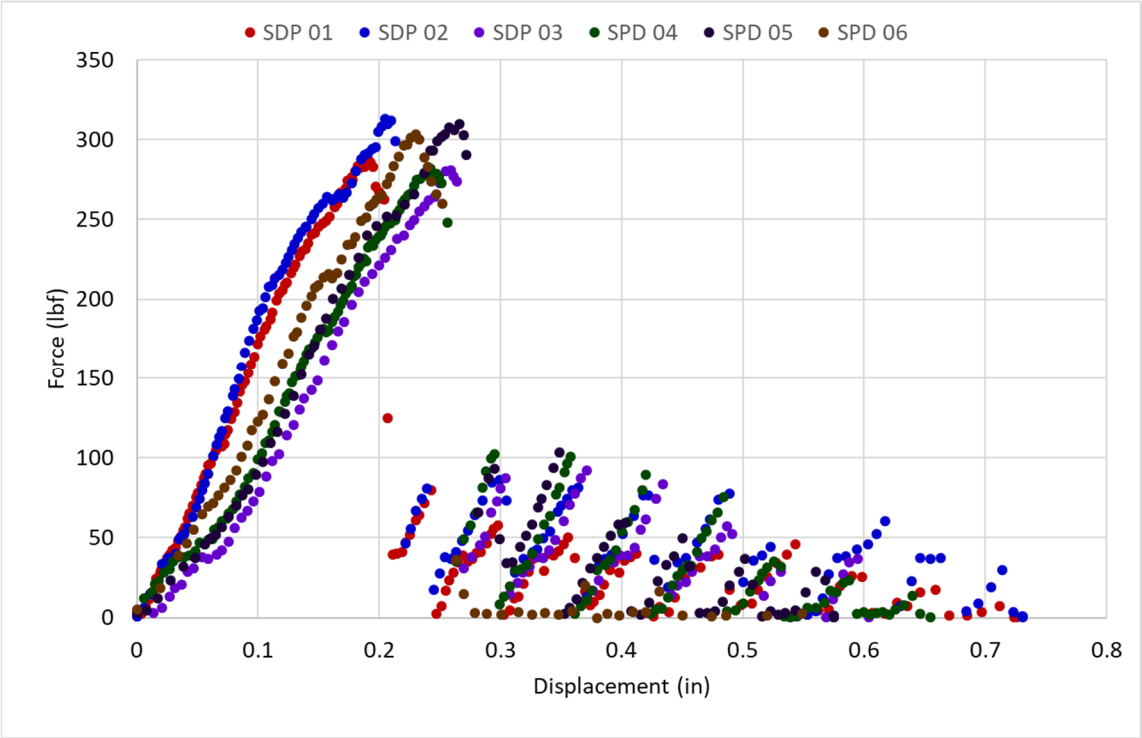

Figure D.1.1-1. Self-drilling screw pullout results.

D.1.2 Machine Screws

Number 10 machine screws were used when to attach the cold-formed knee-wall to the structural steel channel base condition. Depending on which brand of generic machine used determined which limit state would control in these knee-wall testing trials. When the generic machine screws were used, the controlling limit state was the tensile rupture capacity of those machine screws. On the other hand, when the Hillman brand machine screws were used, the tear out capacity of the self-drilling screws used to attach the cold-formed studs to the bottom track controlled. Table D.1.2-1 illustrates the maximum pullout values for the two brand of machine screws used. Figures D.1.2-1 through D.1.2-2 visually represents the reaction of the two machine screw brands in the pullout screw tests.

Table D.1.2-1

Machine Screw Rupture Results

Test	01	02	03	04	05	Average
Generic – Maximum Rupture (lbf)	1391	1379	1338	1495	1413	1403
Hillman – Maximum Rupture (lbf)	1802	1778	1792	1776	1793	1788

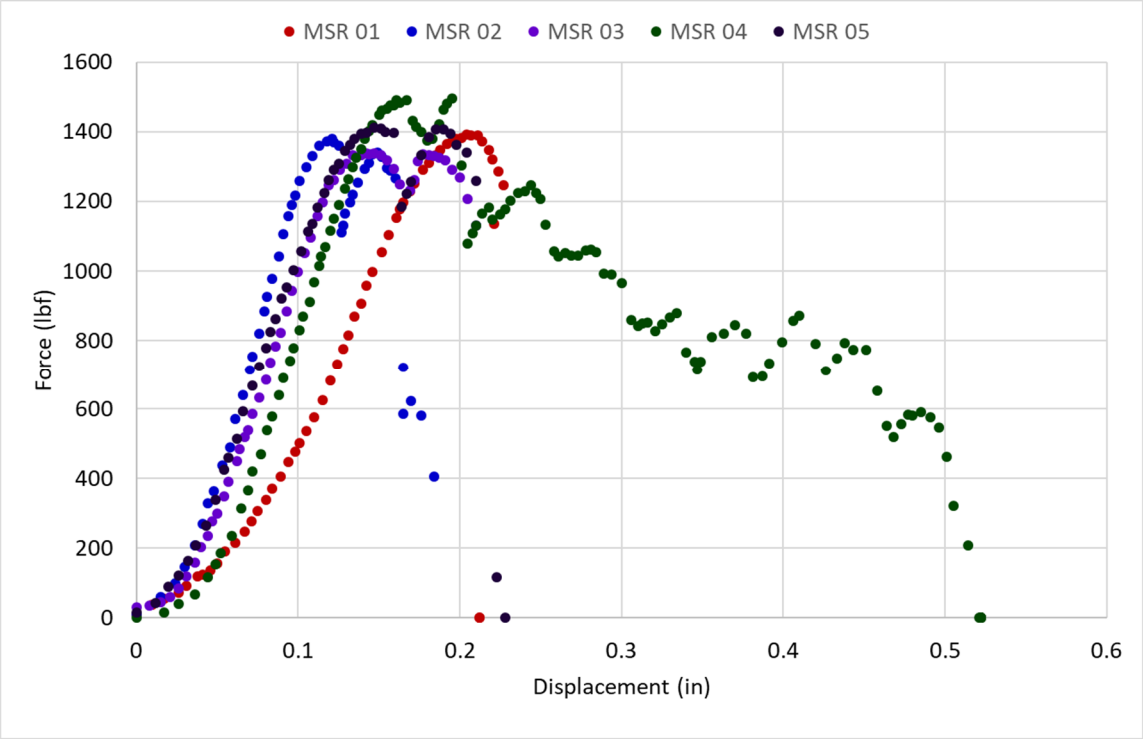

Figure D.1.2-1. Generic machine screw rupture results.

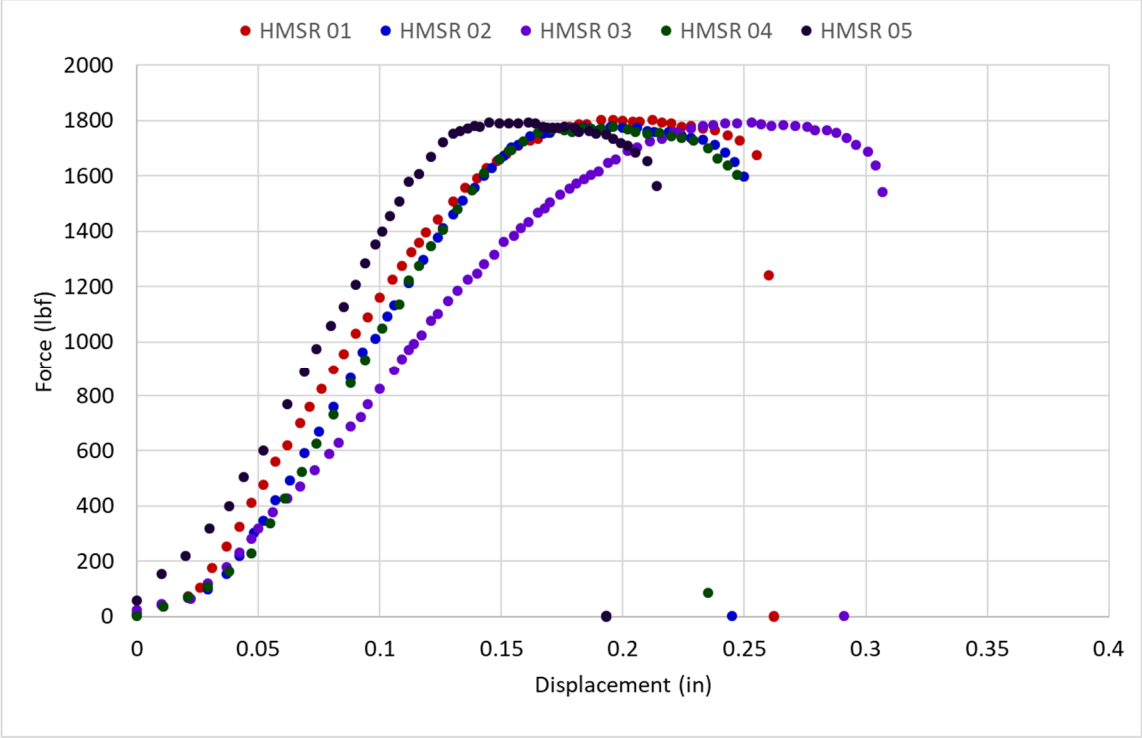

Figure D.1.2-2. Hillman machine screw rupture results.

D.2 Shearing Screw Capacity Testing

D.2.1 Self-Drilling Screws

Under the cold-formed knee-wall testing trials that used the Hillman brand machine screws in the connection of the knee-wall attachment to the structural steel channel, the self-drilling screw shearing in the stud to track connection controlled. The maximum shear screw capacity test results can be seen in Table D.2.1-1 as well as the graphical representation of each test in Figure D.2.1-1.

Table D.2.1-1

Self-Drilling Screw Shear Results

Test	01	02	03	04	05	Average
Maximum Shear (lbf)	1142	957	1104	1198	1018	1084

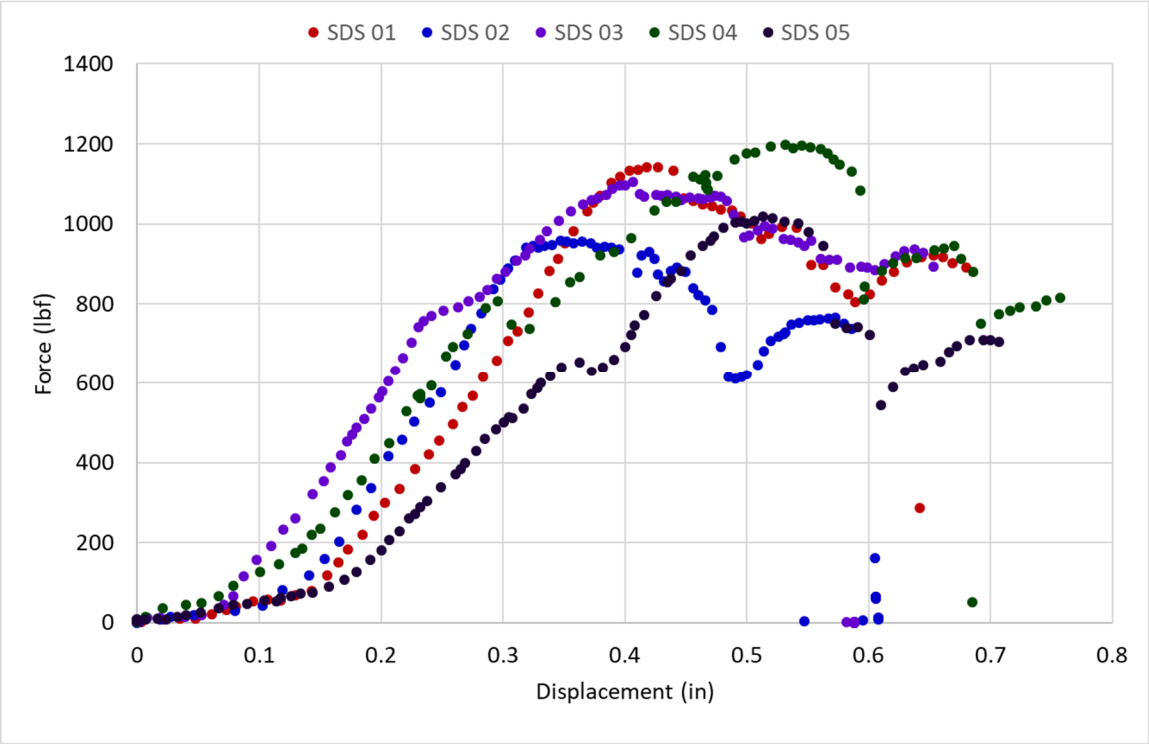

Figure D.2.1-1. Self-drilling screw shear results.

Appendix E: Test Data Output

The experimental data recorded for this research are available upon request. Contact the Milwaukee School of Engineering campus library for further information on how to obtain access to the experimental data.

Structural Engineering

Capstone Report Approval Form

Master of Science in Structural Engineering – MSST

Milwaukee School of Engineering

This capstone report, entitled "Strength of Unclipped Cold-Formed Knee-walls Under Uniform Lateral Loading," submitted by the student Deanna M. Engelmeyer, has been approved by the following committee:

Faculty Advisor: _____ Date: _____

Dr. Christopher Raebel

Faculty Member: _____Date: _____

Dr. Hans-Peter Huttelmaier

Faculty Member: _____Date: _____

Dr. Todd Davis